

Strength development of soft soils

Prediction and verification of undrained shear
strength for loaded soft soils

MSc. Thesis

M.M. Nooteboom

Strength development of soft soils

Prediction and verification of undrained shear
strength for loaded soft soils

by

M.M. Nootboom

Student Name	Student Number
M.M. Nootboom	4706188

Company supervisor	ir. J. Bol
Committee	dr. ir. C. Zwanenburg dr. S. Muraro dr. ir. C. Mai Van
Faculty	Civil Engineering and Geo-sciences

Cover: Manilla International Airport by Anne-Jan Fokkema

Preface

Completing this thesis marks the end of my master's degree journey. The past months have been a mix of challenges and rewarding insights. Now, I want to take a moment to extend my gratitude to everyone who played a role, whether directly or indirectly, in this journey.

First and foremost, a big thank you goes out to the team at Boskalis. Their willingness to assist, their enthusiasm, and the welcoming atmosphere they provided right from the start made a world of difference. I'd like to specifically mention Joris Bol for being an exceptional supervisor. His feedback and shared insights significantly contributed to the positive outcome of the research. Lastly, I'm thankful to Patricia Ammerlaan for giving me the chance and trust to undertake this thesis at Boskalis.

Moving on, I'd like to express my appreciation to Stefano Muraro and Cong Mai Van for their valuable feedback and fruitful discussions. A special mention goes to Cor Zwanenburg, who skillfully chaired our committee. Our regular gatherings to discuss the thesis on Wednesdays truly guided the research in the right direction.

Lastly, I want to acknowledge all those who indirectly supported me during these past months: fellow friends and students in the Civil Engineering faculty. Most importantly, I want to thank my family and my girlfriend Manon for their unwavering support and understanding, even during times when I couldn't always be fully available.

*M.M. Nootboom
Rotterdam, August 2023*

*"Research is a process where you can spend all day being wrong and still feel like you're making progress."
-Paul Graham*

Summary

The concern regarding the subsoil stability of various civil engineering projects often lies in the undrained shear strength of soft soils. Enhancing this strength can be achieved through the application of (pre)loading in conjunction with Prefabricated Vertical Drains (PVDs). To predict strength across different phases—prior to, during, and after the removal of a load—the Stress History And Normalized Soil Engineering Properties (SHANSEP) framework can be applied. Verification of strength is performed through Cone Penetration Tests with pore pressure measurements (CPTu), where CPTu data can be related to undrained shear strength using the strength factor N_{kt} (Karlsrud et al. 2005).

This study utilizes laboratory and site data to predict undrained shear strength via the SHANSEP framework and subsequently validate this strength through CPTu and monitoring data. The research encompasses two datasets. The first dataset involves three field trials for a dike project at 'de Markermeerdijken' in the Netherlands. These trials implement a 5-meter high surcharge alongside Prefabricated Vertical Drains to enhance soil strength. The SHANSEP framework is used to predict undrained shear strength pre-surcharge, just before surcharge removal (at more than 90% consolidation), and post-surcharge removal. Predictions are cross-verified with Cone Penetration Tests (CPTu) and laboratory assessments. The second dataset comprises three field trials for a reclamation project in the Philippines. Here, CPTu tests are conducted during consolidation, CPTu-correlated strength is compared with piezometer-based strength and SHANSEP predictions. The focus pertains to the strength of the seabed's Marine Soft Clay.

Drawing from the analysis of the two case studies, it was determined that the accuracy of predicting undrained shear strength using SHANSEP is influenced by a range of factors. Among these factors, the ones deemed most significant include:

- Uncertainty in Pre Overburden pressure (POP) leads to inaccurate initial strength prediction.
- Small load area relative to depth diminishes preload effectiveness.
- Submersion of surcharge below the phreatic surface due to settlement reduces preload effectiveness and resultant undrained shear strength gain.
- Inclusion of creep in strength prediction necessitates a reduction in SHANSEP S factor.
- Prediction quality relies heavily on high-quality laboratory tests. Constant height DSS yielded consistent SHANSEP S values, while unconsolidated undrained triaxial tests yielded varying and unrealistically low values. Field vane tests yield strength values in line with literature.

When considering the aforementioned points, the SHANSEP framework effectively predicts undrained shear strength in soft soils. SHANSEP predicted strength increments due to surcharge align reasonably with CPTu-measured values. Reliability hinges on quality laboratory tests, and SHANSEP strength shows a poor match with CPTu strength in soils which partially drain during CPTu testing.

Strength prediction and verification during consolidation prove challenging, as excess pore pressure mainly influences strength. Observations include:

- The presence of courser particles in soft soils, indicated by a low pore pressure parameter B_q and higher corrected cone resistance q_t , induces higher strengths in CPTu tests due to partial drainage. This negatively affects correspondence between SHANSEP predicted strength and CPTu correlated strength.
- A poor correspondence between CPTu-based and piezometer-based strengths, with increased mismatch for lower horizontal consolidation coefficients and larger PVD spacing.
- Overestimation of undrained shear strength via piezometer readings may relate to their placement relative to PVDs or within permeable layers.

- Short-term strength increase based on piezometers exceeds CPTu-estimated increase after additional surcharge application.
- CPTu-correlated strength's influence by distance to PVDs peaks initially and diminishes as excess pore pressure dissipates.

Derived from the findings of this investigation, it is advisable to incorporate adjustments for preload submersion, factor in the influence of load distribution, and evaluate the partially drained characteristics during CPTu tests using parameters B_q and q_t for an enhanced SHANSEP strength verification. To ensure reliability and accuracy, it is cautioned against relying solely on CPTu or piezometer data.

Contents

Preface	i
Summary	ii
Nomenclature	ix
1 Introduction	1
1.1 Problem statement	1
1.2 Research method	2
1.2.1 Scope	2
1.2.2 Goal	2
1.2.3 Approach	2
1.3 Data gathering and analysis	3
1.4 Reading Guide	4
2 Background	5
2.1 Soft soils	5
2.2 Societal relevance	5
2.3 Lithology	5
3 Literature study	7
3.1 Undrained shear strength	7
3.2 Consolidation	9
3.3 SHANSEP	13
3.4 Field test	19
4 Methodology	24
4.1 Site Investigation	24
4.2 SHANSEP	24
4.2.1 SHANSEP S	24
4.2.2 SHANSEP m	26
4.2.3 In situ effective vertical stress	26
4.2.4 Preconsolidation stress	26
4.2.5 Coefficient of consolidation	28
4.3 Submersion of preload	29
4.4 Depth influence	30
4.5 CPTu verification of strength	30
4.6 Piezometer verification of strength	30
4.7 Comparison	30
5 Markermeerdijken	32
5.1 Introduction	32
5.2 Site investigation	34
5.2.1 Soil profile	34
5.2.2 CPTu's	35
5.2.3 Geo-hydrology	37
5.2.4 Soil parameters	38
5.2.5 Nkt and SHANSEP S	38
5.2.6 Depth influence	40
5.3 SHANSEP Undrained shear strength	42
5.4 Strength comparison SHANSEP and CPTu	43
5.4.1 de Weel	45

5.4.2 Ethersheim	47
5.4.3 Broeckgouw	48
6 Reclamation Philippines	51
6.1 Introduction	51
6.2 Site Investigation	52
6.2.1 Coefficient of consolidation	55
6.2.2 Geo-hydrology	56
6.2.3 Nkt and SHANSEP S	56
6.2.4 Site investigation summary	59
6.3 Consolidation	59
6.3.1 Consolidation Field Trial 1	60
6.3.2 Consolidation Field Trial 2	61
6.3.3 Consolidation Field Trial 3	61
6.4 Comparison SHANSEP and CPTu	62
6.4.1 Field Trial 1	64
6.4.2 Field Trial 2	68
6.4.3 Field Trial 3	72
7 Project comparison	75
7.1 Strength characteristics	75
7.2 Similarities	75
7.3 Differences	76
8 Discussion	77
8.1 Research Limitations	77
8.2 Suggestions for future research	77
9 Conclusion and Recommendations	79
9.1 Conclusions	79
9.2 Recommendations	81
References	82
A Data Markermeerdijken	84
B Data Philippines reclamation	93

List of Figures

1.1	Reading guide report	4
2.1	Dike reinforcement: https://www.gww-bouw.nl/artikel/markerveerdijken-van-zeedijk-tot-meerdijk/	6
3.1	Mohr circle Unconsolidated Undrained triaxial tests (Verruijt 2017)	7
3.2	Stress paths HOC clay and NC clay	8
3.3	Consolidation solution (Verruijt 2017)	9
3.4	D_s for grid different PVD grid patterns	10
3.5	Comparison of the Conte and Troncone (2009) solution with Barron (1948): (a) loading used in present solution; (b) radial profiles of excess pore pressure, u , for different values of time factor, T_h ; (c) degree of consolidation vs. time factor T_h	11
3.6	Comparison of the Conte and Troncone (2009) solution with Olson (1977): (a) loading used in present solution; (b) radial profiles of excess pore pressure, u , for different values of time factor, T_h ; (c) degree of consolidation vs. time factor T_h	11
3.7	Depth influence of an embankment (Poulos and Davis 1964)	12
3.8	Circular uniform load (Verruijt 2017)	12
3.9	Stress systems for typical in situ modes of failure (Ladd and Foott 1974)	13
3.10	Shear devices and their stress systems for CK_0U testing (Ladd 1991)	14
3.11	Undrained Strength Anisotropy from CK_0U Tests on Normally Consolidated Clay and Silt (Ladd 1991)	14
3.12	Shearing conditions and its effect on the undrained shear strength ratio (Ladd and DeGroot 2003)	15
3.13	Undrained shear strength vs. effective stress (De Koning et al. 2019)	16
3.14	Instant and delayed compression (Bjerrum 1967)	18
3.15	Creep strain and intrinsic time due to (un)loading	19
3.16	Soil behaviour type classification system from CPTu data	22
4.1	Relationship water content and volumetric weight	25
4.2	Direct Simple Shear test on clay	25
4.3	Oedometer test procedure (ASTM-D6535 2011)	27
4.4	C_v determination procedure (ASTM-D6535 2011)	28
4.5	Undrained shear strength in peat (field trial Broeckgouw)	29
5.1	Overview locations field trials: http://www.earth.google.com (2023)	32
5.2	Soil profiles	34
5.3	De Weel: CPTu during Site investigation	36
5.4	Ethersheim: CPTu during Site investigation	36
5.5	Broeckgouw: CPTu during Site investigation	37
5.6	Piezometer data field trial de Weel	37
5.7	N_{kt} and SHANSEP S determination for clay	39
5.8	N_{kt} and SHANSEP S determination for peat	40
5.9	Depth Influence factor	40
5.10	SHANSEP undrained shear strength	42
5.11	Field trial de Weel: CPTu locations	44
5.12	Field trial Ethersheim: CPTu locations	44
5.13	Field trial Broeckgouw: CPTu locations	44
5.14	Field trial de Weel: undrained shear strength comparison SHANSEP and CPTu	45
5.15	Field trial de Weel: B_q parameter	46

5.16	Field trial Ethersheim: undrained shear strength comparison SHANSEP and CPTu . . .	47
5.17	Field trial Ethersheim: B_q parameter	48
5.18	Field trial Broeckgouw: undrained shear strength comparison SHANSEP and CPTu . .	49
5.19	Field trial Broeckgouw: B_q parameter	50
6.1	Overview Site Investigation	52
6.2	Boreholes near Field trials	53
6.3	Marine CPTu-01	53
6.4	Watercontent & Attenberg limits	54
6.5	B_q parameter CPTu-01	55
6.6	BH-01: Coefficient of consolidation	55
6.7	Hydraulic head in the sand fill	56
6.8	N_{kt} and SHANSEP S	57
6.9	Labtests and CPTu	58
6.10	FT1: Radial Consolidation	60
6.11	FT2: Radial Consolidation	61
6.12	FT3: Radial Consolidation	61
6.13	FT1: General strength comparison	64
6.14	FT1: Average strength comparison	66
6.15	FT1: Strength per location	67
6.16	FT2: General strength comparison	68
6.17	FT2: Average strength comparison	69
6.18	FT2: Strength per location	71
6.19	FT3: General strength comparison	72
6.20	FT3: Average strength comparison	73
6.21	FT3: General strength comparison	74
A.1	Volumetric weight measurements Markermeerdijken	84
A.2	Top view de Weel	85
A.3	Top view Ethersheim	86
A.4	Top view Broeckgouw	87
A.5	Markermeerdijken: Isotach model calculation	88
A.6	de Weel stress state	88
A.7	Ethersheim stress state	89
A.8	Broeckgouw stress state	89
A.9	de Weel phase 0	90
A.10	de Weel phase 1	90
A.11	de Weel phase 2	90
A.12	Ethersheim phase 0	91
A.13	Ethersheim phase 1	91
A.14	Broeckgouw phase 0	91
A.15	Broeckgouw phase 1	92
A.16	Broeckgouw phase 2	92
B.1	Site investigation boreholes: BH-01, BH-02, BH-05, BH-06, BH-07	94
B.2	Bulk unit weight	95
B.3	Consolidation during fill, before PVD installation. Fill was completed in approximately 90 days	96
B.4	Monitoring data	97
B.5	FT1: Difference between zero measurement cone resistance prior to CPTu and after CPTu	98
B.6	FT2: Difference between zero measurement cone resistance prior to CPTu and after CPTu	98
B.7	FT3: Difference between zero measurement cone resistance prior to CPTu and after CPTu	99
B.8	FT2: General strength comparison excluding creep	100
B.9	MSC3: better fit with SHANSEP S of 0.22	101
B.10	OCR due to creep in FT1: layers MSC1, MSC2 and MSC3	101
B.11	OCR due to creep in FT2: layers MSC1, MSC2 and MSC3	102
B.12	OCR due to creep in FT3: layers MSC1, MSC2 and MSC3	103

List of Tables

1.1	Data overview	3
3.1	Typical Skempton A parameters	8
3.2	Undrained strength anisotropy of NC Boston Blue clay (Ladd and Foott 1974)	13
3.3	SHANSEP S and SHANSEP m factor based on laboratory testing (De Koning et al. 2019)	16
3.4	Summary of SHANSEP and soil parameters (Yang et al. 2019)	17
3.5	Values for N_{kt} (Rémai 2013)	20
3.6	Application classes and general requirements in EN-ISO 22476-1.	20
3.7	CPTu Application classes with allowable minimum accuracy in EN-ISO 22476-1.	21
5.1	Markermeerdijken: field trial specifications	33
5.2	Class 1 CPTu accuracy	35
5.3	Markermeerdijken: soil parameters	38
5.4	Poulos and Davis geometry parameters	41
5.5	Percentage of effective preload over depth	41
5.6	SHANSEP parameters based on DSS tests	42
6.1	Summary of geotechnical soil properties	59
6.2	C_h based on piezometer data	60
6.3	CPTu information FT1	62
6.4	CPTu information FT2	62
6.5	CPTu information FT3	62
7.1	Strength parameters	75

Nomenclature

Abbreviations

Abbreviation	Definition
1D	One-dimensional
BH	Borehole
CAU	Anisotropically Consolidated Undrained
CIU	Isotropically Consolidated Undrained
CPTu	Cone Penetration Tests with pore pressure measurements
DSS	Direct Simple Shear
ESP	Effective Stress Path
LPE	Lost Point Extensometer
FT	Field Trial
FV	Field Vane
LV	Laboratory Vane
MSC	Marine Soft Clay
MSL	Mean Sea level
NAP	Normaal Amsterdams Peil (Dutch reference level)
NGI	Norwegian Geotechnical Institute
NC	Normally Consolidated
OC	Over Consolidated
OCR	Over Consolidation Ratio
PSA	Plain Strain Active
PSP	Plain Strain Passive
PVD	Prefabricated Vertical Drain
SHANSEP	Stress History And Normalized Soil Engineering Properties
TC	Triaxial Compression
TE	Triaxial Extension
TSP	Total Stress Path
TV	Torvane
USS	Undrained Shear Strength
UU	Undrained Unconsolidated
VWP	Vibrating Wire Piezometer
SP	Settlement Plate

Symbols

Symbol	Definition	Unit
A	Skempton pore pressure coefficient A	[-]
A_k	Fourier Coefficient	[-]
a	Cone area ratio	[-]
B	Skempton pore pressure coefficient B	[-]
B_k	Fourier Coefficient	[-]

Symbol	Definition	Unit
B_q	Pore pressure parameter	[-]
C_α	Secondary compression index	[-]
C_c	Compression index	[-]
C_h	Horizontal coefficient of consolidation	[m ² /s]
CR	Compression Ratio	[-]
C_s	Coefficient of swelling	[-]
C_v	Vertical coefficient of consolidation	[m ² /s]
D	Radius of PVD influence zone	[m]
D_s	Drain spacing	[m]
d_w	Drain diameter	[m]
e	Void ratio	[-]
f_s	Sleeve friction resistance	[MPa]
H	Layer thickness	[m]
h_d	Drainage path length	[m]
h_{d50}	Drainage path length at 50% consolidation	[m]
h_{emb}	Embankment height	[m]
I	Influence factor	[-]
K_0	Neutral earth pressure coefficient	[-]
LL	Liquid Limit	[%]
m	SHANSEP m parameter	[-]
n	Porosity	[-]
$N_{\Delta u}$	Pore pressure factor	[-]
N_{kt}	Cone factor for undrained shear strength	[-]
p	Load	[kPa]
P_c'	Preconsolidation stress	[kPa]
PI	Plasticity Index	[%]
PL	Plastic Limit	[%]
POP	Pre Overburden Pressure	[kPa]
q_c	Cone resistance	[MPa]
q_t	Corrected cone resistance	[MPa]
r	Radius	[m]
R_f	Friction ratio	[%]
RR	Recompression Ratio	[-]
S	SHANSEP S factor	[-]
S_r	Saturation	[%]
s_u	Undrained shear strength	[kPa]
t_{50}	Time at 50% consolidation	[s]
t_{100}	Time at 100% consolidation	[s]

Symbol	Definition	Unit
T_h	Dimensionless horizontal time factor	[-]
T_v	Dimensionless vertical time factor	[-]
U	Degree of consolidation	[-]
u	Pore pressure	[kPa]
u_0	In-situ pore pressure	[MPa]
u_2	Measured pore pressure behind the neck of the cone	[MPa]
w	Watercontent	[%]
z	Depth	[m]
δ	Angle between major stress direction at faillure relative to vertical	[°]
Δu	Pore pressure change	[kPa]
$\dot{\epsilon}$	Strain rate	[%/hr]
γ_{emb}	Embankment unit weight	[kN/m ³]
γ_s	Surcharge unit weight	[kN/m ³]
κ_c	Compressibility of the soil skeleton	[m ² /N]
κ_v	Compressibility of the void fluid	[m ² /N]
ρ	Density	[kg/m ³]
σ_p'	Preconsolidation stress	[kPa]
σ_v'	In situ vertical effective stress	[kPa]
σ_1	Major principle stress	[kPa]
σ_2	Intermediate principle stress	[kPa]
σ_3	Minor principle stress	[kPa]
σ_{tot}	Total stress	[kPa]
τ	Intrinsic time	[days]
τ_v	Uncorrected FVT shear strength	[kPa]
ϕ	Friction angle	[°]
ω	Frequency	[s ⁻¹]

1

Introduction

1.1. Problem statement

Slope stability becomes a critical consideration in various civil engineering undertakings, including projects like land reclamation, dike reinforcement, and embankment construction. Within such endeavors, the underlying soil experiences loading due to the formation of embankments or fills. When dealing with soft soils, the rate of (shear) loading can often surpass the pace at which excess pore water pressure dissipates. In such instances, there is a rise in pore pressure, causing a reduction in effective stress. This reduction can result in slope failures under certain circumstances. To counteract this, a mechanical surcharge is employed, typically in the form of a temporary embankment. Sometimes, this surcharge is combined with drainage systems. The goal is to augment the effective stress and preconsolidation stress within the subsoil, thereby enhancing the soil's shear strength.

The Stress History And Normalized Soil Engineering Properties (SHANSEP) framework by Ladd and Foott (1974) is an established theory to predict the initial strength and the strength as an effect of a temporary or permanent preload. Samples from the field are consolidated to a different over consolidation ratio (OCR) to obtain a relationship between stress state, stress history and undrained shear strength. In this way, a prediction of the undrained shear strength before, after or during loading of the soil is made. The in situ strength can be assessed by means of laboratory tests and Cone Penetration Tests with pore pressure measurements (CPTu) correlations with undrained shear strength s_u . In this relation, the corrected cone resistance is linked to undrained shear strength by the total vertical stress at the depth of the CPTu and a cone factor obtained from laboratory tests or literature.

Marine contractor Boskalis has experience with the design and execution of various reclamation projects and experiences in some cases that the CPTu correlated strength increase does not match with the SHANSEP prediction. Strength development in soft soils is influenced by multiple variables and assumptions, including the quality of site investigations, the idealized behavior of soft soils in the SHANSEP model, uncertainties in CPTu correlations with undrained shear strength, uncertainty in the degree of consolidation, and assumptions regarding the effectiveness of surcharging. This leads to the main questions of this thesis:

- What is the accuracy of SHANSEP undrained shear strength predictions in practical applications?
- How could undrained shear strength development prediction be improved in case of soft soils?

This process of meeting this research objective is guided by the following subquestions:

- How is strength development predicted?
- Which aspects should be taken into consideration for the prediction of strength development?
- Which aspects should be taken into consideration for the verification of strength development?
- How does the strength development (prediction) in different projects compare?
- What site conditions could influence strength development?

1.2. Research method

1.2.1. Scope

This research project has the objective of analyzing field trials executed in two distinct locations: the Markermeerdijken project in the Netherlands and a reclamation project in the Philippines. The main focus of this study is to investigate the development of undrained shear strength in soft soils, including both clay and peat, within the context of dike and reclamation endeavors.

The emphasis lies on assessing the inherent strength of the natural subsoil. In the context of the Markermeerdijken field trials, the investigation delves into the undrained shear strength of the underlying clay and peat layers beneath a surcharge. The evaluation covers the strength of these layers prior to surcharge application, before surcharge removal (following over 90% consolidation), and post surcharge removal.

In contrast, with regard to the reclamation project in the Philippines, the analysis addresses the undrained shear strength during the consolidation process. The study concentrates on analyzing the undrained shear strength of the seabed where the fill material is placed, rather than focusing on the properties of the fill itself.

Furthermore, in the case of the reclamation project, a more pronounced emphasis will be placed on determining the SHANSEP S parameter and the N_{kt} parameter. This determination will be achieved through a combination of laboratory tests and field tests, allowing for a comprehensive understanding of the undrained shear strength characteristics in the context of the reclamation endeavor.

1.2.2. Goal

The primary objective of this thesis is to acquire a comprehensive understanding of the various aspects that play a role in determining the accuracy of predictions generated by the SHANSEP framework. A key focus of interest is to identify and examine the limitations inherent in the SHANSEP framework, as well as to gain insights into the simplifications employed that may result in a reduction of prediction accuracy.

The research also aims to assess the confirmation of undrained shear strength and identify potential factors that may affect the accuracy of such verification.

By conducting a thorough analysis of these aspects, precision of soil strength predictions for future projects can be improved.

1.2.3. Approach

The primary objective is to gain insights into the development of strength in these projects. The approach to achieve this goal can be summarized as follows:

1. Conduct a review of the existing literature focusing on the following areas:
 - (a) Characteristics related to undrained shear strength
 - (b) Consolidation processes in soft soils
 - (c) Methods for predicting and verifying undrained shear strength
2. For each project under consideration, follow these steps:
 - (a) Gather relevant information regarding site conditions and preloading factors
 - (b) Obtain in situ undrained shear strength values through various means such as Cone Penetration Tests (CPTu's), laboratory tests, and field vane tests. Compare these values with the predictions generated by the SHANSEP framework.
 - (c) Utilize the SHANSEP framework to forecast the post-surcharged undrained shear strength.
 - (d) Evaluate the quality of the SHANSEP predictions by comparing them with established CPTu- s_u correlations.
3. Assess the variations in strength enhancement observed across the different projects.
4. Utilize both empirical data and theoretical analysis to elucidate the factors contributing to differences in strength development and subsequent predictions.

5. Utilize the insights gained from the previous point to refine and enhance the prediction strategy for future projects.

By following this research plan, the thesis aims to provide a comprehensive understanding of undrained shear strength prediction using the SHANSEP framework, analyze its effectiveness in different projects, identify potential areas for improvement, and contribute to the advancement of prediction methodologies for future endeavors.

1.3. Data gathering and analysis

Each project provides a significant amount of CPTu data, which will be utilized to establish soil stratification combined with borehole data. CPTu- s_u correlations will be employed to determine the undrained shear strength during various project phases. Utilizing laboratory tests, SHANSEP parameters necessary for strength prediction can be obtained. The research places great emphasis on organizing and interpreting the data, with a comprehensive overview of the project data presented in table 1.1.

Table 1.1: Data overview

	Dike project (Netherlands)	Reclamation project (Philippines)
Subsoil	Clay, Peat	Marine Clay
Fill	-	Sand
<i>Before preload</i>		
Laboratory data	Triaxial tests, index tests	Triaxial, 1D consolidation, lab vane, index tests
Field data	Boreholes, CPTu	Field vane tests, CPTu, Boreholes
<i>During preload</i>		
Field data	CPTu, settlement plates, piezometers, extensometers	CPTu, settlement plates, piezometers, extensometers
<i>After preload removal</i>		
Laboratory data	DSS	-
Field data	CPTu	-

1.4. Reading Guide

Figure 1.1 illustrates the report's structure and captures the primary subjects addressed within each chapter.

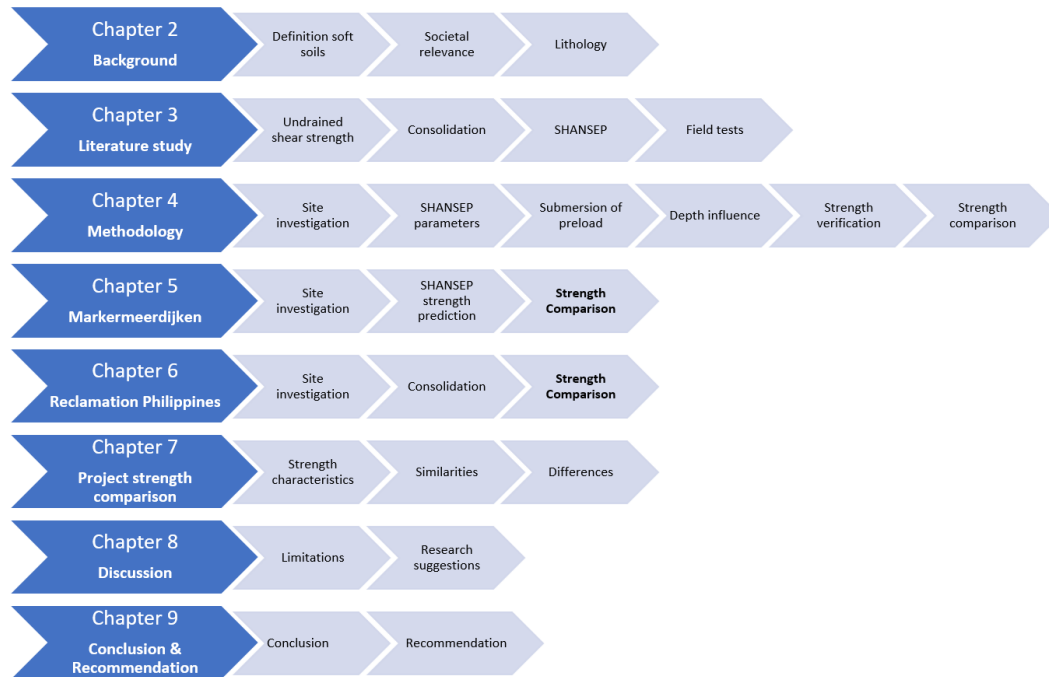


Figure 1.1: Reading guide report

Chapter 2 introduces the concept of soft soils, emphasizes the importance of undrained shear strength in society, and provides background information on the composition of the studied soils. Chapter 3 reviews existing literature about predicting strength, verifying strength, and consolidation. In Chapter 4, the methods employed to study the development of strength are explained, along with relevant examples. The findings of the research for the dike and reclamation projects are outlined in Chapters 5 and 6, respectively. Chapter 7 is dedicated to comparing these results. Chapter 8 critically discusses the limitations of the research and suggests potential directions for future studies. Finally, Chapter 9 summarizes the conclusions drawn and offers recommendations, particularly focusing on strength prediction.

2

Background

2.1. Soft soils

Soft soils refer to soil materials that possess usually low shear strength and high compressibility. Soft soils typically consist of fine-grained materials, such as silt, clay, and organic-rich material. The engineering properties of soft soils are influenced by various factors, including soil composition, mineralogy, void ratio, consolidation state, and pore water pressure. Soft soils may be found in various geological settings, such as coastal areas, river deltas, estuaries, and lacustrine deposits.

2.2. Societal relevance

Enhancing undrained shear strength prediction accuracy holds significant societal relevance for multiple reasons. Reclamation's and dikes rely on the stability and strength of the underlying soil. Accurate strength prediction is crucial for ensuring the safety of these structures in final and temporary construction phases.

Geotechnical failures can be extremely costly, resulting in significant financial losses and project delays. Enhancing strength prediction accuracy helps reduce the risks associated with uncertainties in the stability of the subsoil.

Accurate strength prediction enables engineers to optimize construction techniques and minimize the environmental impact of these activities. Optimization of preload steps will lead to a faster execution of dike reinforcement projects. Figure 2.1 shows the importance of an efficient execution: dike reinforcement projects can have a negative influence on quality of life for local inhabitants. A higher accuracy of strength prediction in reclamation projects allows for steeper slopes, reducing material use therefore environmental impact.

2.3. Lithology

Markermeerdijken

The soft soil layers under investigation at the Markermeerdijken field trials have their origins in the Holocene era and were deposited as a result of the rising sea levels (Technische Adviescommissie voor de Waterkeringen 1989). These layers were initially classified as the 'Calais formation' and 'Duinkerke formation' but were later renamed as 'Oude (Blauwe) Zeeklei' and 'Jonge Zeeklei'. Both layers are classified within the Naaldwijk formation.

The Calais formation, dating back 8000-4000 years, was deposited in a lacustrine environment resulting from the breach of coastal sand dunes by the North Sea, leading to the formation of lagoons. Within the Calais formation, the lower section is primarily composed of sand, while the upper part is predominantly comprised of clay. On the other hand, the Duinkerke formation, formed approximately 3000 years ago, is mainly characterized by sandy clay or clay. In certain locations, peat acts as a separation layer between the clay of the Calais formation and the clay of the Duinkerke formation.

To ensure practicality, this research will adopt the conventional terminology and refer to these clay lay-

ers using their traditional names.



Figure 2.1: Dike reinforcement: <https://www.gww-bouw.nl/artikel/markerveerdijken-van-zeedijk-tot-meerdijk/>

Philippines

The reclamation site rests on the Quaternary Diliman Tuff and Recent Deposits, including various sediment types like fluvial, lacustrine, paludal, and beach deposits. The Guadalupe-Diliman Plateau is underlain by the Diliman Tuff, while the Marikina Basin and coastal area sit on Recent alluvial deposits (Luna et al. 2020).

The Diliman Tuff comprises thick welded tuff and thinner tuffaceous sandstones, shales, and siltstones, with visible ancient soil layers. Recent deposits over the Diliman Tuff consist of loose sands, silts, and clay. These sedimentary deposits are thicker towards Manila Bay in the west and encounter the Diliman Tuff at shallow depths towards Quezon City in the east.

3

Literature study

This chapter focuses on the background of SHANSEP strength prediction and CPTu verification, which serve as the basis for the SHANSEP validation research. The outcomes of this validation study are discussed in detail in Chapter 5 and Chapter 6.

3.1. Undrained shear strength

Soft soils such as clay and peat are characterized by their low hydraulic conductivity. The rate at which these soils dissipate pore pressures is low relative to the rate of loading in construction projects. Pore pressures build up as water is unable to escape during loading. Undrained shear strength does not increase under relatively fast loading conditions since the load is transferred to the water in the soil rather than the soil skeleton, increasing pore pressure rather than effective stress. This principle is visualized in figure 3.1. An increase in normal stress does not result in additional shear strength. The undrained shear strength s_u is defined as half the difference between major principle stress σ_1 and minor principle stress σ_3 :

$$s_u = \frac{1}{2}(\sigma_1 - \sigma_3) \quad (3.1)$$

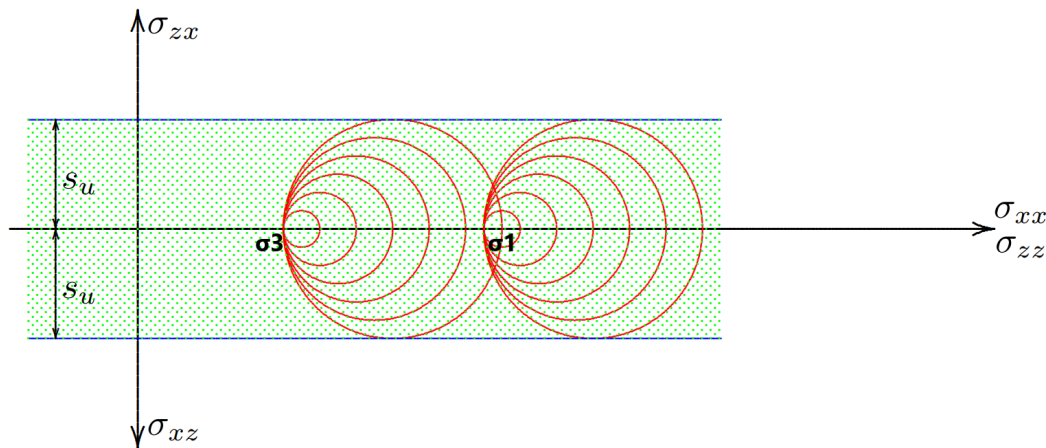


Figure 3.1: Mohr circle Unconsolidated Undrained triaxial tests (Verruijt 2017)

The pore pressure change Δu under total stress change must be known in case of loading a soft soil. The relation between stresses and pore pressure change was established by Skempton (1954) with pore pressure coefficients A and B :

$$\Delta u = B[\Delta\sigma_3 + A(\Delta\sigma_1 - \Delta\sigma_3)] \quad (3.2)$$

A and B are determined experimentally in undrained triaxial tests. Parameter B relates to the ratio between the compressibility of the pore fluid and the soil skeleton, defined by formula:

$$B = \frac{1}{1 + \frac{n\kappa_v}{\kappa_c}} \quad (3.3)$$

With n being the porosity, κ_v being the compressibility of the void fluid and κ_c the compressibility of the soil skeleton. In case of a saturated soil, the compressibility of the skeleton is very large compared to water. Consequently, $B = 1$ for a fully saturated soil. For a dry soil, $B = 0$.

Coefficient A is derived using triaxial tests. It indicates the effect of shear on pore pressure generation. In the case of a saturated soil, $B = 1$, the induced pore pressure is described by formula:

$$A = \frac{\Delta u - \Delta\sigma_3}{\Delta\sigma_1 - \Delta\sigma_3} = \frac{\Delta u}{\Delta\sigma_1} \quad (3.4)$$

Approximate Skempton A parameters for different types of clay are summarized in table 3.1.

Table 3.1: Typical Skempton A parameters

Type of Clay	A
Clays of high sensitivity	+0.75 to + 1.5
Normally consolidated clays	+0.5 to + 1
Compacted sandy clays	+0.25 to +0.75
Lightly over-consolidated clays	0 to +0.25
Compacted clay-gravels	-0.25 to +0.25
Heavily over-consolidated clays	-0.5 to 0

In case of a Normally Consolidated (NC) clay, shear causes the grain skeleton to compact. The compaction leading to volume decrease is prevented by the pore pressure, resulting in shear induced pore pressure. The effective stress path (ESP) curves away from the Total Stress Path (TSP) to the failure line due to the excess pore pressure, as can be seen in figure 3.2 (right). In case of an Highly Over Consolidated (HOC) clay, shearing leads to dilation due to the already dense particle arrangement. Volume expansions is prevented by the pore water, resulting in negative pore pressures. The negative pore pressure causes an increases in effective stress, the ESP curves towards the TSP as shown in figure 3.2 (left), therefore showing a higher strength.

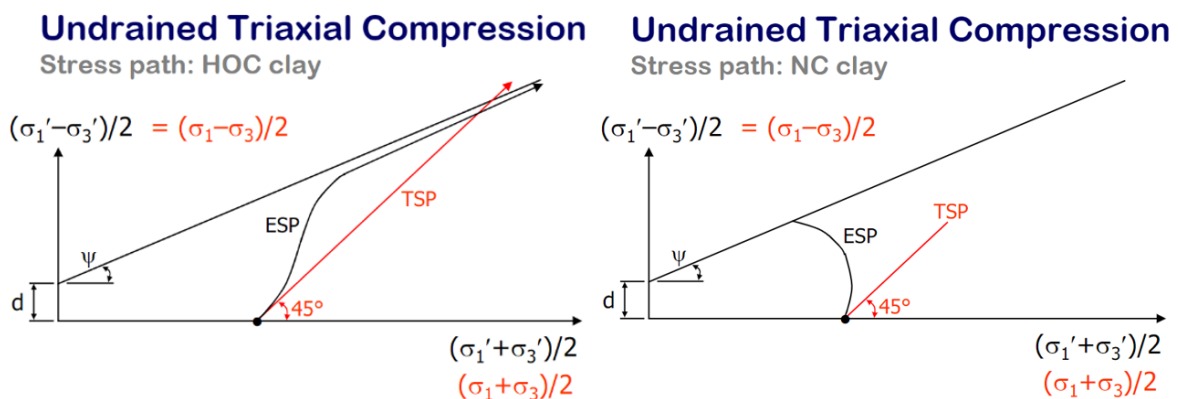


Figure 3.2: Stress paths HOC clay and NC clay

3.2. Consolidation

Time dependent settlement in saturated cohesive soils was described by Terzaghi and Peck (1948). In this 1D consolidation theory it is assumed that the soil is homogeneous, isotropic and saturated. Drainage is assumed to be vertical and water flow is one-dimensional. Under these assumptions, the relationship between degree of consolidation U and time t can be written as:

$$U = 1 - \sum_{m=0}^{m=\infty} \frac{2}{M^2} \exp(-M^2 T_v) \quad (3.5)$$

$$M = \frac{\pi}{2}(2m + 1) \quad (3.6)$$

$$T_v = \frac{C_v t}{h_d^2} \quad (3.7)$$

Where:

- h_d is the length of the drainage path
- T_v is the vertical dimensionless time factor
- C_v is the vertical coefficient of consolidation

The analytical solution of pore pressure relative to the load as function of normalized depth is shown in figure 3.3a. The degree of consolidation for the dimensionless time factor $\frac{c_v t}{h_d^2}$ is plotted in figure 3.3b.

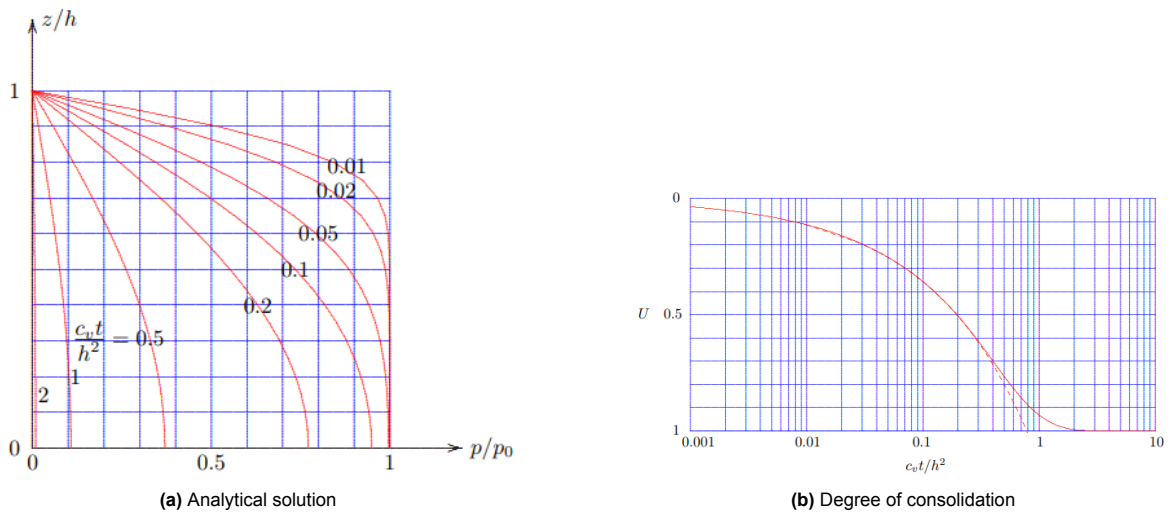


Figure 3.3: Consolidation solution (Verruijt 2017)

The radial consolidation theory Barron (1948) extends Terzaghi's one-dimensional consolidation theory to account for the radial flow of water in saturated soils during consolidation. This theory provides a more accurate representation of consolidation behavior in situations where the flow of water is not purely vertical, such as in embankments, earth dams, circular foundations and in case of using Prefabricated Vertical Drains (PVD's).

Barron's theory assumes that the soil is homogeneous, isotropic, and fully saturated. It also assumes that the consolidation process is axisymmetric, and the drainage occurs radially outward from a central point. The radial consolidation theory is often used when consolidation is improved by prefabricated vertical drains. The average degree of consolidation in the radial direction is formulated as:

$$U_h = 1 - \exp\left(\frac{-8}{F(n)} T_h\right) \quad (3.8)$$

with

$$T_h = \frac{c_h t}{D^2} \quad (3.9)$$

$$n = \frac{D}{d_w} \quad (3.10)$$

$$F(n) = \frac{n^2}{n^2 - 1} \ln(n) - \frac{3n^2 - 1}{4n^2} \quad (3.11)$$

Parameter d_w is the diameter of the drain, the radius of influence zone D depends on the grid pattern and drain spacing D_s , the value for a triangular grid and a square grid are respectively $D = 1.05D_s$ and $D = 1.13D_s$ as shown in figure 3.4.

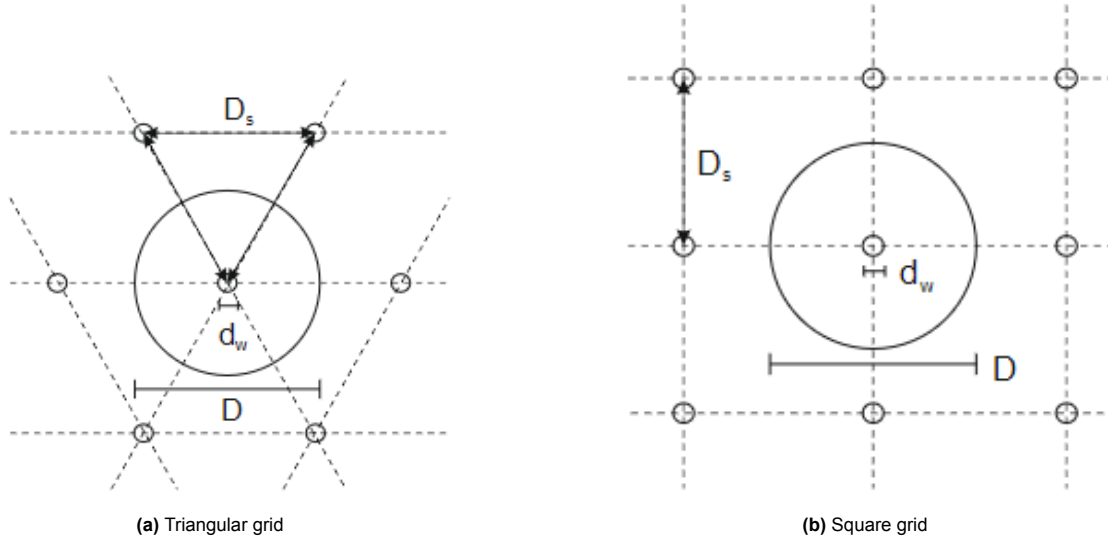


Figure 3.4: D_s for grid different PVD grid patterns

Conte and Troncone (2009) extended the equal strain relationship by Barron using Duhamel's theorem to calculate the consolidation of a loaded soil with PVD's. The excess pore pressure at time t at distance r from the drain due to a general time-dependent loading is defined as:

$$u_w(r, t) = X(r)Y(t) \quad (3.12)$$

With

$$X(r) = \frac{F_1}{R^2 F_0} \quad (3.13)$$

$$Y(t) = \frac{F_0}{F_0^2 + 4\zeta_r^2} \{ (A_k F_0 + 2B_k \zeta_r) [\cos(\omega t) - \exp(-2T_h/F_0)] + (B_k F_0 - 2A_k \zeta_r) \sin(\omega t) \} \quad (3.14)$$

$$\zeta_r = \frac{c_h}{wR^2} \quad (3.15)$$

$$T_h = \frac{c_h t}{R^2} \quad (3.16)$$

$$F_0 = \frac{N^2}{N^2 - 1} \ln(N) - \frac{3N^2 - 1}{4N^2} \quad (3.17)$$

$$F_1 = R^2 \ln\left(\frac{r}{r_d} - \frac{r^2 - r_d^2}{2}\right) \quad (3.18)$$

N is the ratio between the distance from the drain and the diameter of the drain ($N = R/r_d$). A_k and B_k are Fourier parameters which describe the general time dependent loading. This solution shows excellent agreement with solutions by Barron (1948) and Olson (1977), see figure 3.5 and figure 3.6. The solution is capable to consider smear effects by introducing factors F_3 and F_4 .

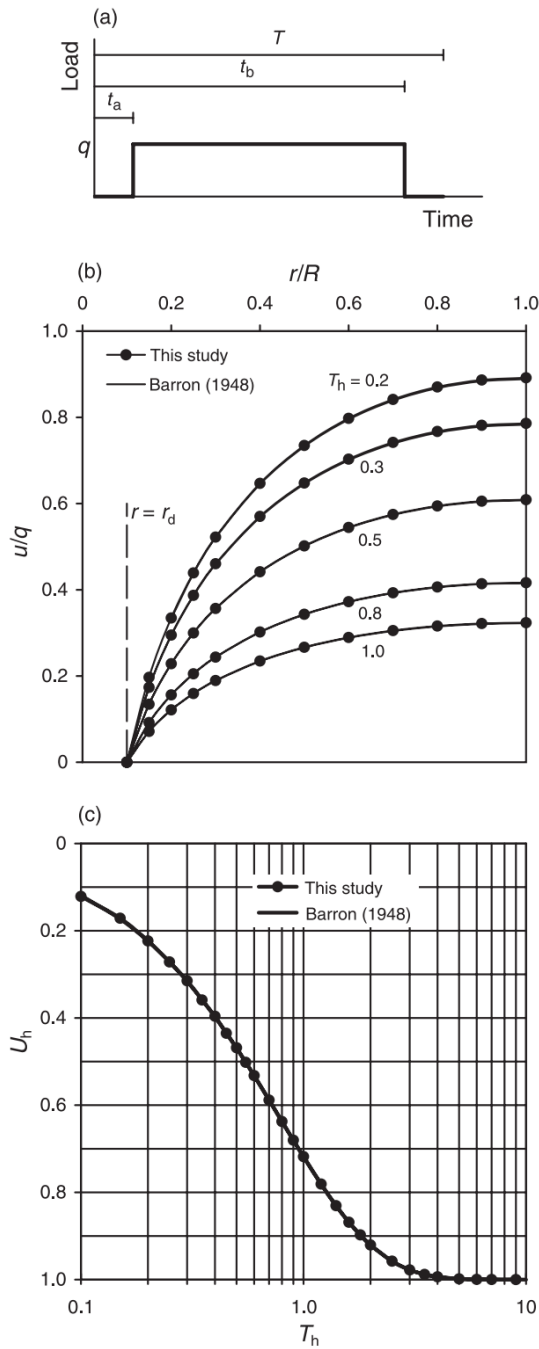


Figure 3.5: Comparison of the Conte and Troncone (2009) solution with Barron (1948): (a) loading used in present solution; (b) radial profiles of excess pore pressure, u , for different values of time factor, T_h ; (c) degree of consolidation vs. time factor T_h

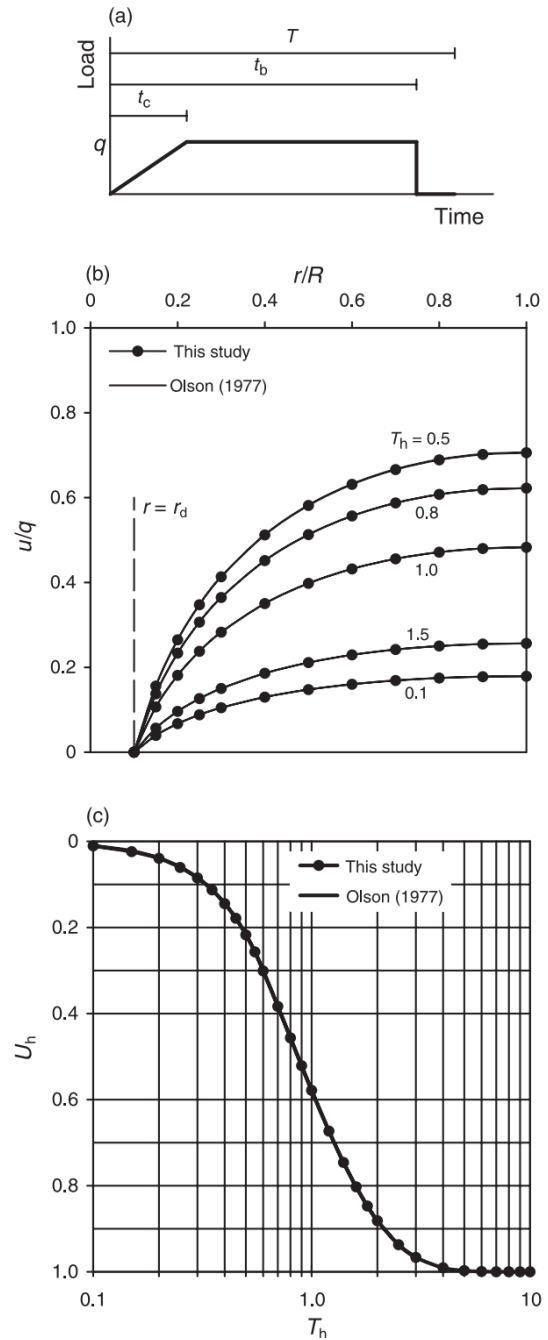


Figure 3.6: Comparison of the Conte and Troncone (2009) solution with Olson (1977): (a) loading used in present solution; (b) radial profiles of excess pore pressure, u , for different values of time factor, T_h ; (c) degree of consolidation vs. time factor T_h

The consolidation process is often induced by the application of a preload. The effect of the preload reduces over depth, as the preload induced stress distributes. Stress distribution is important to consider especially in cases where the area of the preload is relatively small compared to the depth where consolidation of the soil is required. Poulos and Davis (1964) extensively investigated the weight distribution of embankments over depth. The portion of the embankment weight increasing stress at depth z , under the center of an embankment, is described by influence factor I . The influence factor is dependent on the length of the crest of the embankment defined by parameter b , the length of the slope of the embankment defined by parameter a , and the depth under the embankment z . Figure 5.9 can be

used to determine the influence factor I . The stress increase $\Delta\sigma_v$ can be computed with the formula:

$$\Delta\sigma_v = 2I * \gamma_{emb} * h_{emb} \tag{3.19}$$

where γ_{emb} is the unit weight of the embankment material and h_{emb} the height of the embankment.

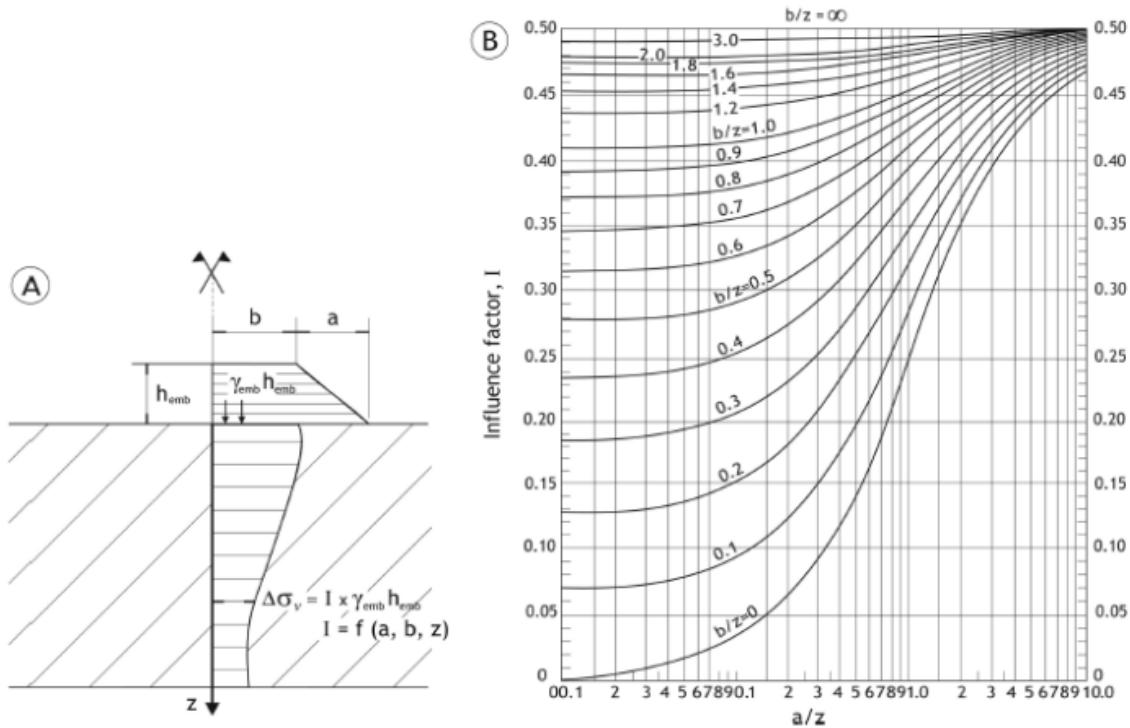


Figure 3.7: Depth influence of an embankment (Poulos and Davis 1964)

A solution for stresses and strains in a linear elastic homogeneous half space, loaded by a vertical point force was obtained by Boussinesq in 1885. The assumption of linear elastic material implies that superposition can be applied. An example of this is a case of a uniform load p applied over a circular area with radius r , as described by Goodier and Timoshenko (1970). The stress below the center of the load σ_{zz} was found to be:

$$\sigma_{zz} = p \left(1 - \frac{z^3}{s^3} \right) \tag{3.20}$$

with

$$s = \sqrt{z^2 + r^2} \tag{3.21}$$

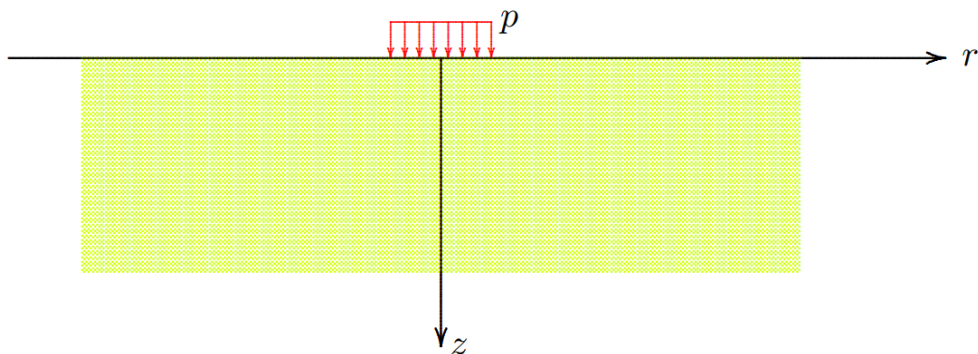


Figure 3.8: Circular uniform load (Verruijt 2017)

3.3. SHANSEP

Ladd and Foott (1974) summarized that undrained shear strength obtained from testing is affected by sample disturbance, stress-strain anisotropy, strain-rate effects and normalized behaviour.

Sample disturbance occurs as a sample is recovered from deep in the ground. The prevention of swelling induces negative pore pressures. Disturbance typically leads to a 20% to 50% lower undrained shear strength in the lab, compared to a perfect sample.

Stress-strain anisotropy can be divided into inherent anisotropy due to difference in soil structure occurred during the formation and stress induced anisotropy resulting from rotation of principal stresses. The effect of anisotropy can be modelled by a stress system that represents in situ conditions.

Figure 3.9 demonstrates the stress system along a typical failure surface including the major principle stress direction. Table 3.2 demonstrates the obtained ratio between vertical stress and undrained shear strength for various tests representing different stress systems. The tests were performed on Boston Blue Clay, a sensitive marine clay.

Table 3.2: Undrained strength anisotropy of NC Boston Blue clay (Ladd and Foott 1974)

Type of Test (1)	$s_u/\bar{\sigma}_{vc}$ (2)	γ_f , as a percentage ^a (3)	s_u/s_u (TC) (4)
CK_oU Plane strain active (PSA)	0.34	0.8	1.03
CK_oU Triaxial compression (TC)	0.33	0.5	1.00
CK_oU Direct-simple shear (DSS)	0.20	6	0.61
CK_oU Plane-strain passive (PSP)	0.19	8.5	0.57
CK_oU Triaxial extension (TE)	0.155	15	0.47

^a γ_f = shear strain at failure.

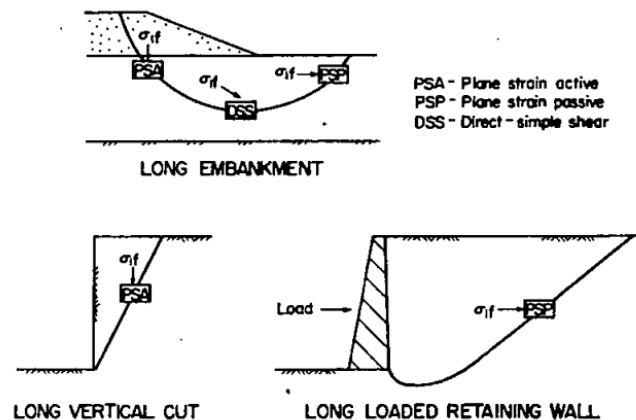


Figure 3.9: Stress systems for typical in situ modes of failure (Ladd and Foott 1974)

The ratio between vertical stress and undrained shear differs for different stress systems, as displayed in table 3.2. Ladd and DeGroot (2003) summarized that the difference in strength ratio can be described by two variables:

- The relative magnitude of intermediate principal stress, defined by parameters b :

$$b = (\sigma_2 - \sigma_3)/(\sigma_1 - \sigma_3) \quad (3.22)$$

- The angle δ between the direction of the applied major principal stress at failure relative to vertical deposition direction.

Combinations of b and δ achievable through shear devices are depicted in Figure 3.10. Figure 3.11 illustrates the peak undrained shear ratio as a function of the Plasticity Index (PI) for Triaxial Compression (TC), Direct Simple Shear (DSS), and Triaxial Extension (TE) tests. The TC test ratio exhibits little correlation with PI, while the DSS test ratio increases with higher PI values. The increase is even more pronounced for TE tests.

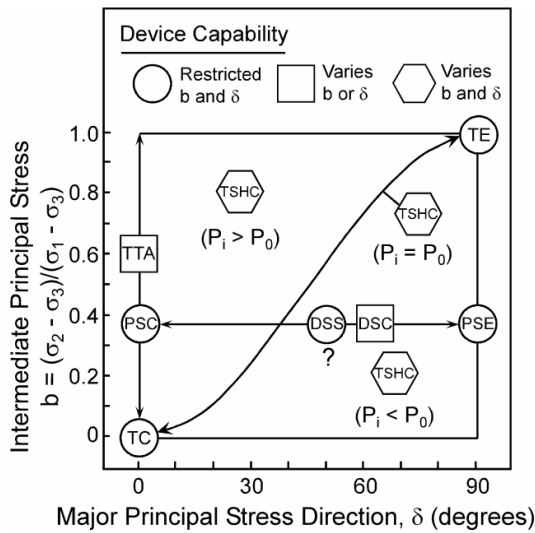


Figure 3.10: Shear devices and their stress systems for CK₀U testing (Ladd 1991)

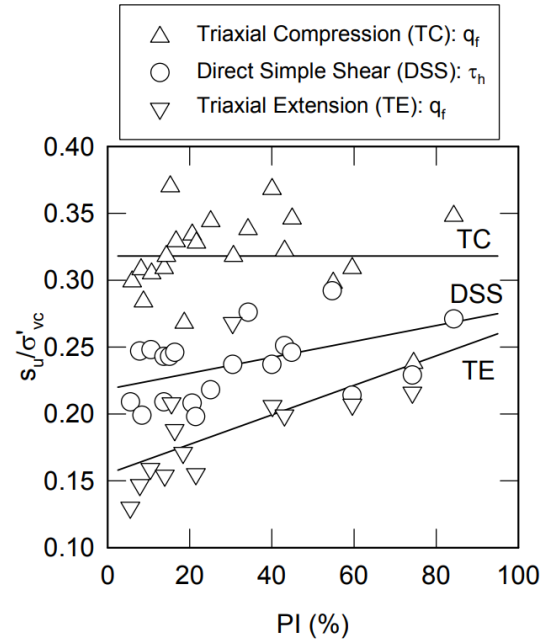


Figure 3.11: Undrained Strength Anisotropy from CK₀U Tests on Normally Consolidated Clay and Silt (Ladd 1991)

Strain rate influences the undrained shear strength as a result of creep. The lower the strain rate, the more time for creep to generate additional pore pressure, lowering the effective stress and therefore the undrained shear strength. Sheahan et al. (1996) studied the strength ratio under different axial strain rates $\dot{\epsilon}$ for different OCR values, by performing several CK₀UC tests on Boston Blue clay. Based on the results, the graph as depicted in figure 3.12 was made. This figure displays the strain rate of shearing and its effect on the strength ratio relative to CK₀U tests for various soil investigation methods and field loading conditions.

- CPTu, and lab strength index tests yield up to 50% higher strength ratio due to its extremely fast shearing (≈ 5 sec)
- The rate of shearing in Field Vane Tests (≈ 5 min) increases strength ratio by approximately 15%
- The low rate of shearing as possibly occurs in the field (≈ 2 weeks), reduces the strength ratio by 10%

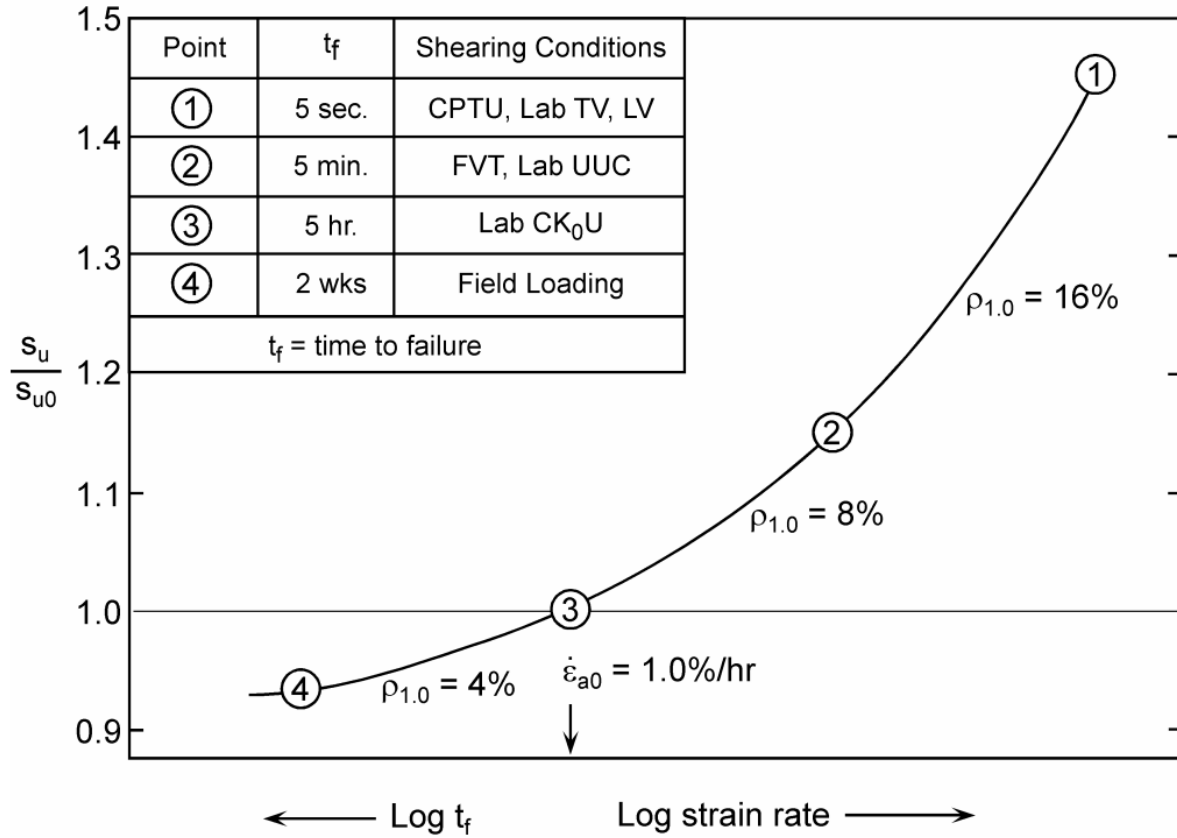


Figure 3.12: Shearing conditions and its effect on the undrained shear strength ratio (Ladd and DeGroot 2003)

Ladd and Foott (1974) proposed to a method to reduce the effect of sample disturbance and anisotropy on undrained shear strength in lab testing. The following steps should be followed:

1. Divide the soil profile into layers based on site investigation data.
2. Obtain good undisturbed samples, check whether the soil shows normalized behavior. Select samples and determine preconsolidation stress (σ'_{pc}).
3. Determine which laboratory tests resemble the in situ stress state.
4. Tests the shear strength of the samples. The ratio between preconsolidation stress and undrained shear strength should be reasonably constant in order to use SHANSEP. This ratio is the SHANSEP S parameter.
5. Consolidate the sample to 1.5, 2.5 and 4.0 times the preconsolidation stress. The sample is consolidated along the K_0 stress path to replicate condition in the field.
6. Unload the sample to known OCR's. Perform undrained shear tests and plot $\log(s_u/\sigma'_{v0})$ on the y-axis and $\log(\text{OCR})$ on the x-axis. SHANSEP parameter m is the slope of the line, SHANSEP parameter S the offset at $\text{OCR}=1$.

The undrained shear strength can be predicted using equation 3.23 and is valid for uniform saturated soils:

$$\frac{s_u}{\sigma'_{v0}} = S \cdot \text{OCR}^m = S \left(\frac{\sigma'_{pc}}{\sigma'_{v0}} \right)^m \quad (3.23)$$

Where σ'_{v0} is the in situ vertical stress, σ'_{pc} is the maximum preconsolidation stress, S is the ratio of $\left(\frac{s_u}{\sigma'_{v0}} \right)$. Exponent m is based on the "Critical state" concept:

$$m = 1 - \left(\frac{C_s}{C_c} \right) \quad (3.24)$$

With C_s being the slope of the swelling line and C_c being the slope of the virgin compression line in a 1D compression test.

The limitation of the SHANSEP procedure is that the method can only be applied in regular deposits with a well known stress history. Another limitation of the SHANSEP framework is the possibility that the consolidation beyond the preconsolidation stress destroys the structure of the soil, this is the case for cemented clay and sensitive quick clay.

De Koning et al. (2019) investigated the SHANSEP S parameter through a series of experiments. They conducted 102 static CAU triaxial tests on (silty)clay and 62 Direct Simple Shear tests on peat under in situ stress conditions, and with an OCR of 1. The samples were collected from a dike located between Krimpen aan den IJssel and Gouderak in the Netherlands. The strength ratio for clay was determined at an axial strain of 25%, while for peat, it was determined at a radial strain of 40%. The undrained shear strength corresponding to the effective vertical stress was plotted in Figure 3.13. To determine the SHANSEP m parameter, the researchers conducted and interpreted 160 oedometer tests. The values for SHANSEP S and m can be found in Table 3.3.

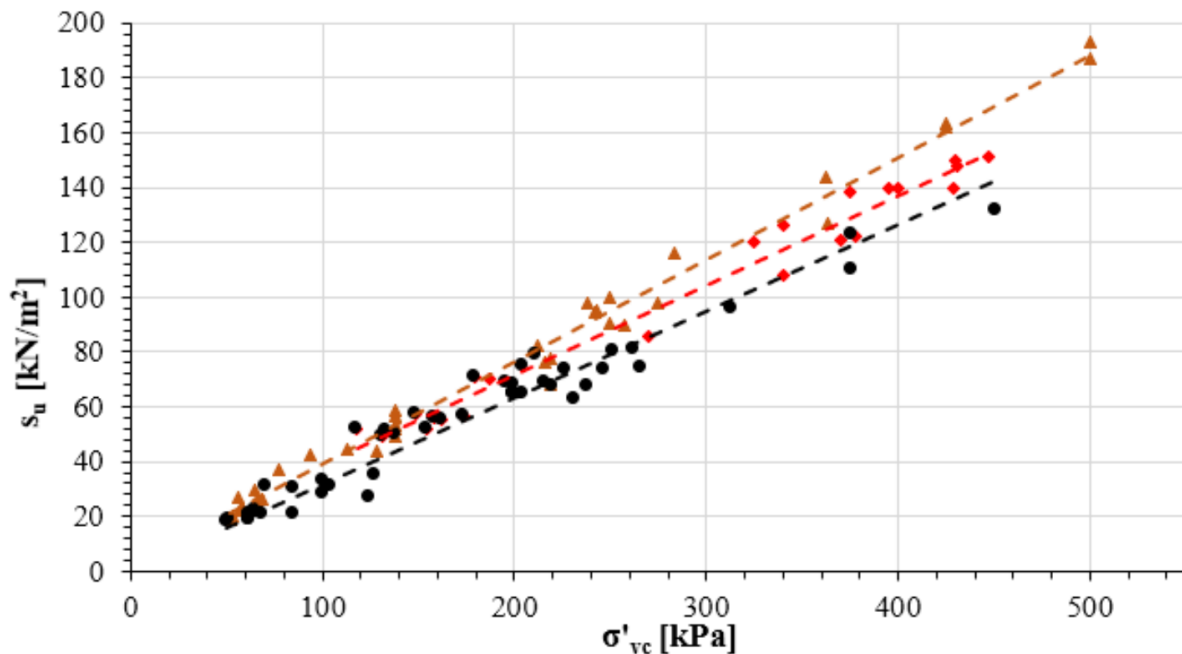


Figure 3.13: Undrained shear strength vs. effective stress (De Koning et al. 2019)

Table 3.3: SHANSEP S and SHANSEP m factor based on laboratory testing (De Koning et al. 2019)

Soil type	μS	σ_S	μm	σm
Clay	0.32	0.02	0.88	0.01
Dikes-material	0.37	0.02	0.88	0.02
Peat	0.39	0.02	0.85	0.02

Yang et al. (2019) collected data from several (marine) sites that were studied by the Norwegian Geotechnical Institute and summarized the parameters in table 3.4. The SHANSEP S parameter, here mentioned as strength ratio, was determined by performing triaxial compression tests on the clay samples. For triaxial compression, a SHANSEP S value ranging between 0.26 to 0.31 was found except for two clay types, which led to a strength ratio of 0.18 and 0.19. Most SHANSEP m parameters lie between 0.7 and 0.8. Higher values up to 0.98 are also possible, those generally seem to have a higher water content.

Table 3.4: Summary of SHANSEP and soil parameters (Yang et al. 2019)

Site	water content %	plastic limit %	Liquid limit %	Plasticity index %	Liquidity index -	Clay content %	Sensitivity -	OCR -	m -	strength ratio at OCR=1 -	Source, reference
Tangawizi	36	27.9	69.9	42.0	0.2	55.0		1.1	0.80	0.29	
Egypt	100	46.1	109.3	63.2	1.2	56.0	4.2	1.3	0.96	0.27	
Egypt	110	43.8	87.5	50.0	1.3	67.7	6.2	1.3	0.87	0.28	
	102	28.8	89.8	61.0	1.2	41.0	4.0	1.2	0.89	0.35	
Shah Deniz	104	30.0	90.0	60.0	1.2	40.0	4.0	1.2	0.98	0.30	
	65	27.3	68.1	40.7	0.9	58.2	3.3	1.5	0.75	0.32	NGI project
	41	28.3	76.3	40.0	0.3	59.8	2.0	1.1	0.75	0.31	
Norwegian Sea	54	27.8	70.0	42.2	0.6	51.1	4.0	1.2	0.77	0.31	
Onsoy	66	27.2	69.9	42.7	0.9	50-65		1.3	0.75	0.31	
Lierstranda	34	21.3	39.9	18.6	0.7	33.0			0.74	0.30	
				12-25		30-40			0.70	0.32	
Ormen Lange				>25		45-65			0.70	0.28	
Bonneville	58-67	23-26	36-47	10-23.5		34-38			0.82	0.32	Bay, et al., 2005
Bangkok	68.0	24.0	65.0	41.0	1.1				0.74	0.27	Seah and Lai, 2003
Klang	66-107	30-45	75-95	41-60					0.78	0.26	Amin et al., 1997
	38-40	20-24	40-47	20-24	0.7-0.9	48-57			0.71-0.77	0.28-0.33	Abdulhadi et al., 2012
Boston											
Connecticut		30	45	15	>1				0.73	0.18	Degroot, 1999
Boston		25	45	20					0.75	0.19	Degroot, 1999

The OCR plays a prominent role in the undrained shear strength, as is described by equation 3.23. Jamiolkowski (1985) described 4 mechanism that cause overconsolidation in clay deposits:

1. Mechanical overconsolidation, due to overburden removal or a lowering of the ground water table. This results in a constant Pre Overburden Pressure (POP) over depth.
2. Desiccation due to evaporation or freezing. Usually the preconsolidation pressure decreases with depth.
3. Aging, due to creep
4. Physico-chemical, due to cementation. This results in a variable preconsolidation stress over depth.

Mechanism 1 is generally exploited to artificially increase the strength of the subsoil: a preload is applied and later removed to mechanically overconsolidate the subsoil. This process automatically activates mechanism 3, as the preload increases the creep rate. The effect of creep on the OCR can be described by for instance the Isotach model by Den Haan and Edil (1994).

Bjerrum (1967) described a system in the form of Figure 3.14, illustrating a compression curve during sedimentation. At a certain point, the sedimentation process halts, but settlement continues due to creep, referred to as delayed compression. As time progresses, the rate of creep strain slows down, as predicted by equation 3.25. The creep strain between 3 years and 30 years in figure 3.14 is identical to the strain between 30 years and 300 years. However, it takes 10 times longer to reach the same amount of strain in the latter case. This pattern persists for the strain developed between 300 years and 3000 years, and so on.

The lines representing ages, such as 3 years, 30 years, etc., run parallel to the instant compression line. Regardless of the stress level applied to the load, after 3 years of creep, the combination of strain and $\log(\sigma'_v)$ falls precisely on the 3-year line. The same holds true for the 30-year, 300-year, and 3000-year lines. These age lines also indicate constant strain rates. This relationship stems from the time derivative of equation 3.25:

$$\frac{d\epsilon}{d\tau} = \frac{d}{d\tau} \left(C_\alpha \log \left(\frac{\tau_2}{\tau_1} \right) \right) = \frac{C_\alpha}{\ln(10)} \frac{\tau_1}{\tau_2} = \frac{C_\alpha}{2.3\tau} \quad (3.25)$$

where τ_1 is the time when creep starts and τ_2 the age.

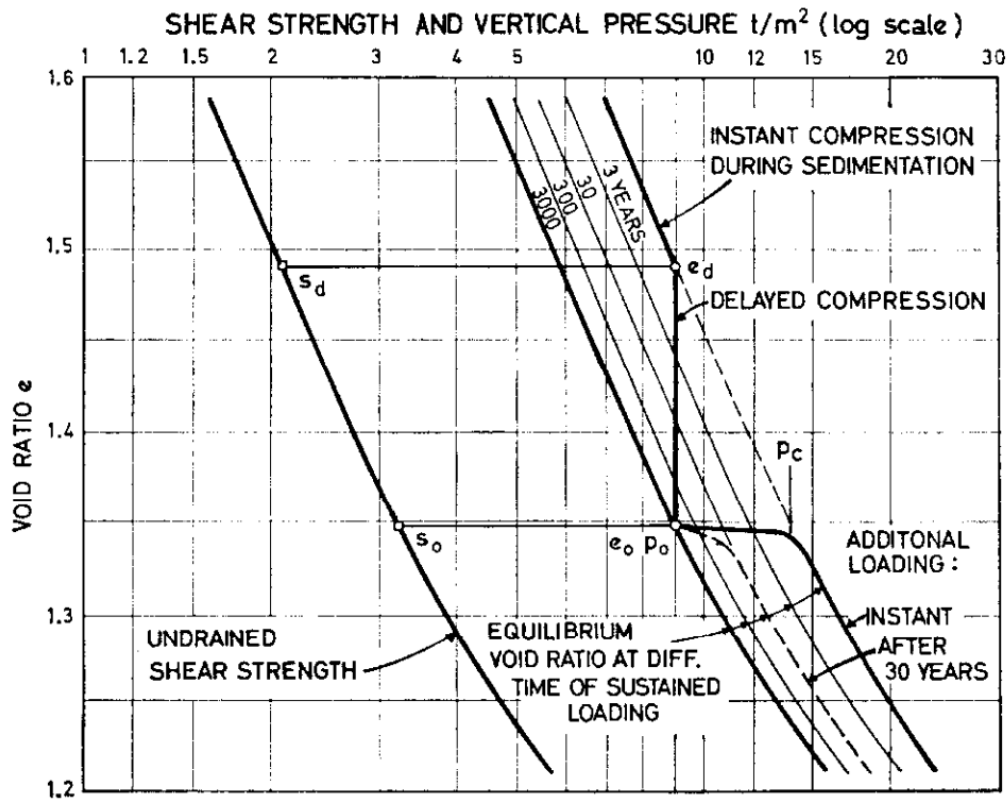


Figure 3.14: Instant and delayed compression (Bjerrum 1967)

There is thus a difference between the time scale for the rate at which creep develops and for the time the construction or a laboratory test ($t = 0$) started. Den Haan and Edil (1994) introduced the intrinsic time τ of a soil, characterizing the isotach of a soil, which describes the stress-strain and strain rate conditions of the soil. In Figure 3.15, point a corresponds to an intrinsic time of 1 day, while point b corresponds to an intrinsic time of 100 days, and so on.

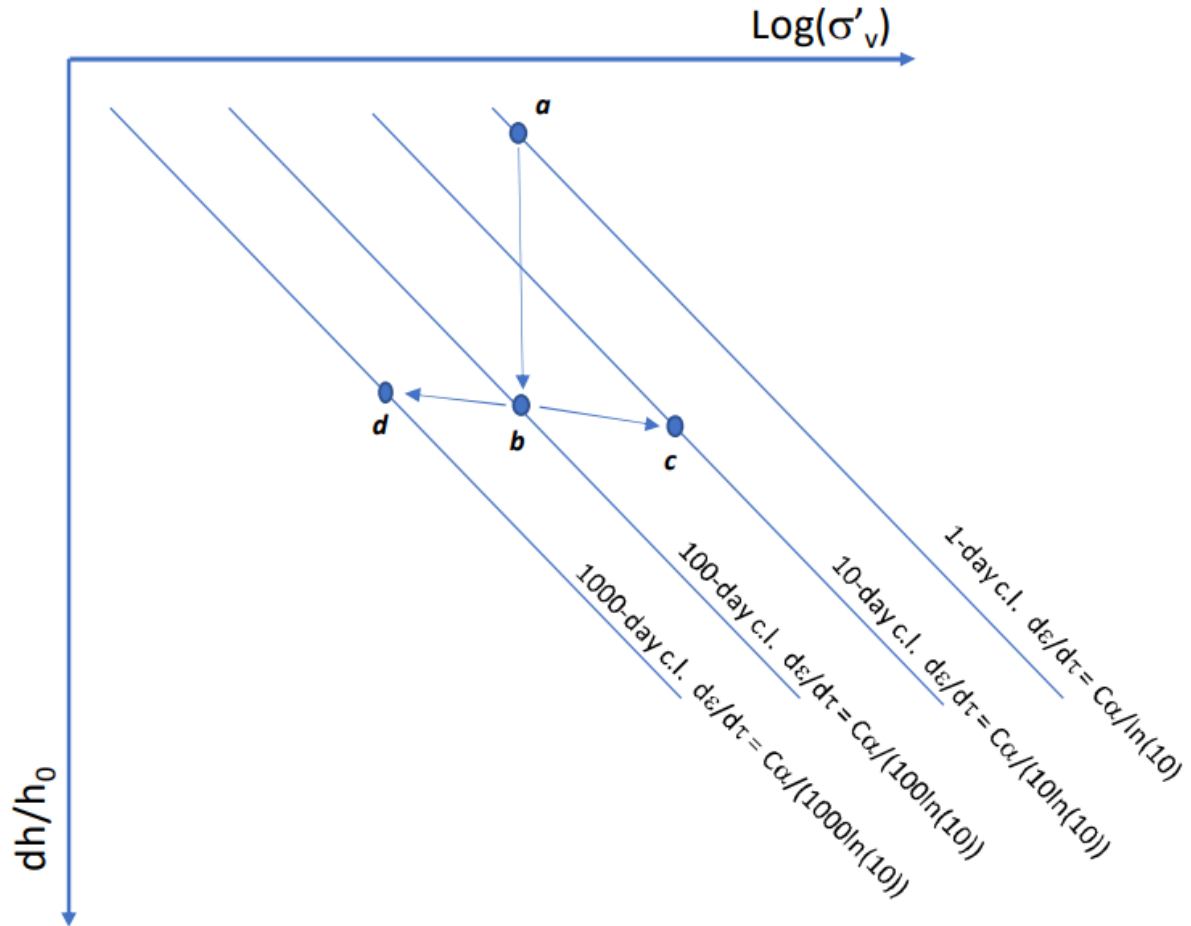


Figure 3.15: Creep strain and intrinsic time due to (un)loading

The intrinsic time prior to loading can be obtain using equation: 3.26.

$$\tau = \tau_0 \left(\frac{\sigma'_{vy}}{\sigma'_v} \right)^{\frac{CR-RR}{C_\alpha}} = \tau_0 OCR^{m_{isotach}} \quad (3.26)$$

In which τ_0 is the 1-day reference isotach, CR is the Compression Ratio, RR the Recompression ratio, C_α the Creep index and OCR the overconsolidation ratio. The new intrinsic time after a load has been applied can be calculated by the formula:

$$\tau_{i+1} = \tau_i \left(\frac{\sigma'_{v,i+1}}{\sigma'_{v,1}} \right)^{m_{isotach}} \quad (3.27)$$

Where τ_{i+1} is the new intrinsic time, τ_i is the duration of the load, $\sigma'_{v,i+1}$ the new vertical effective stress due to the loading step and $\sigma'_{v,1}$ the old vertical effective stress.

3.4. Field test

Karlsrud et al. (2005) analyzed a large data set of lab and CPTu tests results for multiple clay samples. The undrained shear strength is in practise often related to the corrected cone resistance q_t rather than the directly measured cone resistance q_c . The cone resistance is corrected to account for the difference in area of the cone and the cone rod. The corrected cone resistance is defined as:

$$q_t = q_c + u_2(1 - a) \quad (3.28)$$

where u_2 is the pore pressure measured just behind the neck of the cone and a is the ratio of the area of the central part of the cone over the gross area of the cone. The undrained shear strength is measured

via the normalized expression:

$$s_u = \frac{q_t - \sigma_{v0}}{N_{kt}} \quad (3.29)$$

with q_t being the corrected cone resistance, N_{kt} the cone factor and σ_{v0} the total vertical stress.

A large amount of research on N_{kt} values is performed, Rémai (2013) summarized ranges of N_{kt} values obtained from several researches. Most of the researches used the triaxial compression tests as reference tests. The results are displayed in table 3.5.

Table 3.5: Values for N_{kt} (Rémai 2013)

N_{kt} value range	Reference test	Comments	Reference
8-16	triaxial compression, triaxial extension and direct shear	For clays ($3\% < I_p < 50\%$) N_{kt} increases with I_p	Aas et al. (1986)
11-18		Found no correlation between N_{kt} and I_p	La Rochelle et al. (1988)
8-29	Triaxial compression	N_{kt} varies with OCR	Rad and Lunne (1988)
10-20	Triaxial compression		Powell and Quarterman (1988)
6-15	Triaxial compression	N_{kt} decreases with B_q	Karlsrud (1996)
7-20	Triaxial compression	Busan clay, Korea $25\% < I_p < 40\%$	Hong et al. (2010)
4-16	Vane shear	High plasticity, soft clay, $42\% < I_p < 400\%$	Almeida et al. (2010)

Sandven (2010) presented the state-of-the-art on CPTu equipment and test procedures. Four application classes are introduced in which performance depends on test type and geological conditions, see table 3.6. According to this table, class 1 can not be obtained when denser layers are present even in case of predrilling through the dense layer. The allowable minimum accuracy of measured parameters in CPTu's are presented in table 3.7. Here the lower limit is defined for small values, a percentage is defined for the higher values.

Table 3.6: Application classes and general requirements in EN-ISO 22476-1.

Application class	Test type	Soil conditions	Application
1	TE2: $q_c, u_2, f_s + i$	Soft soils. Stratified deposits should be avoided.	Only CPTU is performed. Interpretation of parameters possible.
2	TE1: $q_c, f_s + i$ TE2: $q_c, u_2, f_s + i$	Layered deposits with both soft and stiff soils.	Interpretation in stiff soils possible, indicative interpretation in soft soils.
3	TE1: $q_c, f_s + I$ TE2: $q_c, u_2, f_s + i$	Layered deposits with both soft and stiff soils.	Soil profiling. Interpretation in very stiff soils possible, indicative interpretation in stiff soils.
4	TE1: q_c, f_s	Layered deposits with both soft and stiff soils.	Indicative profiling in all soils. No parameter interpretation.

Table 3.7: CPTu Application classes with allowable minimum accuracy in EN-ISO 22476-1.

Application class	Test type	Measured Parameter	Allowable minimum accuracy	Maximum measurement interval	Use			
					Soil	Interpretation		
1	TE2	Cone resistance	35 kPa or 5 %	20 mm	A	G, H		
		Sleeve friction	5 kPa or 10%					
		Pore pressure	10 kPa or 2 %					
		Inclination	2°					
		Penetration length	0.1 m or 1%					
2	TE1	Cone resistance	100 kPa	20 mm	A	G, H*		
	TE2	Sleeve friction	15 kPa or 15%				B	G, H
		Pore pressure	25 kPa or 3%				C	G, H
		Inclination	2°				D	G, H
		Penetration length	0.1 m or 1%					
3	TE1	Cone resistance	200 kPa or 5%	50 mm	A	G		
	TE2	Sleeve friction	25 kPa or 5%				B	G, H*
		Pore pressure	50 kPa or 5%				C	G, H
		Inclination	5°				D	G, H
		Penetration length	0.2 m or 2%					
4	TE1	Cone resistance	500 kPa or 5%	50 mm	A	G*		
		Sleeve friction	50 kPa or 20%				B	G*
		Penetration length	0.2 m or 1%				C	G*
							D	G*

Soil classification:

- A: Homogenously bedded soils with very soft to stiff clays and silts ($q_c < 3$ MPa)
 B: Mixed bedded soils with very soft to stiff clays (1.5 MPa $< q_c < 3$ MPa) and medium dense sands (5 MPa $< q_c < 10$ MPa)
 C: Mixed bedded soils with stiff clays ($q_c < 3$ MPa) and very dense sands ($q_c > 10$ MPa)
 D: Very stiff to hard clays ($q_c < 3$ MPa) and very dense coarse soils ($q_c > 20$ MPa)

Use:

- G: Profiling and material identification with low uncertainty level
 G*: Indicative profiling and material identification with high uncertainty level
 H: Interpretation in terms of design with low uncertainty level
 H*: Indicative interpretation in terms of design with high uncertainty level

The main factors influencing test accuracy in CPTu testing are:

1. Choice of equipment for in situ soil conditions: the cone should have sufficient capacity to penetrate the softer and stiffer layers. A high capacity probe shouldn't be applied to soft soils as the cone is not able to make accurate measurements. A low capacity cone should not be used in dense soils since the transducer could be overloaded and damaged.
2. Probe geometry and tolerances: the geometry of the probe should be checked since wear changes the geometry, therefore the measured parameters.
3. Temperature influence and zero shift: the zero values of the transducers should be read before and after the test. The cone temperature should be stable. The zero shift gives an indication of the calibration of the cone. Permanent zero shifts can be caused by dense layers, stones and damage.
4. Saturation of the pore pressure system: all components of the cone should be saturated with water. Lack of saturation is caused by improper saturation procedures or passing through unsaturated zones
5. Maintenance: CPTu cones should be cleaned after used. The cone should be checked for damages and the parts should be lubricated. Other accessories such as rods and the acquisition system should be checked.

Extra care should be taken in case of gas or air pockets in the soil. Entrapped pockets may lead to sluggish pore pressure response. Penetration pore pressure do not reach full magnitude especially at small depths.

Lunne et al. (1986) stated that sleeve friction is considered by many as the most inaccurate parameter measured by a CPTu. The pore pressure acting on both ends of the sleeves influences the recorded friction. The difference in area between both sides has to be corrected for, this correction is often inaccurate since pore pressure are usually not measured on both locations (u_2 and u_3). Caution is required using correlations with this parameter.

To overcome the problem of inaccurate measurements of the sleeve friction, classification charts based on pore pressure ratio were proposed by K. Senneset (1954). Pore pressure parameter B_q is defined as:

$$B_q = \frac{u_2 - u_0}{q_c - \sigma_{v0}} \tag{3.30}$$

where u_2 is the pore pressure measured at the neck of the cone, u_0 the equilibrium pore pressure, q_c the cone resistance and σ_{v0} the total overburden stress. The equilibrium pore pressure is the measured pore pressure by a CPTu after the pore pressure caused by the penetration of the cone has been dissipated. Later it was generally agreed that the cone resistance should be replaced by the corrected cone resistance. Robertson (1986) defined a system that includes q_t , B_q and R_f in the form of figure 3.16.

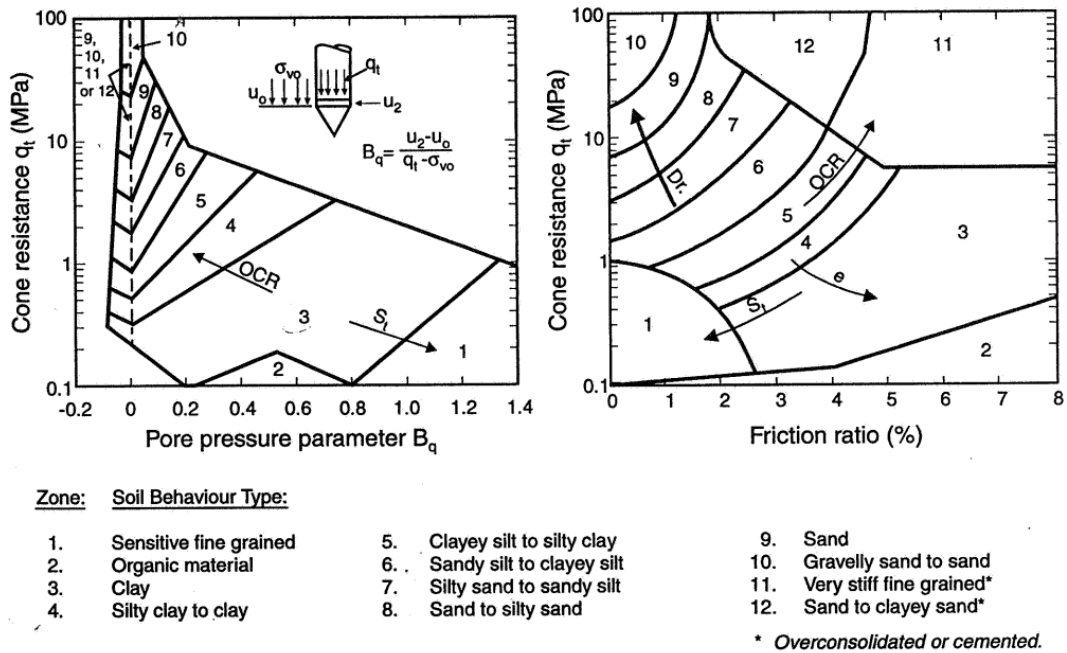


Figure 3.16: Soil behaviour type classification system from CPTu data

R. Larsson and Åhnberg (2005) discussed the assessment of undrained shear strength and preconsolidation pressure, using commonly conducted field tests in clay soils. Field Vane Tests (FVT) are commonly calibrated to load tests and full scale failures by the relationship (R. Larsson, Bergdahl, et al. 1984):

$$s_u = \tau_v \left(\frac{0.43}{LL} \right)^{0.45} \tag{3.31}$$

with s_u being the corrected undrained shear strength, τ_v the uncorrected FVT shear strength and LL the liquid limit. For over consolidated soils, an extra correction is required to match FVT results with those obtained from advanced lab tests. This correction is based on empirical data:

$$\mu_{OCR} = OCR^{-0.15} \tag{3.32}$$

This correction factor is valid for soil with an OCR of approximate 1.3. The corrected shear strength for FVT's in over consolidated soils can be written as:

$$c_u = \tau_v \left(\frac{0.43}{LL} \right)^{0.45} \left(\frac{OCR}{1.3} \right)^{-0.15} \quad (3.33)$$

4

Methodology

4.1. Site Investigation

The research on undrained shear strength of the subsoil for the field trials at Markermeerdijken and for the field trial at the Philippines reclamation starts with collecting data from laboratory tests and field tests. Boreholes, index tests and CPTu's are used to construct a soil profile with adjacent soil layers. The properties of those layers are determined by laboratory tests on borehole samples.

4.2. SHANSEP

The SHANSEP framework will be used to predict the in situ strength, strength during surcharge and if applicable and strength after surcharge removal. This section describes how the SHANSEP parameters S , m , σ'_{v0} and σ'_{pc} will be obtained.

4.2.1. SHANSEP S

For the Markermeerdijken field trials, multiple sets of constant volume Direct Simple Shear (DSS) are performed in order to derive the SHANSEP S for clay Calais, clay Duinkerke and peat. A cylindrical undisturbed representative sample is placed inside the DSS apparatus, surrounded by a rubber membrane and laterally confined by a stack of metal rings. Subsequently, the sample is consolidated to a pressure substantially higher than the preconsolidation pressure. After the consolidation phase, the shearing phase can be initiated with a constant sample height. The variation in vertical load must be measured, from which the change in pore water pressure is derived. The SHANSEP S value will be determined for two clay types and a peat soil for the Markermeerdijken case study.

Full saturation is required to obtain consistent DSS tests results. The volumetric weight is plotted against the water content in figure 4.1. The water content based theoretical line of volumetric weight for a saturation (S_r) of 100% and a measured soil particle weight of 2530kg/m^3 is plotted. The test results of one outlier are not taken into account as the sample is likely to be unsaturated, this outlier is plotted in red.

Figure 4.2 is one of the DSS used to obtain the SHANSEP S factor as further explained in section 5.2.5. For this research, peak values of the DSS tests are used for the determination of the SHANSEP S parameter. Tests leading to significant higher SHANSEP S values than average were discarded.

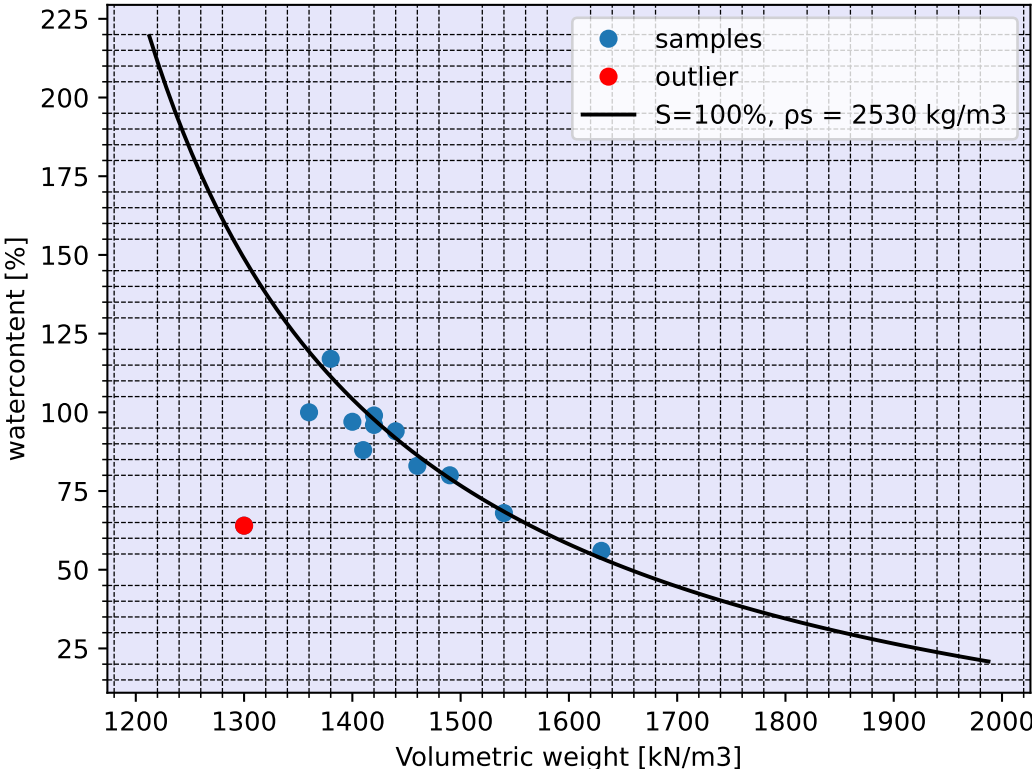


Figure 4.1: Relationship water content and volumetric weight

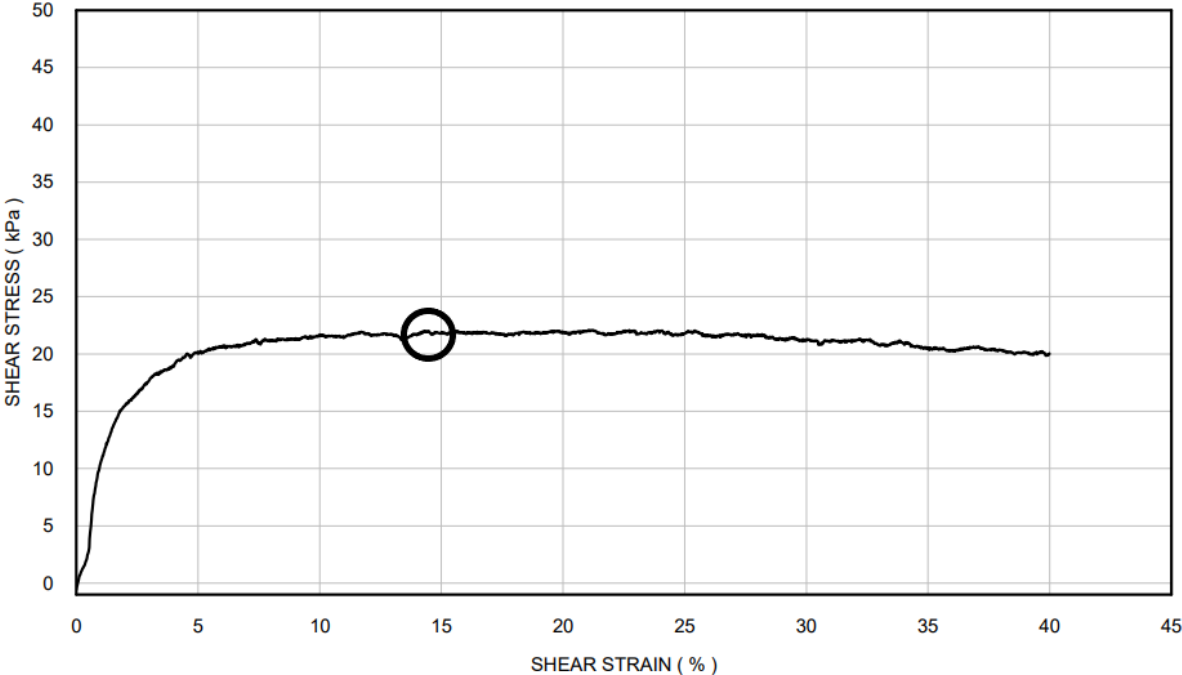


Figure 4.2: Direct Simple Shear test on clay

The SHANSEP S parameter for the Philippines case study is based on Field Vane (FV) tests, Unconsolidated Undrained (UU) triaxial tests and Laboratory Vane (LV) tests. The Field Vane test is corrected as proposed by R. Larsson and Åhnberg (2005):

$$s_u = \tau_v \left(\frac{0.43}{LL} \right)^{0.45} \left(\frac{OCR}{1.3} \right)^{-0.15} \quad (4.1)$$

More information regarding the laboratory tests can be found in section 6.2.3.

4.2.2. SHANSEP m parameter

In the context of the Markermeerdijken project, the SHANSEP m value for clay is determined based on 1D consolidation tests. The same is done for the SHANSEP m value for peat, which is determined through the execution of 10 1D consolidation tests. These tests involve measuring the compression ratio (CR), recompression ratio (RR) and creep index (C_α) of the peat samples.

To calculate the recompression ratio RR , the average of the swelling and reloading steps is taken. Subsequently, the SHANSEP m parameter is determined using equation 4.2 which results from the Cam-Clay theory:

$$m = \frac{CR - RR}{CR} \quad (4.2)$$

For the Philippines reclamation field trials, the SHANSEP m parameter is determined by the same equation 4.2, values of CR , RR and C_α can be found in appendix B.

4.2.3. In situ effective vertical stress

The effective stress is defined as portion of the total stress carried by the soil skeleton. The other portion of the total stress is carried by the pore water pressure. The effective stress can be formulated as followed:

$$\sigma'_{v0} = \sigma_{v0} - u \quad (4.3)$$

Here, σ_{v0} is the total vertical stress and u is the pore water pressure. The total stress is a summation of the weight of the soil above a certain point in depth. The bulk unit weight for each soil layer is required in order to compute the total stress profile. The bulk unit weight is determined by weighting samples and by deriving weight based on water content. The results of the investigation for the Markermeerdijken is displayed in appendix A, figure A.1. The sample is classified as peat for unit weights lower than 11kN/m^3 , as clay for unit weights larger than 13kN/m^3 . Values within these boundaries are classified by visual inspection. The clay samples retrieved from above a present peat layer are classified as clay Duinkerke, the other clay samples as clay Calais. The results of the weight tests are discussed in section 5.2.4.

The bulk unit weight for the Philippines reclamation project is derived by weighting samples from 5 different borehole locations and plotting the results over depth, as shown in Appendix B, figure B.2. The unit weights used for the computation of the stress profile is summarized in section 6.2.4.

The pore pressure distribution is derived by evaluating field data. In the case of the Markermeerdijken field trials, piezometers and CPTu data is employed to accomplish this task. To simplify the modeling process, a uniform hydraulic head was assumed in the soft layers. This decision was supported by data suggesting limited influence length from the deviating hydraulic head of deeper layers. Further elaboration on this can be found in section 5.2.3.

For the reclamation in the Philippines, the initial pore pressure distribution is based on the mean sea level. Subsequently, excess pore pressure resulting from fill placement is estimated using a radial consolidation model and is incorporated into the pore pressure distribution. Additional information is available in section 6.2.2.

4.2.4. Preconsolidation stress

The preconsolidation stress, denoted as σ'_{pc} , represents the peak apparent stress magnitude that a soil has encountered during its history. It is crucial to note that σ'_{pc} is not solely dependent on past stress conditions but is also influenced by phenomena like creep and cementation. Estimation of the initial σ'_{pc} is performed using 1D consolidation tests. During the loading process of the sample, initially, minimal strain is observed due to the stiffness increase resulting from past conditions. However, after

surpassing the preconsolidation stress point, the sample exhibits a softer response. The preconsolidation stress is determined by using the method by Casagrande (1936). An example of this procedure is displayed in figure 4.3. The following steps were followed:

1. Determine the point of maximum curvature (point B)
2. Draw a tangent line through point B (line c)
3. Draw a horizontal line through point B (line d)
4. Draw a line that splits the area between line c and line d in equal parts (line e)
5. Extend the tangent through the linear steep portion of the curve (line f)
6. Mark the intersect of line e and line f as preconsolidation stress

The change in stress-strain response indicates the preconsolidation stress. The difference between the current vertical effective stress and preconsolidation stress for a soil layer is known as parameter POP (pre-overburden pressure). The ratio between the current vertical effective stress and preconsolidation stress is defined as the Over Consolidation Ratio (OCR).

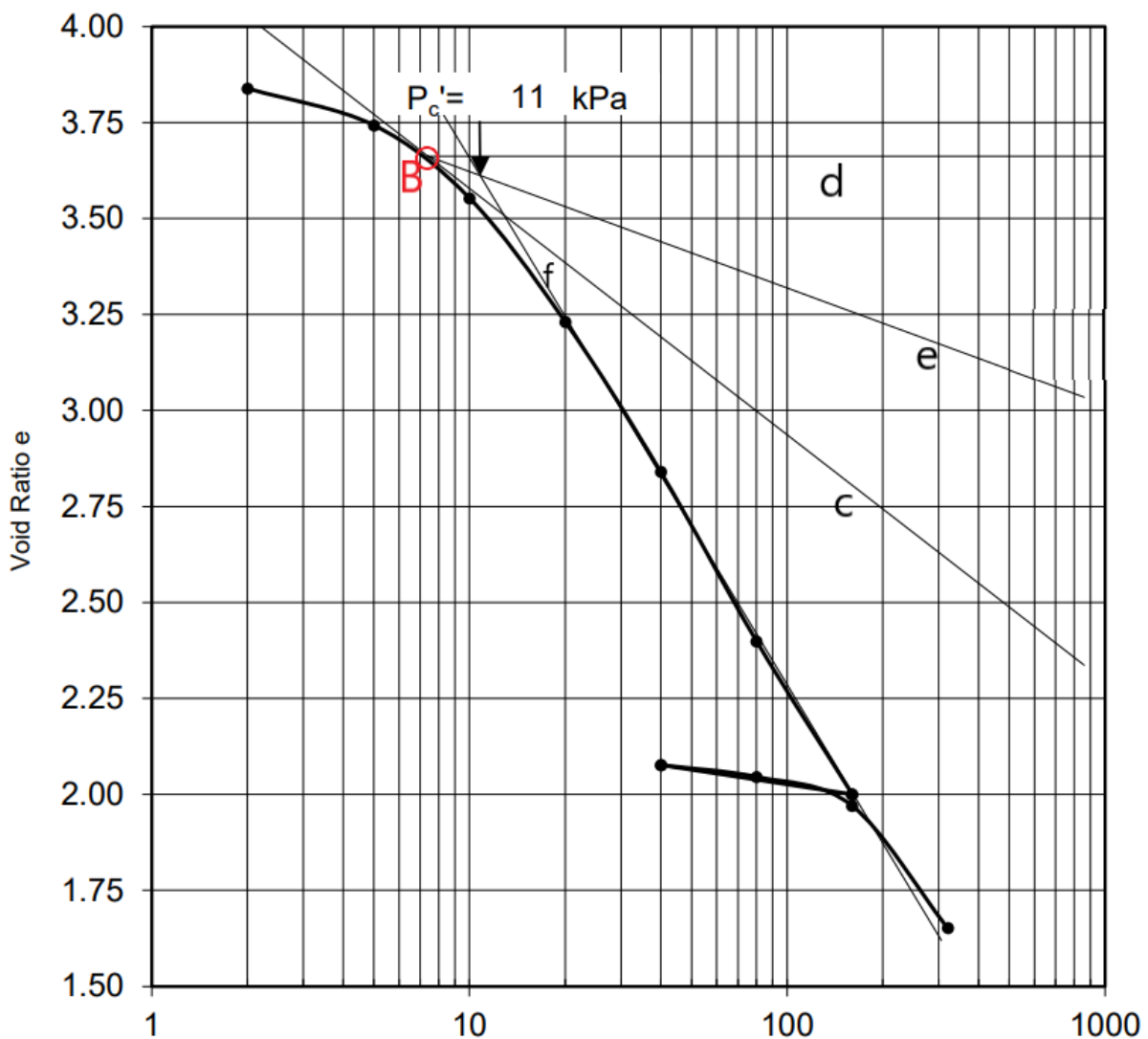


Figure 4.3: Oedometer test procedure (ASTM-D6535 2011)

To determine the OCR after removing a surcharge, the pre-consolidation stress resulting from its application is calculated. The preconsolidation pressure caused by surcharging depends on factors such as the degree of consolidation, creep, the weight of the surcharge, and the depth to which the surcharge

is submerged below the groundwater level. When dealing with significant depths relative to the surcharge area, it is important to take into account the distribution of the load. Preconsolidation stress σ'_{pc} is calculated with the following formula:

$$\sigma'_{pc} = \sigma'_{vc} + U * (\gamma_s h_s) \quad (4.4)$$

Here, U is the degree of consolidation, γ_s is the weight of the surcharge material and h_s is the effective height of the surcharge material, corrected for submersion and load distribution.

4.2.5. Coefficient of consolidation

The vertical coefficient of consolidation C_v is determined in a 1D oedometer tests for multiple load steps using the Log of Time Method. The procedure of determining C_v was followed using the standard ASTM-D6535 (2011), an example of this procedure is showed in figure 4.4. The following procedure is followed:

1. A straight line (D) is drawn through the steepest section of the slope and the straight part at the end of the test (line C).
2. The intersection of line C and line D is assumed to be the end of primary consolidation, at time t_{100} . The time at 50% of consolidation t_{50} can be found graphically.

The vertical coefficient of consolidation is calculated using the equation:

$$C_v = \frac{TH_{D50}^2}{t} \quad (4.5)$$

where T is a dimensionless time factor, t a time corresponding to a degree of consolidation and H_{d50} the length of the drainage path at 50% consolidation. The log time method is used, here $T = T_{50} = 0.197$ and $t = t_{50}$. The sample is able to drain double sided, H_{d50} equals half of the specimens height.

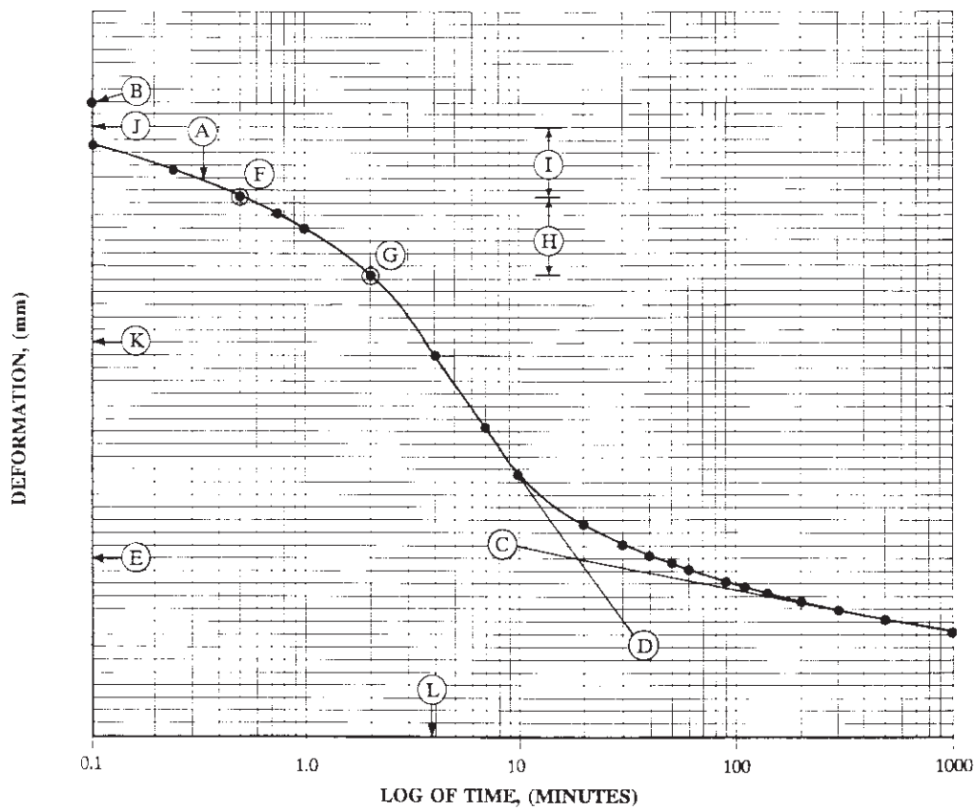


Figure 4.4: C_v determination procedure (ASTM-D6535 2011)

4.3. Submersion of preload

When surcharge is applied to soft soils, significant settlements can occur. In situations where the water table is high, a portion of the surcharge will submerge below the phreatic surface. According to the effective stress theory, the contribution of the submerged surcharge below the phreatic surface is determined by the difference in weight between the surcharge material and the weight of water. The undrained shear strength of the soil is influenced by the (past) effective stress, as defined within the SHANSEP framework. Failing to consider submersion would lead to an overestimation of the undrained shear strength during and after the preloading process.

In the specific field trial at Broeckgouw, the phreatic surface was found to be located 0.1m below the initial ground level. Settlement plates recorded a settlement of 1.4m at the interface between the surcharge and the ground level. Approximately 1.3m of the 5-meter high surcharge sank below the phreatic surface line. The effective weight of this submerged portion is calculated to be 7.6kPa per meter, while the effective weight of the part above the phreatic surface is 17.6kPa. Neglecting to consider sinkage would lead to an overestimation of the effective surcharge of approximately 14kPa.

Figure 4.5 presents a comparison between the undrained shear strength calculated using the SHANSEP approach and the shear strength determined through CPTu measurements. Within the depth range of -3.5m NAP to -4.2m NAP, there exists a peat layer with a SHANSEP S factor of 0.43.

Neglecting the effect of submersion, the undrained shear strength of this layer is overestimated by 6kPa at the end of the surcharge phase (Phase 1) due to the earlier mentioned 14kPa overestimation of effective stress. Figure 4.5a illustrates a poor fit due to the strength overestimation resulting from using SHANSEP without accounting for submersion correction. However, Figure 4.5b demonstrates a better fit when submersion is considered, particularly during the surcharge phase, although the strength after surcharge removal (Phase 2) is slightly underestimated.

This example clearly highlights the necessity of sinkage correction, especially when dealing with soils exhibiting large SHANSEP S factors, combined with high water tables and significant settlements. It should be noted that the overestimation for clay layers with smaller SHANSEP S values than the SHANSEP S of peat layers results in a smaller overestimation.

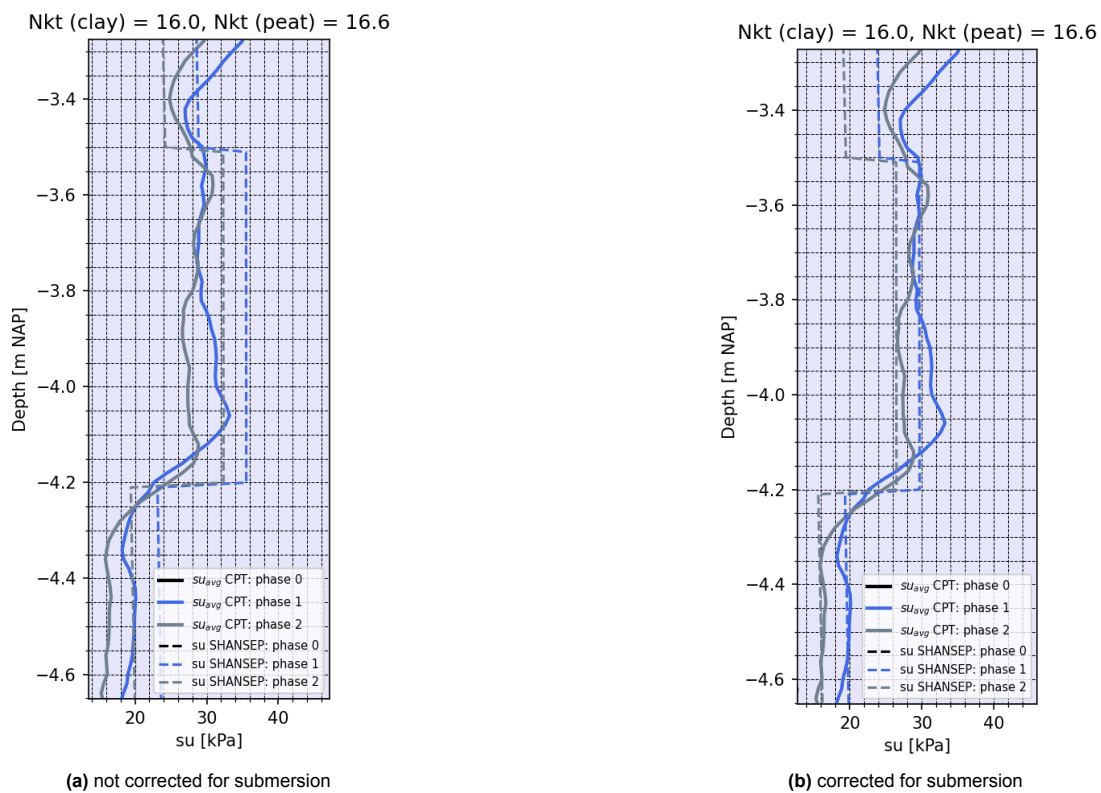


Figure 4.5: Undrained shear strength in peat (field trial Broeckgouw)

4.4. Depth influence

Effective stress increase due to preloading reduces over depth due to load distribution. In case of the Markermeerdijken field trials, reduction in preload effectiveness is expected considering the small loading area. The preload contribution to effective stress will be computed for the SHANSEP strength prediction profiles using equation 3.20. The required load radius r will be verified by comparing the obtained influence factor with the influence factor by Poulos and Davis (1964).

4.5. CPTu verification of strength

The undrained shear strength of the soft soils will be derived from the CPTu- s_u relationship as described in chapter 3. A Python script is used to load CPTu data. The undrained shear strength (s_u) is calculated using equation 3.29. For each location, the total vertical stress profile is calculated, which is required for the relationship between CPTu and s_u . The following steps will be performed:

1. Load the Cone Penetration Test (CPTu) data
2. Compute the corrected cone resistance (q_t) using the cone resistance (q_c), the area ratio (a), and the pore pressure (u_2).
3. Calculate the total vertical effective stress (σ_{tot}) profile.
4. Utilize the CPT- s_u relation (equation 3.29) to calculate the undrained shear strength via the N_{kt} factor.
5. Combine the CPTu data into a single dataframe, ensuring the depths are corrected and converted to meters below a reference level NAP/MSL (Normal Amsterdams Peil or Mean Sea Level).
6. Generate a plot of the undrained shear strength over depth. Additionally, calculate and plot the average s_u over depth.

When dealing with projects characterized by significant variability, such as the Philippines reclamation, the CPTu data can be grouped based on location to facilitate meaningful comparisons. However, it is important to note that relying solely on the average undrained shear strength (s_u) value does not provide a complete picture of the soil strength. This is because the average strength can be greatly influenced by the high variability in soil strength within the project area.

Moreover, it is important to consider the pore pressure parameter B_q , which is calculated using equation 3.30. Taking into account partially drained behavior during a Cone Penetration Test with pore pressure measurements is essential as it can significantly impact the correlated undrained shear strength.

4.6. Piezometer verification of strength

For the Philippines reclamation project, the undrained shear strength of the marine clay during consolidation under a surcharge will be estimated using CPTu correlations with undrained shear strength. Another method of estimating the undrained shear strength involves utilizing piezometers to measure in-situ pore pressure. By estimating the total vertical stress at the depth of the piezometer and measuring the pore pressure with the piezometer, the effective stress level can be determined at the piezometer location. This effective stress can be multiplied by the SHANSEP S factor and the OCR due to creep to estimate the undrained shear strength. The OCR due to creep is estimated by the Isotach framework by Den Haan and Edil (1994), calculation of the OCR's due to creep for the different field trials are attached in Appendix B: figures B.10, B.11 and B.12.

During consolidation, the piezometers settle up to 1.7m. To account for this settlement, the measured values are corrected by subtracting the estimated pressure increase caused by settlement. This settlement is estimated using data from the Lost Point Extensometers (LPE's) installed within 2m of the piezometers.

4.7. Comparison

The predicted undrained shear strength over depth by the SHANSEP framework will be plotted against the measured undrained shear strength with the CPTu- s_u correlations to gain insight in the accuracy of the prediction/verification process. An evaluation will be conducted to analyze the enhancement of strength resulting from preloading, as well as the subsequent reduction in strength following the removal

of the surcharge. In the context of the Markermeerdijken field trial, the graph will incorporate laboratory test data to ensure the consistency and compatibility between the methods used in laboratory tests and field tests. In case of the Philippines reclamation field trials, undrained shear strength based on piezometer data will be compared to strength measurements by CPTu during consolidation.

5

Markermeerdijken

5.1. Introduction

Between Amsterdam and Hoorn, 33km of dike is reinforced to comply to national safety standards. The dike is built on soft soils, consisting of clay and peat layers. Three field trials were investigated to understand the consolidation and strength development of the soft clay and peat. From north to south, these field trials are located at de Weel, Ethersheim and Broeckgouw as displayed in Figure 5.1. The Broeckgouw field trial site features a 1.5m thick layer of peat, whereas the two northern field trials contain clay and sand only.

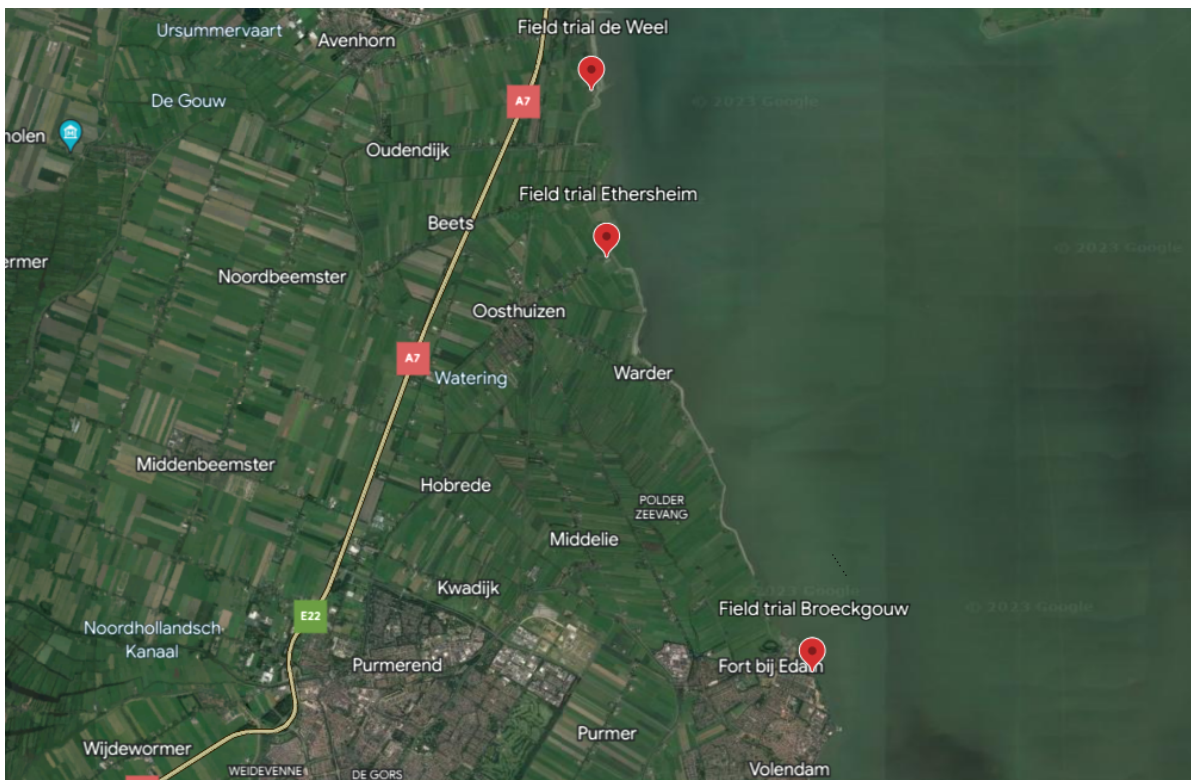


Figure 5.1: Overview locations field trials: <http://www.earth.google.com> (2023)

The field trials will undergo loading through the placement of a 5-meter-high sand embankment. To expedite the consolidation process by reducing drainage path length, Prefabricated Vertical Drains (PVD's) will be installed. For the de Weel field trial, drains will be installed up to a depth of -13.5m NAP, employing a triangular spacing of 1.5 meters. The same drain spacing will be utilized for the

Broeckgouw field trial reaching a depth of -15.0m NAP. In the case of the Ethersheim field trial, drains will extend down to -14.5m NAP, arranged in a triangular grid with a spacing of 1.0 meter.

The top view of the field trials can be observed in Appendix A. Each field trial exhibits a slope of 1:3, with a crest height measuring 5 meters. The dimensions of the field trials are approximately 70m x 50m for de Weel, 65m x 45m for Ethersheim, and 40m x 40m for Broeckgouw.

Geotextiles are placed at ground level after the ground surface has been leveled. After the first preload step, drains are installed through the first preload layer and the geotextiles. Drain depth and drain spacing are summarized in table 5.1. The preload is applied in steps of 0.5m – 1.0m to ensure slope stability. The maximum preload height for all field trials is 5 meters. The average degree of consolidation should reach a minimum of 90% before removal of the surcharge, which was computed with piezometer measurements.

Table 5.1: Markermeerdijken: field trial specifications

	Unit	De Weel	Ethersheim	Broeckgouw
Crest	[m ²]	20 x 40	20 x 40	20 x 20
Drain spacing	[m]	1.5 (triangular)	1.0 (triangular)	1.5 (triangular)
Ground water level	[m NAP]	-4.2	-4.6	-1.43
Preload height	[m]	5	5	5
Preload magnitude	[kPa]	85	85	85
Slope	[-]	1:3	1:3	1:3

5.2. Site investigation

Before the field trials were constructed, various site data was collected. The site investigation mainly consists of Class 1 CPTu's and boreholes. For the computation of the soil profiles, mainly CPTu data is used since those were performed at the exact location of the field trials. Borehole sampling was performed several hundreds meters away from the field trials.

Standpipe data and piezometers are used to compute the pore pressure distribution, details on this investigation are given in section 5.2.3.

5.2.1. Soil profile

The soil profiles for the initial situation are based on boreholes and CPTu's. The resulting soil profiles from the ground investigation are displayed in figure 5.2.

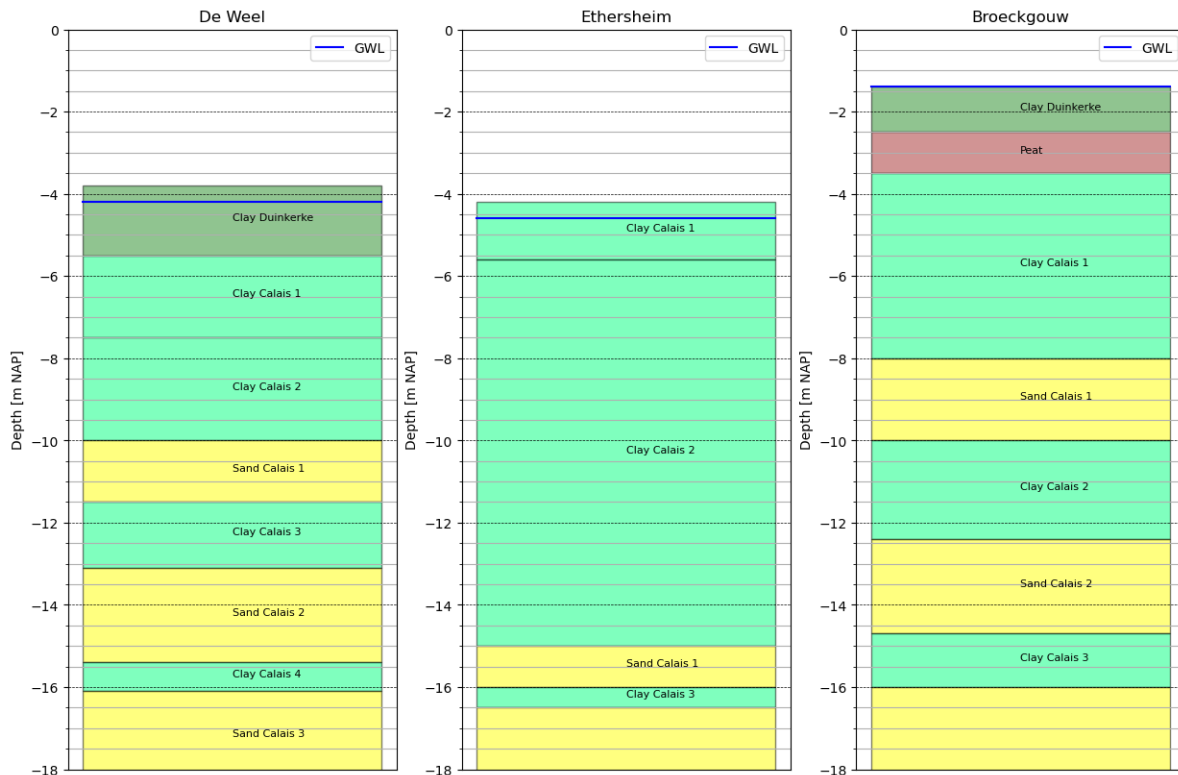


Figure 5.2: Soil profiles

At De Weel trial site, there is a layer of topsoil consisting of clay Duinkerke with an approximate thickness of 1.4m. Below this, between depths of -6m NAP and -10m NAP, clay Calais is encountered. However, this layer can be further divided into two distinct layers due to the presence of a spiky pattern observed in the CPTu's for the first two meters of this zone. Refer to Figure 5.3 for visualization. Below -10m NAP, both sand Calais layers and clay Calais layers are present. The Ethersheim field trial site comprises a clay Calais layer with a thickness of 10.8m, starting at -4.2m NAP and extending down to -15m NAP. Beneath this layer, there is a sand Calais layer approximately 1m thick, followed by an additional 0.5m of clay Calais.

The Broeckgouw field trial consists of a 1m thick peat layer located beneath the topsoil. Extending from -3.5m NAP to -8m NAP, the clay Calais layer is encountered. It is important to note that this layer exhibits relatively high cone resistance values compared to the clay Calais found in other field trials. Below -8m NAP and up to -10m NAP, a sand Calais layer is present. This layer is followed by a thin layer of clay.

5.2.2. CPTu's

The results of the CPTu's taken before the application of preload (phase 0) at field trial de Weel, Etherseim and Broeckgouw are shown in figure 5.3, 5.4 and 5.5 respectively. The figures show from left to right:

- Cone resistance q_c [MPa] in log scale
- Friction ratio Rf [%]
- Pore pressure u_2 [MPa]
- Sleeve friction resistance f_s [MPa] in log scale
- Corrected cone resistance q_t [MPa]

In order to improve the accuracy of pore pressure measurements, an initial pre-drilling procedure was conducted on the upper 1.3 meters of soil to eliminate the unsaturated zone. To facilitate differentiation between clay and sand layers while including data for both, cone resistance, sleeve friction, and corrected cone resistance values were plotted on a logarithmic scale.

The CPTu tests were performed at a constant speed of 20mm/sec (± 5 mm), ensuring that the maximum distance between consecutive measurements did not exceed 20mm. All CPTu tests were classified as Class 1 applications, with the minimum accuracy requirements for the measured parameters summarized in table 5.2. To assess the influence of accuracy on the estimation of undrained shear strength obtained from the Class 1 CPTu tests, the minimum accuracy was divided by the N_{kt} value. For cone resistance values smaller than 0.7MPa, the cone resistance contributes to a maximum deviation of 2.2kPa for an N_{kt} value of 16. Similarly, for u_2 values smaller than 0.5MPa, the pore water pressure u_2 causes a maximum deviation of 0.63kPa. The estimated total vertical stress has a small effect on the accuracy of strength estimation, as it is determined reasonably accurate.

Based on these observations, it can be concluded that the minimum measurement accuracy for s_u obtained from the CPTu tests is approximately 3kPa for an N_{kt} value of 16.

Table 5.2: Class 1 CPTu accuracy

	Minimal accuracy
Cone resistance q_c	35kPa or 5%
Sleeve friction f_s	5kPa or 10%
Pore water pressure cone shoulder u_2	10kPa or 2%
Angle	2°
Penetration length	0.1m or 1%
X-coordinate entry	<0.50m
Y-coordinate entry	<0.50m
Z-coordinate entry	<0.05m

Figure 5.3 displays the CPTu data obtained from the field trial at de Weel. The plot reveals that up to a depth of -10m NAP, there are relatively low cone values and high u_2 values, indicating the presence of clay. However, between -6m NAP and -7.5m NAP, higher cone values and lower u_2 values suggest the presence of coarser material. Starting from -10m MSL, high cone values and low u_2 values indicate the presence of sand. It is also noticeable that a softer layer exists at -12.5m NAP.

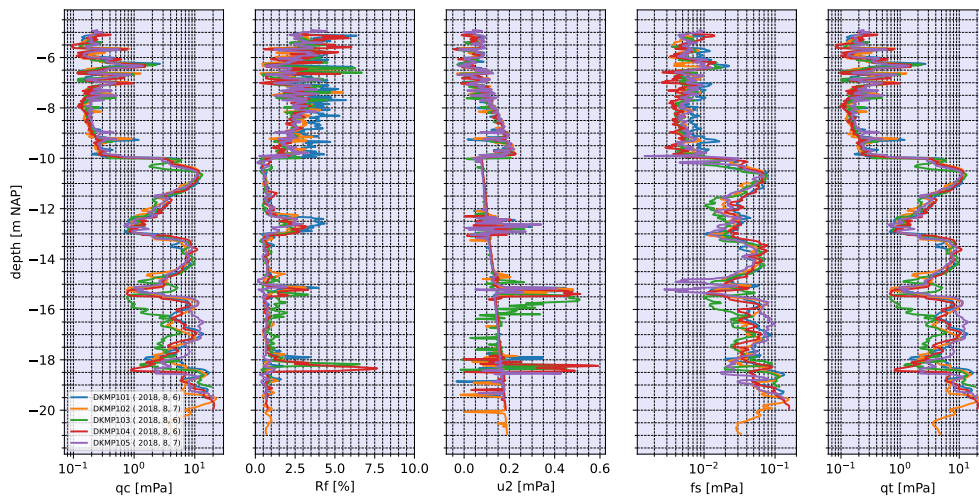


Figure 5.3: De Weel: CPTu during Site investigation

The field trial at Ethersheim begins with an uninterrupted clay layer that is 10m thick, as depicted in Figure 5.4. Below this clay layer, at a depth of -15m NAP, there is a layer classified as sand, characterized by higher cone resistances and low values of u_2 . A thin layer of clay separates this sand layer from the underlying sand layers.

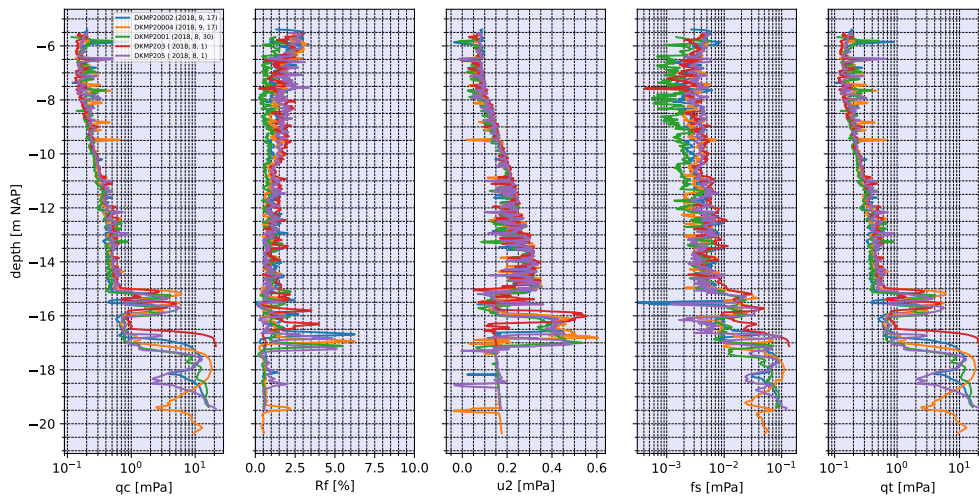


Figure 5.4: Ethersheim: CPTu during Site investigation

The CPTu's performed at field trial Broeckgouw measures high friction ratio's between -2.5m NAP and -3.5m NAP. The combination of high friction ratio and low cone resistance indicates the presence of peat. The peat layer is followed by 13m of clay, which seem to include coarser particles from around -7m NAP.

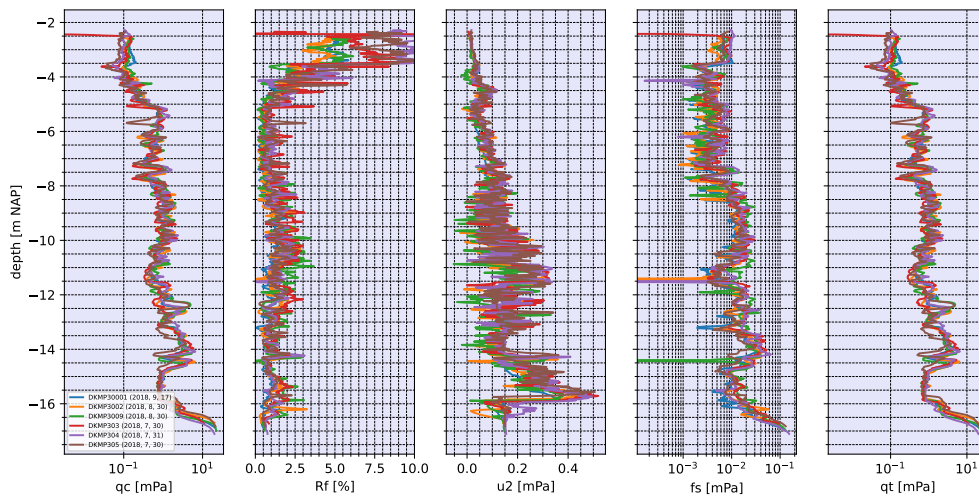


Figure 5.5: Broeckgouw: CPTu during Site investigation

5.2.3. Geo-hydrology

The distribution of pore pressure plays a role in the determination of the effective stress profile, thereby influencing the SHANSEP strength profile. This relationship is particularly significant in the Marker-meerdijken region. In this area, the hydraulic head in deeper layers differs from the groundwater level. To assess the pore pressure distribution, data from Cone Penetration Testing with pore pressure readings (u_2) and piezometers are utilized.

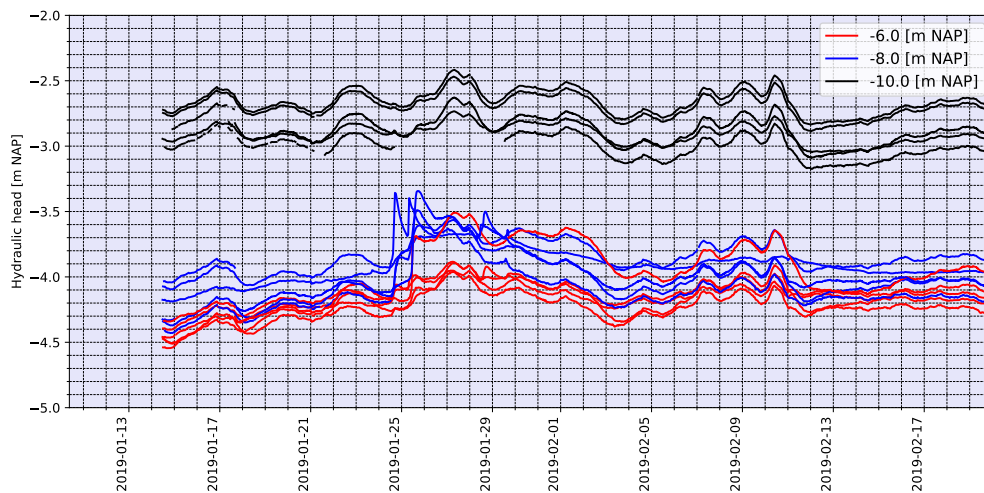


Figure 5.6: Piezometer data field trial de Weel

At the field trial location de Weel, the groundwater level is recorded at -4.1m NAP. In the deeper sand Calais 1 at -10m NAP, the CPTu cone measures a hydraulic head of -2.8m NAP with pore pressure reading, as shown in Figure 5.3. This measurement aligns with the piezometer reading at -10m NAP, shown in Figure 5.6. Similar observations of pore pressure distribution are made at the Ethersheim field trial. There, the groundwater level is located at -4.6m NAP, and the hydraulic head in sand Calais 1 is -2.8m NAP.

At both field trials, de Weel and Ethersheim, the higher hydraulic head in the deeper layers has little

impact on the hydraulic conditions of the soft layers above, as indicated by piezometer measurements. For example, at de Weel, the piezometer located at -8m NAP, two meters above sand Calais 1, records values comparable to the groundwater level. Similarly, at Ethersheim, where the first sand layer is at -15m NAP, there is no significant influence of higher hydraulic levels observed at -10m NAP, with the measured hydraulic head around -4.5m NAP, similar to the groundwater level.

However, at the Broeckgouw field trial, a different hydraulic condition is observed with the groundwater level higher than the hydraulic head in the deeper layers. This lower hydraulic head at greater depths could result in an increase in effective stress, potentially affecting the SHANSEP predicted strength. Piezometers located at -2.7m NAP, -4.0m NAP, and -9.0m NAP indicate a hydraulic head of -1.42m NAP. Similar to the previous cases, the influence length of this different hydraulic head at deeper layers appears to be limited.

Considering this, a pore pressure distribution based on the groundwater level in the soft layers is used, and the effect of a different hydraulic head in the underlying layers is disregarded due to its small influence length. The 2m influence length of the higher hydraulic head will be considered qualitatively.

5.2.4. Soil parameters

To create stress profiles utilized in generating a SHANSEP prediction, the parameters listed in Table 5.3 are employed. The stress profiles for the de Weel, Ethersheim, and Broeckgouw field trials are provided in Appendix A. The parameters were determined by laboratory tests as was described in chapter 4.

Table 5.3: Markermeerdijken: soil parameters

	γ_{sat}	C_v	RR	CR	C_α	POP
unit	[kN/m ³]	[m ² /s]	[-]	[-]	[-]	[kPa]
Peat	10.0	2.4e-7	0.079	0.489	0.029	7
Clay Calais	14.0	2.7e-7	0.035	0.229	0.011	10
Clay Duinkerke	13.5	9.2e-8	0.038	0.247	0.012	14
Sand Calais	20.0	0.4	0.001	0.004	0	-
Sand preload	17.6	-	-	-	-	-

5.2.5. N_{kt} and SHANSEP S

The determination of the N_{kt} factor for the correlation between undrained shear strength (s_u) and corrected cone resistance involves plotting s_u values obtained from constant height DSS tests against the corrected cone resistance reduced by the in situ total stress. The DSS tests are conducted on samples taken from a borehole located 1km away from the de Weel field trial site and is adjusted to match the in situ stress conditions at de Weel.

The q_t values used for computation of N_{kt} are average values derived from the CPTu tests performed at de Weel. By fitting a line through the plotted points, a suitable N_{kt} value can be determined. The N_{kt} fit is presented in figure 5.7. It is worth noting that at a depth of -7.4m NAP, the subsoil contains pockets of silt, resulting in relatively high cone values compared to the rest of the clay layer. This discrepancy leads to a poor fit with the chosen N_{kt} factor.

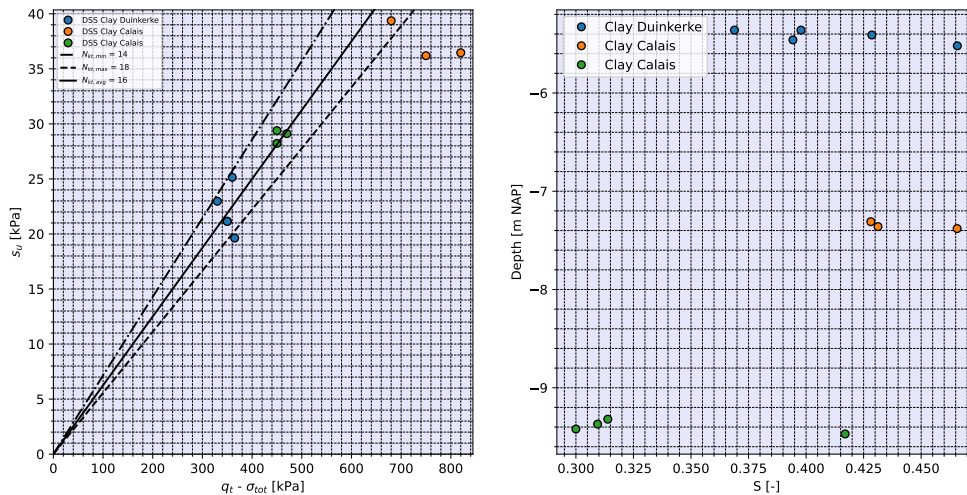


Figure 5.7: N_{kt} and SHANSEP S determination for clay

The determination of the N_{kt} factor for peat follows a similar approach as that for clay. In this case, samples obtained from a borehole at the Broeckgouw field trial were utilized to conduct 20 constant height DSS tests at two different preconsolidation stresses.

In Figure 5.8 (right), the SHANSEP S factors derived from the DSS tests are plotted. To determine the in situ s_u value, the SHANSEP S factor is multiplied by the in situ effective stress during the surcharge. The s_u values obtained are then plotted against the corrected cone resistance, adjusted by subtracting the total stress. This allows for fitting a suitable N_{kt} factor to the data.

For this specific dataset, a N_{kt} factor of 16.0 for clay, along with a SHANSEP S value of 0.30 for Clay Calais and a SHANSEP S value of 0.35 for Clay Duinkerke, provides a satisfactory fit. These values enable a strong correlation between the undrained shear strength and the corrected cone resistance at the de Weel field trial and Ethersheim field trial, as will be shown later. Additionally, these findings align with the research conducted by De Koning et al. (2019), who obtained a N_{kt} of 16.1 and a SHANSEP S value of 0.32 in their triaxial tests for clay below another dike in the Netherlands.

The results from the DSS tests on peat are presented in Figure 5.8. The DSS tests consistently demonstrate that the SHANSEP S value for peat is estimated to be 0.43, while the N_{kt} value is 16.6. Similarly, De Koning et al. (2019) observed a SHANSEP S value of 0.39 and a N_{kt} of 15.2 using the DSS apparatus, which closely aligns with the results obtained from the Markermeerdijken test.

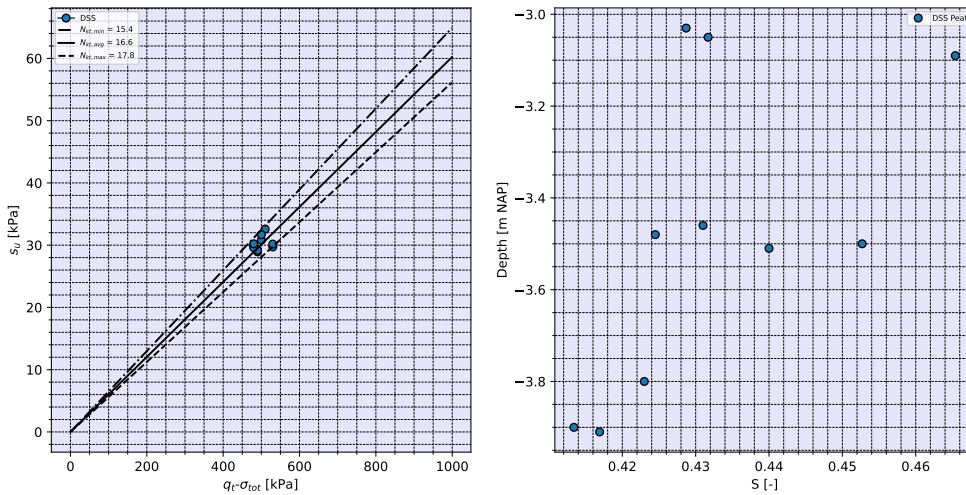


Figure 5.8: N_{kt} and SHANSEP S determination for peat

5.2.6. Depth influence

The role of depth influence on effective stress increase by preloading is estimated by computing influence factor I . The influence factor is valid for points under the central axis of the embankment. The CPTu's are performed up to 4m from the central axis, a lower-bound solution in the form of $b = 10$ (0m from the central axis) and an upper-bound solution in the form of $b = 6$ (4m from the central axis) is therefore provided using equation 3.19 (Poulos and Davis 1964). Table 5.4 summarizes the required parameters a and b from figure 3.7 for field trials de Weel, Ethersheim and Broeckgouw. For field trial Broeckgouw, parameter a is reduced to 10m to account for the 20m shorter length of the field trial. The upper and lower bound influence factors over depth are shown in figure 5.9.

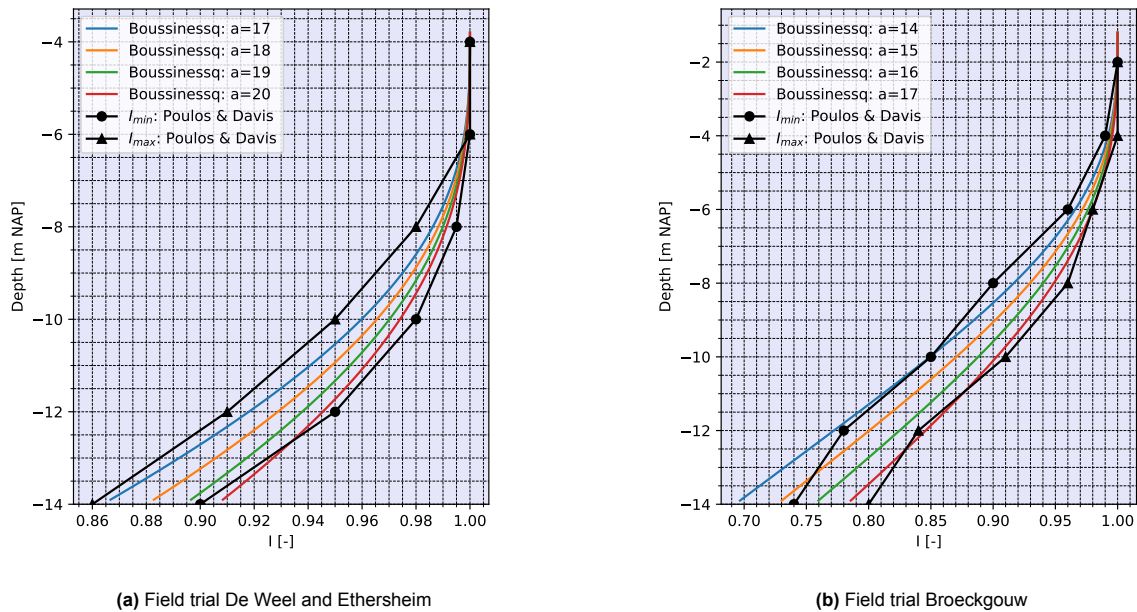


Figure 5.9: Depth Influence factor

Table 5.4: Poulos and Davis geometry parameters

	De Weel	Ethersheim	Broeckgouw
a [m]	15	15	10
b [m]	6-10	6-10	6-10
Groundlevel [m NAP]	-3.8	-4.2	-1.4

Equation 3.20, based on theorem by Boussinesq, is used to correct the SHANSEP profiles for depth influence. The required load area radius r is chosen using figure 5.9. For field trial de Weel and Ethersheim, a value of $r = 18$ was found. The smaller area of field trial Broeckgouw results in a values of $r = 16$.

Table 5.5 displays the percentage of effective preload over depth relative to the preload at the interface between preload and subsoil, based on graph 3.7. Depth effects will have a limited impact for field trial de Weel, since the effective preload is reduced by only 2-5% for the depth of interest (-4.0m NAP to -10.0m NAP). For field trial Ethersheim, the effective preload is reduced by approximately 8-14% for a depth of -14.0m NAP.

Table 5.5: Percentage of effective preload over depth

	De Weel	Ethersheim	Broeckgouw
Depth [m NAP]	Preload effectiveness [%]	Preload effectiveness[%]	Preload effectiveness[%]
-6	100	100	96-98
-8	100	100	90-96
-10	95-98	95-98	85-91
-12	90-95	90-95	78-84
-14	86-92	86-92	74-80

5.3. SHANSEP Undrained shear strength

This section will cover the prediction of undrained shear strength for the three field trials. The derived SHANSEP parameters are summarized in table 5.6.

The SHANSEP S including creep is derived by dividing the test determined SHANSEP S by the OCR due to creep just before preload removal. The OCR value is calculated using equation 3.26, the calculation can be found in figure A.5. The advantage of using the lowered SHANSEP S while including creep is that the strength increase due to creep can be included when a prediction of future strength is made. Due to removal of the surcharge, the effect of creep on the CPTu correlated strength could not be assessed. Therefore, the test derived SHANSEP S was used for the comparison of SHANSEP with CPTu strength.

Table 5.6: SHANSEP parameters based on DSS tests

	S	S + creep	m	POP
unit	[-]	[-]	[-]	[kPa]
Peat	0.43	0.33	0.88	7
Clay Duinkerke	0.35	0.27	0.85	14
Clay Calais	0.30	0.22	0.85	10

The undrained shear strength over depth is shown in figure 5.10. The profile is not continuous due to the presence of sand layers which are not considered. The shift in starting point of the profile is a result of settlement.

The strength profile includes three phases:

- Phase 0: initial strength profile with POP as shown in table 5.6.
- Phase 1: strength profile during surcharge at a minimal degree of consolidation of 90%.
- Phase 2: strength profile after removal of the surcharge.

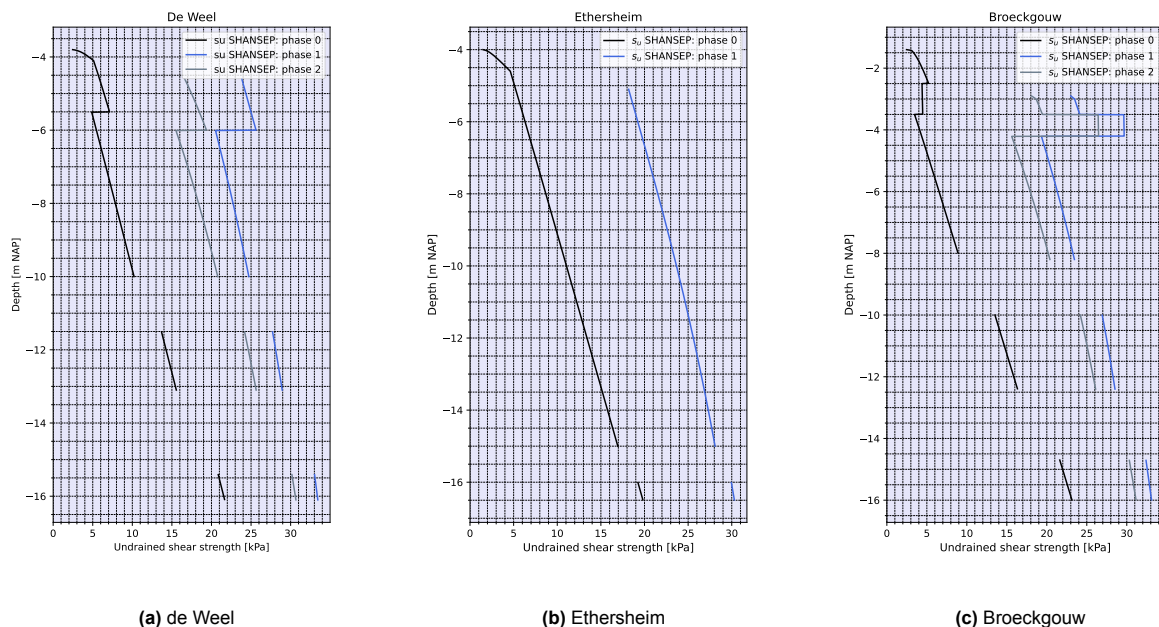


Figure 5.10: SHANSEP undrained shear strength

In phase 0, the top of the undrained shear strength profile exhibits curvature, primarily caused by the overconsolidation ratio (OCR) approaching infinity while the effective stress approaches zero. However, this curvature is not observed in phase 1 and phase 2. This is because the top of the clay layers

is covered by a layer of sand. In phase 1, this is due to the preload, and in phase 2, it occurs because a portion of the surcharge is left in place to compensate for settlement. The effect of the load distribution correction is clearly visible, as the strength in phase 1 and phase 2 curves towards initial strength at larger depths.

The SHANSEP strength profiles of field trial de Weel are displayed in figure 5.10a. A decrease in strength at -5.5m NAP is visible, this is the transition from clay Duinkerke to clay Calais. The decrease is caused by the lower SHANSEP S factor of clay Calais compared to clay Duinkerke. The strength in phase 0 ranges between 4kPa and 11kPa for the clay layers up to -10m NAP. The deeper layers at -12m NAP and -15.5m NAP have a strength of 15kPa and 23kPa respectively. Due to preloading, the strength increased with 20kPa in all layers except for the top layer. The top layer shows a slightly larger strength increase because of a higher SHANSEP S factor. Removal of the preload decreases the strength with 10kPa in the top soil to 5kPa in the deepest clay layer.

Field trial Ethersheim (figure 5.10b) shows a smooth strength profile as little variations of soil types are present. The strength in phase 0 ranges from 3kPa at the top of the clay layer to 17kPa at -15m NAP. Due to preloading, the strength increases by approximately 22kPa over the whole depth. The effect of preload removal is not considered for this field trial since no CPTu data is available for phase 2.

Field trial Broeckgouw (figure 5.10c) includes a peat layer located at -2.5m NAP to -3.5m NAP. The strength in phase 0 is estimated to be 3kPa in clay Duinkerke and peat. The strength increases quite linear from 6kPa at -5.5m NAP to 24kPa at -16m NAP. Due to preloading, the strength increases with 17kPa in the clay layers. Although the preload height is equal to the other field trials, strength increase is less due to the large settlement reducing the effective preload. The peat has a significant higher SHANSEP S factor therefore showing an strength increase of 24kPa. Removal of the preload decreases the strength with 4kPa. This is less than in the other field trials: more settlement occurred on this location while the initial ground elevation was maintained. Less preload had to be removed in order to maintain the original ground level.

5.4. Strength comparison SHANSEP and CPTu

It should be noted that for the Ethersheim field trial, no CPTu data was available for phase 2 (after preload removal). Phase 2 is therefore left out in the plot. The locations of the CPTu's and PVD's for the three field trials are shown in figure 5.11, figure 5.12 and figure 5.13.

Figures 5.14 to 5.18 display the undrained shear strength over depth for different stress states during the field trial experiment. From left to right the figure shows:

- Profiles of undrained shear strength over depth for all CPTu's conducted during phase 0 (initial situation), along with the corresponding predictions of undrained shear strength using SHANSEP.
- Profiles of undrained shear strength over depth for all CPTu's performed during phase 1 (preloading at 90% consolidation), along with the corresponding predictions of undrained shear strength using SHANSEP.
- Profiles of undrained shear strength over depth for all CPTu's carried out during phase 2 (after preload removal), along with the corresponding predictions of undrained shear strength using SHANSEP.
- Average undrained shear strength for each phase based on CPTu data, along with the predicted shear strength using SHANSEP.

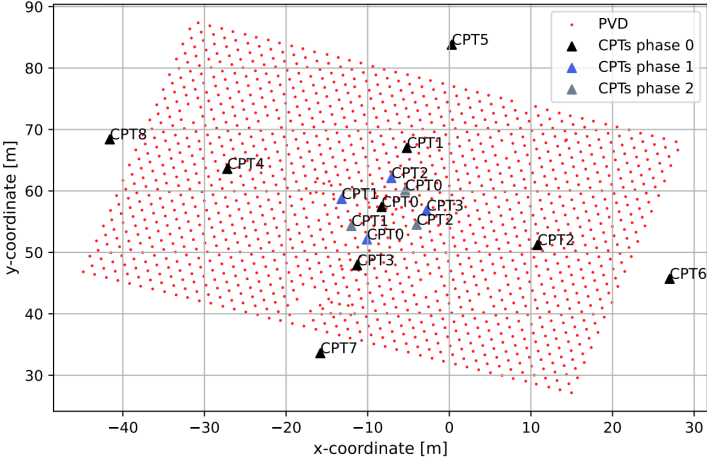


Figure 5.11: Field trial de Weel: CPTu locations

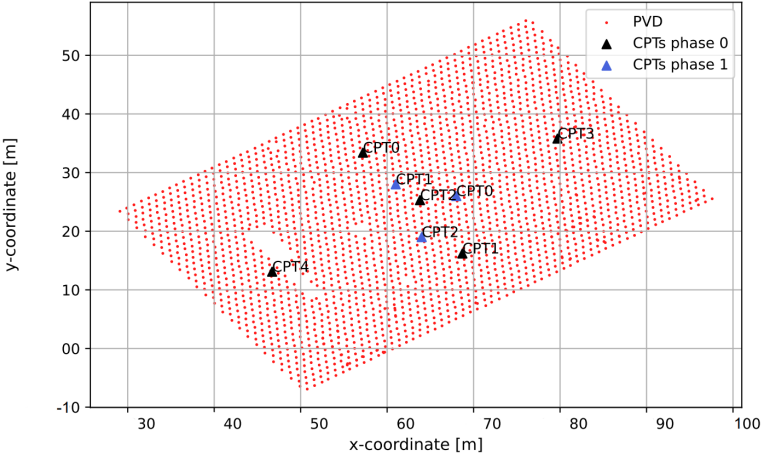


Figure 5.12: Field trial Ethersheim: CPTu locations

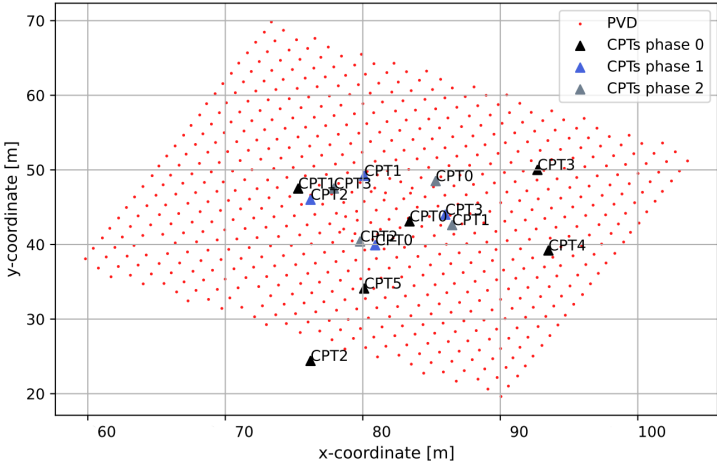


Figure 5.13: Field trial Broeckgouw: CPTu locations

5.4.1. de Weel

Phase 0

The SHANSEP predicted strength and CPTu correlated strength for field trial de Weel are displayed in figure 5.14. Due to 1.3m predrilling, no CPTu data is available for the first layer. No conclusion can be drawn regarding the accuracy between SHANSEP and CPTu- s_u relationships for the first 1.3m. Overall the initial strength prediction by SHANSEP shows a decent match with the values obtained from the CPTu's. For the clay Duinkerke (-5.0m NAP to -5.5m NAP), the SHANSEP prediction is on the conservative side. The strength of the soil located between -5.6m NAP and -7.0m NAP (clay Calais) shows sharp peaks and shows considerably higher undrained shear strength than predicted by SHANSEP. The measured strength between -7.0m NAP and -9.8m NAP is lower than predicted, around 4kPa difference between SHANSEP and CPT- s_u values of strength. This mismatch could be the consequence of a overestimation of the initial POP for this layer. The clay layer at -12.5m NAP is thinner than predicted with the borehole data. Given the positioning of the layer between two sand layers, it is probable that the layer contains a significant amount of sand or silt, explaining the high CPTu correlated undrained shear strength.

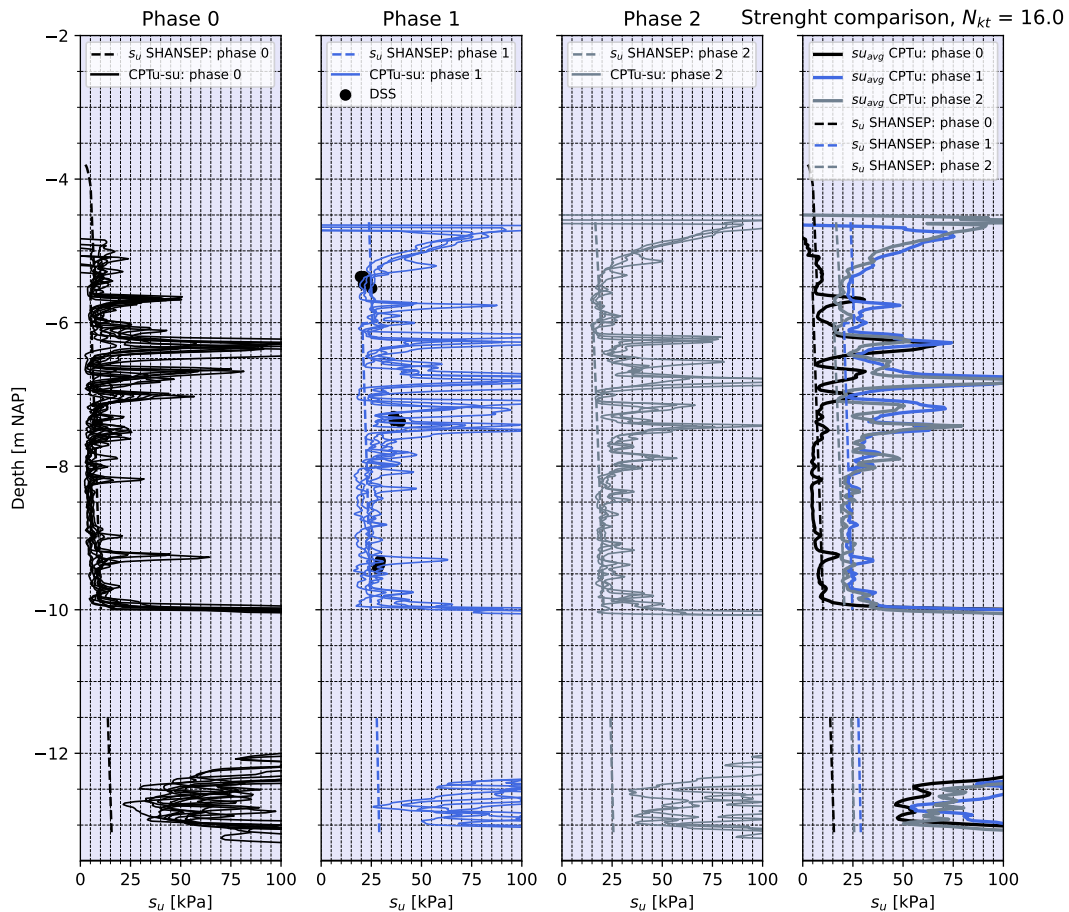


Figure 5.14: Field trial de Weel: undrained shear strength comparison SHANSEP and CPTu

Phase 1

The undrained strength measured by CPTu's during surcharge corresponds well with the SHANSEP prediction and the strength of DSS tests. The spiky section between -6.0m NAP and -8.0m NAP is un-

derestimated by SHANSEP, this was expected since the same conclusion was drawn for Phase 0. The DSS tests and the CPTu values indicate a higher SHANSEP S value is applicable for this layer. The SHANSEP prediction for the soil between -7.0m NAP and -9.8m NAP seems to be a good estimation.

Phase 2

Based on the SHANSEP framework, a significant portion of the strength is expected to remain even after the removal of the surcharge. The strength predicted by SHANSEP fits well with the CPTu correlated strength, the silty layer between -6.0m NAP and -8.0m NAP excepted.

The increase in strength due to preloading is clearly evident in Figure 5.14, as the measured strength has increased throughout the entire depth. The SHANSEP prediction of strength reduction due to surcharge removal matches the strength loss measured with the CPTu. This indicates that the determined SHANSEP m is suitable for this subsoil. The peaks of strength are not located at the exact same depths in different project phases, which is a combination of settlement and local variability. A surface settlement of 0.8m was measured, which represents the cumulative strains between the ground level and the sand layer located at -10m NAP. It is worth noting that the sand layer at -10m NAP did not experience any settlement.

The B_q parameter over depth for field trial de Weel is plotted in figure 5.15(left). The q_t value for each point is linked to the color bar on the right of the plot. In all phases, the SHANSEP prediction shows a poor match with the CPTu data from -5.5m NAP to -7.5m NAP. The subsoil at this depth has B_q values as low as 0.1 and q_t values of 1 MPa. This B_q values indicates partially drained CPTu behaviour, resulting in an underestimation of the undrained shear strength.

The Right graph in figure 5.15 plots the CPTu correlated undrained shear strength in dots, with the color dependent on the B_q value. The SHANSEP predicted strength is plotted in black. For this site, SHANSEP prediction and CPTu- s_u correlation shows a decent match for B_q values larger than 0.45. Points with a B_q smaller than 0.45 (green), show less correspondence with the SHANSEP prediction.

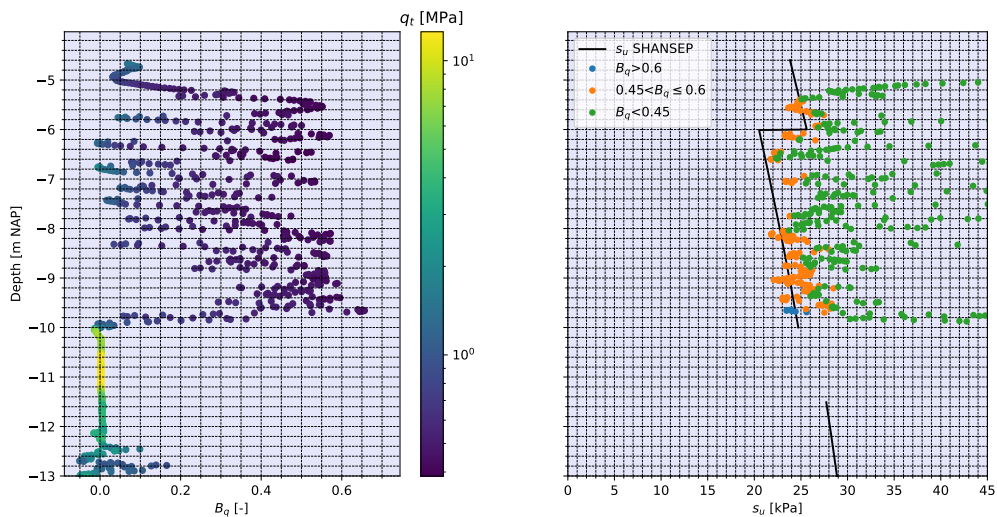


Figure 5.15: Field trial de Weel: B_q parameter

5.4.2. Ethersheim

The SHANSEP predicted strength and CPTu correlated strength for field trial Ethersheim are displayed in figure 5.16. The first 1.3m of CPTu data is not available due to predrilling. The undrained shear strength of clay Calais 1 is underestimated by on average 3kPa using SHANSEP prediction. The predicted strength of clay Calais 2 (-6m NAP to -10m NAP) corresponds well with the measured strength. From -10m NAP to -15m NAP, SHANSEP underestimates the CPTu based strength by 5kPa.

The match between SHANSEP and CPTu data in phase 1 is reasonable but less accurate than described in phase 0. The strength increase is less than predicted, this might be due to a small overestimation of the SHANSEP S factor. From -11m NAP to -14m NAP, the prediction is more accurate than phase 0.

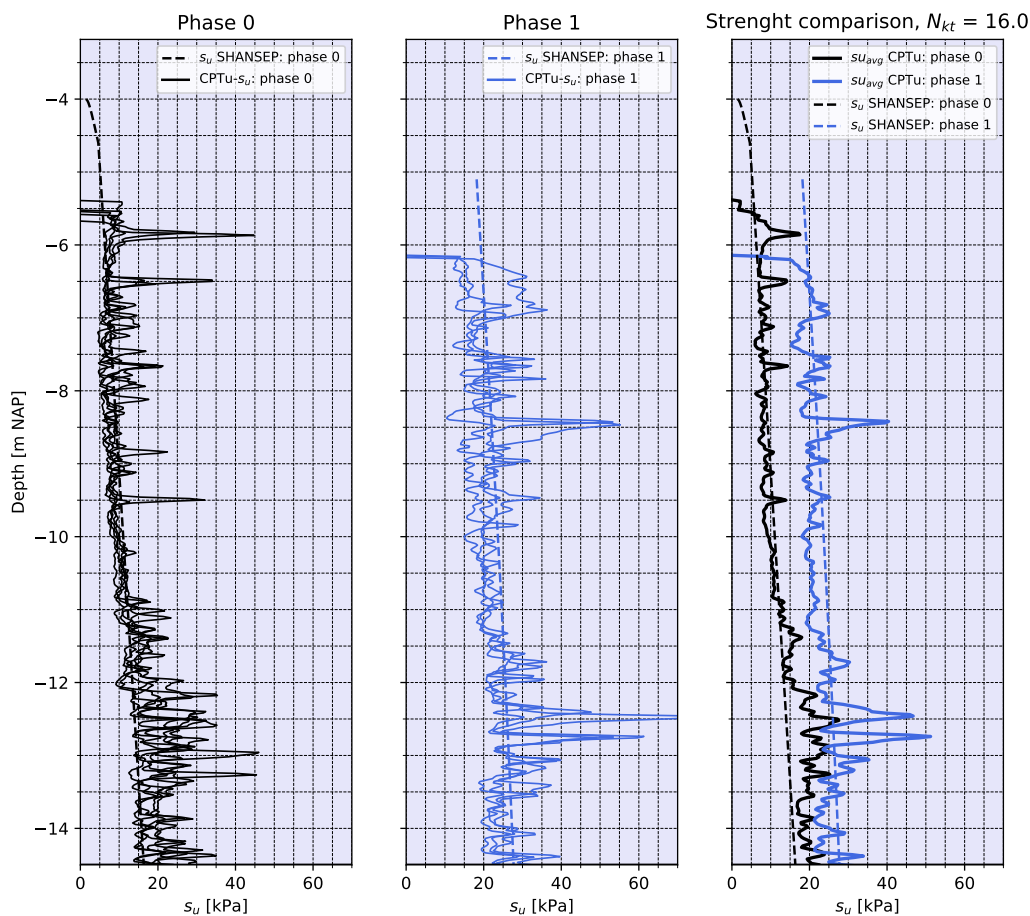


Figure 5.16: Field trial Ethersheim: undrained shear strength comparison SHANSEP and CPTu

The strength increase is displayed in figure 5.16 and corresponds reasonably with the predicted SHANSEP strength. Strength increase from -11m NAP is smaller than above this point. This smaller strength gain could be explained by two theories:

- An underestimated POP: As discussed earlier, the shear strength by SHANSEP is smaller than the measured shear strength in phase 0. This could be due to a underestimated POP parameter. The lack of strength increase is in this case caused by the higher preconsolidation pressure in this layer. Preloading is less effective on a soil with a larger preconsolidation stress.

- A conservative SHANSEP S parameter and a stronger depth influence: a conservative S value for the layer between -11m NAP and -14.5m NAP causes initial the strength to be underestimated. This theory only holds if the load distribution was underestimated. The predicted strength in phase 1 is quite accurate, a higher SHANSEP S factor would lead to overestimation of the strength if a higher distribution of load is not present.

The B_q parameter in figure 5.17 is relatively constant over depth, while the corrected cone resistance increases from -11m NAP. A higher POP is most likely causing a higher CPTu correlated undrained shear strength. Similar to what was observed for field trial de Weel, CPTu correlated strength deviates from the SHANSEP prediction for B_q values lower than approximately 0.45.

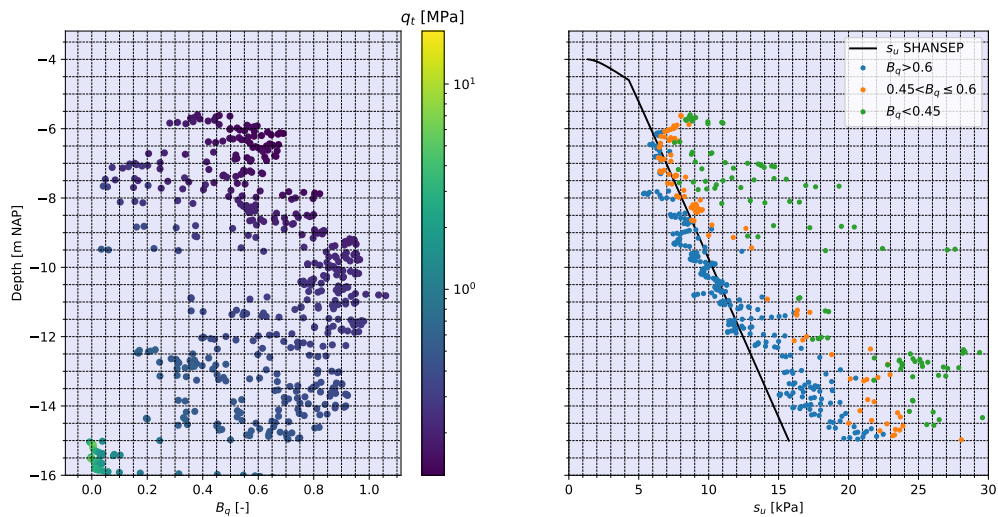


Figure 5.17: Field trial Ethersheim: B_q parameter

5.4.3. Broeckgouw

The SHANSEP predicted strength and CPTu correlated strength for field trial Broeckgouw are displayed in figure 5.18. No information regarding the top layer, clay Duinkerke, was obtained due to 1.0m of predrilling. For phase 0, the undrained shear strength prediction of the peat layer matches the undrained shear strength values obtained by the CPTu's. The measured strength ranges from 3kPa to 8kPa. The prediction of the clay Calais 1 layer corresponds with the CPTu- s_u values to a depth of -4.2m NAP. From -4.2m NAP to -8.0m NAP, the clay Calais 1 layer shows a 10kPa to 50kPa higher strength than predicted by SHANSEP. This strength underestimation is likely consequence of a higher silt/sand content. The second clay Calais layer is located at -10.0m NAP to -12.4m NAP. This layer shows a larger strength then predicted as well, likely a consequence of a higher silt content. The part from -11.0m NAP to -11.6m NAP shows a reasonable match with the prediction.

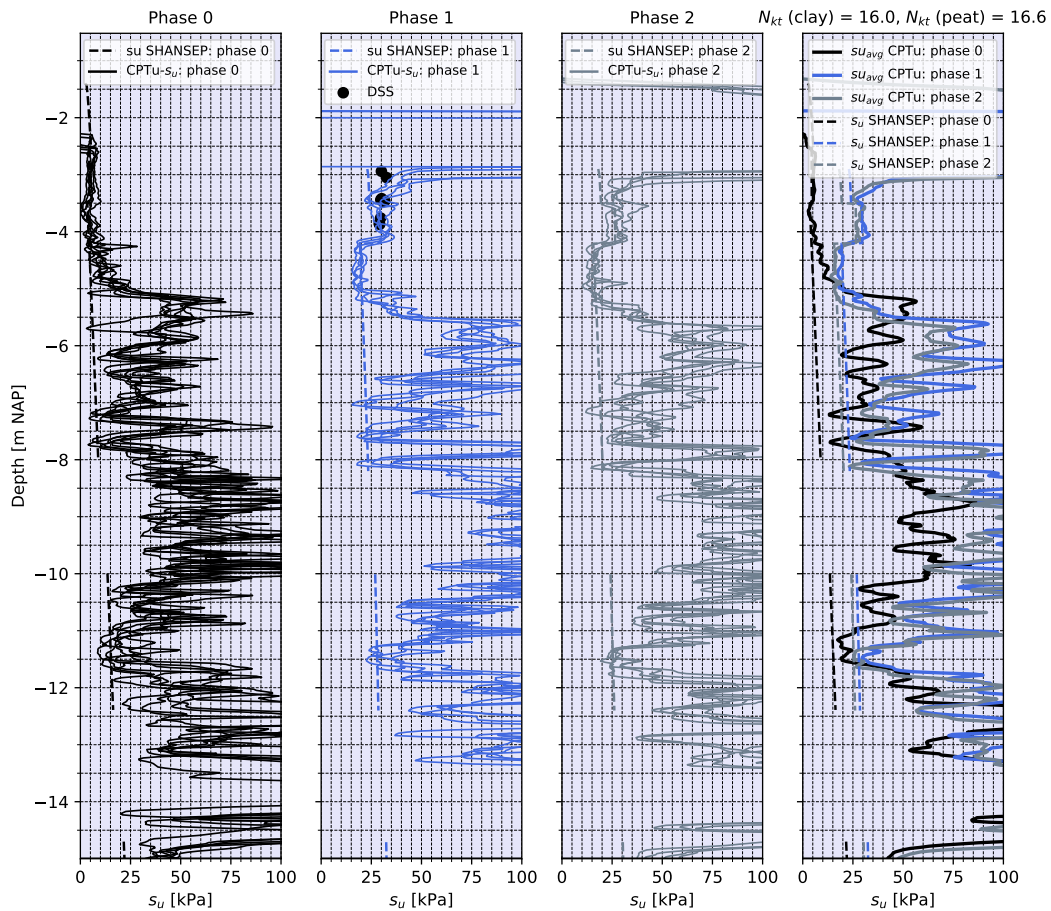


Figure 5.18: Field trial Broeckgow: undrained shear strength comparison SHANSEP and CPTu

The prediction for phase 1 shows similar performance as phase 0. The predicted strength of the peat layer corresponds with the strength correlated to the CPTu measurements and the DSS tests. The strength in the clay Calais layers is again underestimated except for some thin layers with a lower silt content.

The strength prediction for phase 2 is accurate for at least the peat layer and under laying clay layer. From -5m NAP, the prediction does not match with the measured values except for the thin clay layer at -11.5m NAP.

The average strength increase due to preloading is predicted with good accuracy for the peat layer and the clay layers with low silt content. The strength loss due to preload removal is similar to the loss predicted by SHANSEP. Strength increase due to preload is clearly measurable. Part of the strength remains as predicted by SHANSEP.

B_q parameter

The B_q parameter in combination with the q_t value indicates the presence of silt and sand from -5m NAP, hence the high values of undrained shear strength at field trial Broeckgow. Again, SHANSEP and CPTu strength match poorly for B_q smaller than 0.45.

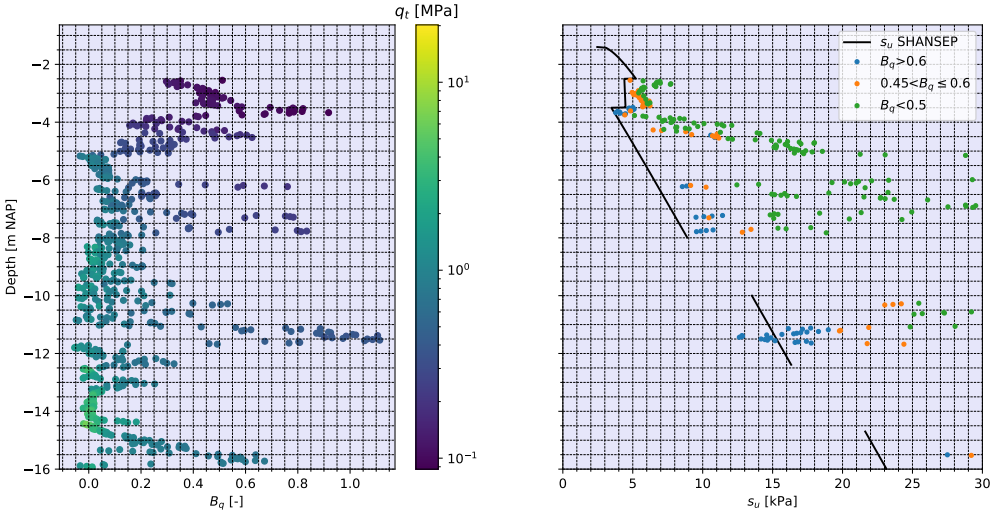


Figure 5.19: Field trial Broeckgouw: B_q parameter

6

Reclamation Philippines

6.1. Introduction

In the Philippines, a reclamation project involved the placement of a sand fill on the Marine Soft Clay (MSC) along the shore. To enhance the consolidation of the Marine Soft Clay, Prefabricated Vertical Drains (PVD's) were installed. The project included three designated field trial areas, each measuring 50m x 50m, to investigate the strength development in the Marine Soft Clay.

The SHANSEP framework was utilized to estimate the minimum and maximum undrained shear strength at six different time points during consolidation, covering a period of 10 months after the installation of the PVD's. The following factors were taken into account for the undrained shear strength estimation:

- The SHANSEP S factor, which was determined through laboratory tests and field vane tests.
- The excess pore pressure using the radial consolidation model proposed by Barron (1948), with the coefficient of consolidation derived from 1D consolidation tests.
- The total stress increase, estimated by calculating the weight of the sand fill.
- The increase in OCR due to creep, determined with the isotach model by Den Haan and Edil (1994).

To verify the increase in undrained shear strength during consolidation, Cone Penetration Test (CPTu) data and monitoring data is used. The CPTu tests were conducted at various time intervals, ranging from 1 month to 6 months, thereby covering approximately 10 months of consolidation time. The obtained undrained shear strength values from the CPTu tests were compared with the SHANSEP prediction of strength.

Furthermore, a comparison was made between the strengths obtained from the CPTu tests and the SHANSEP prediction, and the monitoring data collected from Vibrating Wire Piezometers (VWP), Lost-Point Extensometers (LPE), and Settlement Plates (SP). The monitoring data allowed for the back-calculation of undrained shear strength, providing additional insights into the consolidation process and strength development in the Marine Soft Clay.

Information such as fill construction time, drain spacing, grid pattern and additional preload is summarized below.

- Trial area FT1 has a triangular drain pattern with a spacing of 1.0m center-to-center. The seabed was located at -12.57m MSL and hydraulically filled to 1.50m MSL in 81 days. After drain installation, the area was filled to 6.1m MSL.
- Trial area FT2 has a triangular drain pattern with a spacing of 2.5m center-to-center. The seabed was located at -12.29m MSL and hydraulically filled to 1.50m MSL in 60 days. After drain installation, the area was filled to 6.0m MSL.
- Trial area FT3 has a triangular drain pattern with a spacing of 2.5m center-to-center. The seabed was located at -12.30m MSL and hydraulically filled to 1.50m MSL in 60 days. After drain installation, the area was filled to 8.2m MSL.

6.2. Site Investigation

The site investigation for the reclamation consists of Boreholes and CPTu's. The field trials are situated closest to the boreholes: BH-01, BH-02, BH-03, BH-04, BH-05, BH-06, and BH-07. Figure 6.1 gives an overview of the performed site investigation and the location of the field trials. Borehole samples were taken to perform laboratory tests, such as:

- Index tests: watercontent (w), plastic limit (PL), Liquid Limit (LL) and Plasticity Index (PI).
- Undrained shear strength tests: Torvane (TV), Labvane (LV) and Unconsolidated Undrained (UU) triaxial tests.

The Samples were collected by undisturbed piston sampling (Shelby tube) and undisturbed open tube sampling (Mazier Tube). A Field Vane (FV) apparatus is used in BH-03 and BH-04 to acquired the in situ undrained shear strength.



Figure 6.1: Overview Site Investigation

A simplified representation of the soil profile according to the description of the borehole samples is displayed in Figure 6.2. In the reclamation area, the soil profile comprises a layer of very soft clay, followed by layers of sand, silt, gravel, and clay. Those layers are underlain by the much stiffer Guadalupe Tuff Formation (GTF). The boreholes show a great variability in soil types and layer thickness. The focus of the investigation will be on the undrained shear strength of the upper 15 to 20 meters of soil, which predominantly consists of Marine Soft Clay.

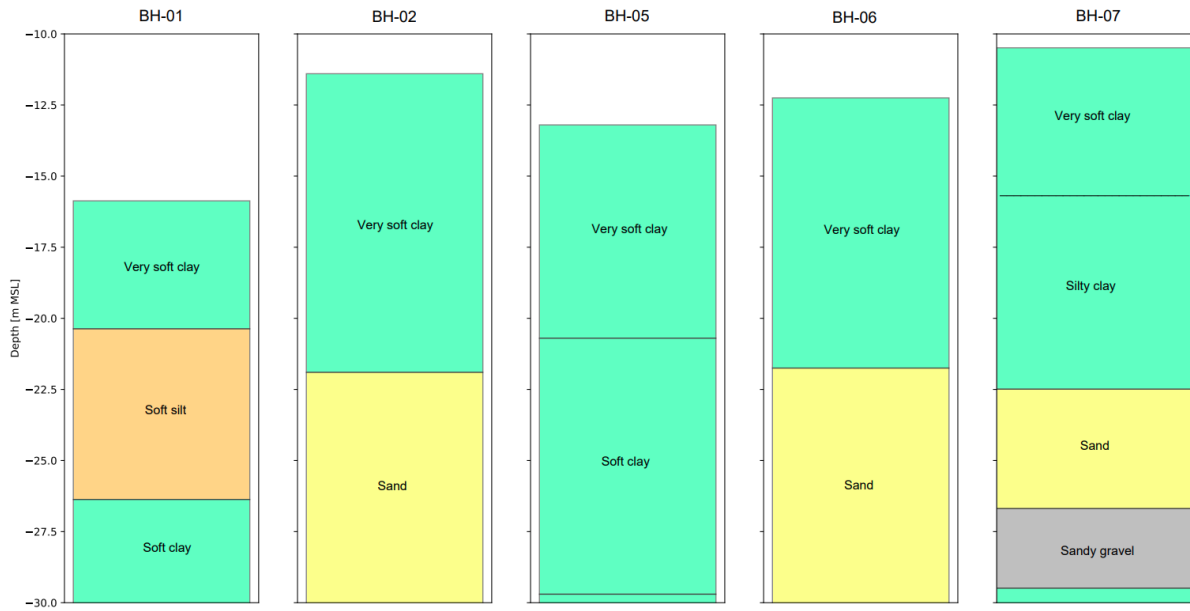


Figure 6.2: Boreholes near Field trials

CPTu data is essential to compute a representative soil profile for the 3 field trials. The boreholes can be used as a conformation of the soil layering based on the CPTu, although care must be taken due to the large variability encountered between the boreholes.

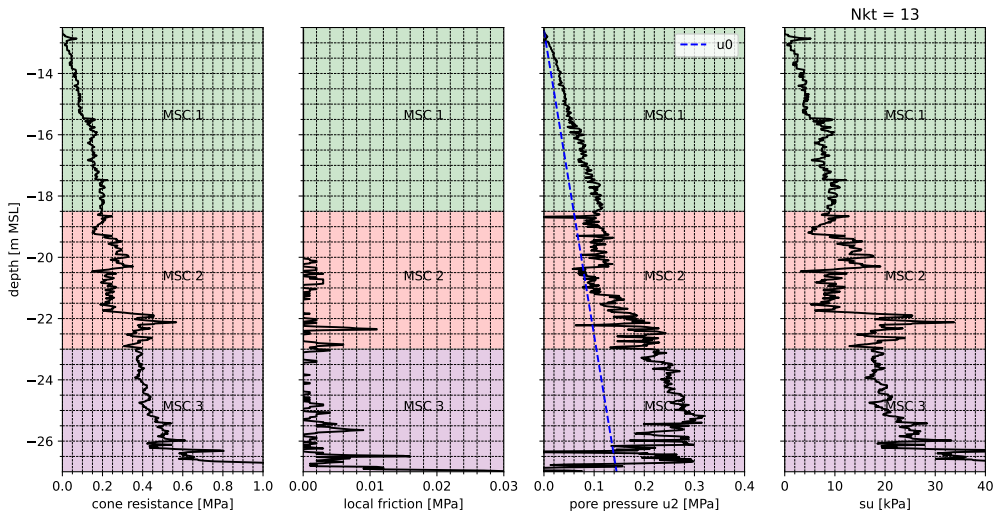


Figure 6.3: Marine CPTu-01

Figure 6.3 presents the data obtained from a marine Cone Penetration Test with dissipation (CPTu) conducted near FT2 and FT3. The test reveals the presence of three distinct layers. The first layer, known as Marine Soft Clay 1 (MSC1), exhibits a very low cone resistance ranging from 0.0MPa to 0.2MPa. Additionally, the pore pressure u_2 displays a linear increase. Moving from approximately -18.5m MSL to -23.0m MSL, the second layer, referred to as Marine Soft Clay 2 (MSC2), is encountered. This layer exhibited lower pore pressure u_2 values closer to the hydrostatic pore pressure u_0 line, indicating the presence of coarser materials. Continuing down to approximately -23.0m NAP to -26.5m NAP, the third layer, identified as Marine Soft Clay 3 (MSC3), is observed. In this layer, the pore pressure u_2 exhibits a significant response relative to the u_0 line, while the cone resistance shows minimal increase.

The MSC3 layer terminates around -26.5m MSL, marked by a rapid increase in cone resistance, which indicates the transition into the stiffer GTF formation.

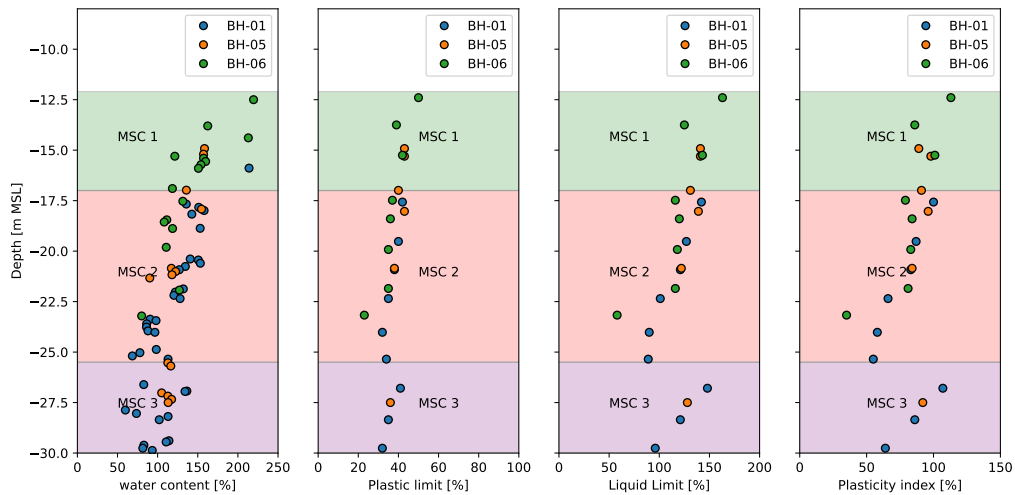


Figure 6.4: Watercontent & Attenberg limits

Figure 6.4 displays the result of index testing on samples from boreholes BH-01, BH-05 and BH-06. The index tests comply with the soil profile based on CPTu-01, although interface depth between MSC2 and MSC3 is located 2.5m deeper. This is due to spacial variation in layer thickness combined with the distance between the boreholes and the CPTu.

The B_q parameter was calculated for the initial situation, as shown in figure 6.5. MSC1 is categorized as clay, with a B_q value of about 0.4 and q_t values ranging from 0.05MPa to 0.4MPa. MSC2 is classified as silty clay due to lower B_q values and higher q_t values. For MSC3, the soil consists of clay with B_q values of approximately 0.45 and a q_t value around 0.6MPa. The relationship between B_q value and matching CPTu strength with the SHANSEP predicted strength is less prominent in this project, as is noticeable in figure 6.5(right). This might be a consequence of the very low cone resistance values: partial drainage has a smaller effect on the correlated strength.

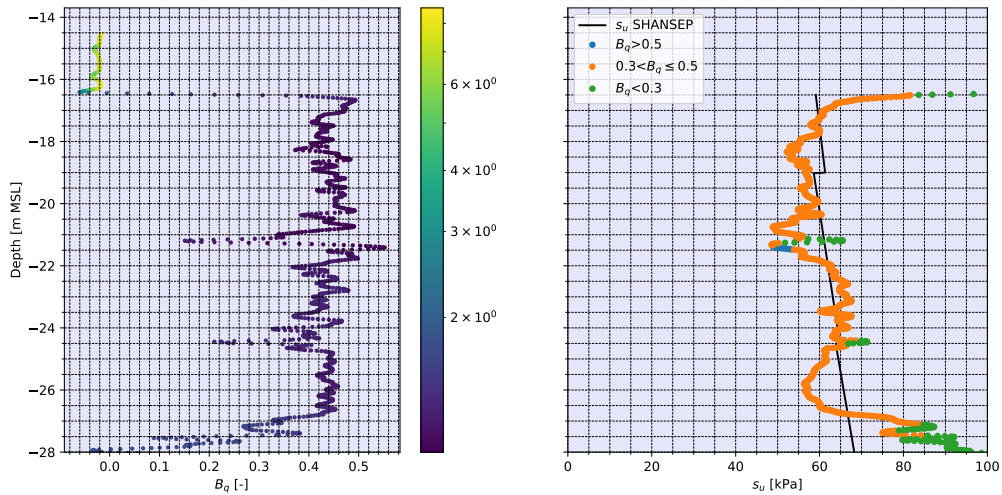


Figure 6.5: B_q parameter CPTu-01

6.2.1. Coefficient of consolidation

The results of 1D consolidation tests on samples extracted from borehole BH-01 and BH-07 are depicted in figure 6.6. The coefficient of vertical consolidation (C_v) is determined for various load steps, namely 5kPa, 10kPa, 20kPa, 40kPa, 80kPa, and 160kPa. For the method of estimating the vertical consolidation coefficient, please refer to section 4.2.5. Values of C_v obtained from load steps lower than the in situ preconsolidation stress, augmented by an additional 10kPa to account for uncertainties in preconsolidation stress estimation, have been excluded from the analysis. Load steps lower than the in situ preconsolidation stress result in values of C_v representing unloading/reloading conditions rather than primary consolidation.

The top layer exhibits C_v values of $1.0e-8m^2/s$ to $2.0e-8m^2/s$. For the intermediate clay layer, the C_v value is estimated to between $2.5e-8m^2/s$ and $7.0e-8m^2/s$. The third layer has consolidation properties similar to the top soil, with minimum C_v values of $1.0e-8m^2/s$ in the middle of the layer to $3.0e-8m^2/s$ at the bottom of the layer.

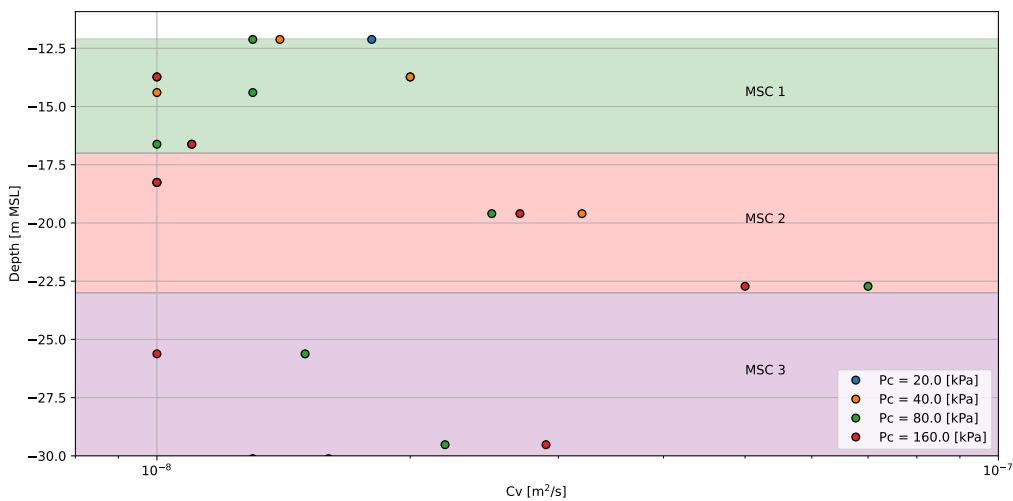


Figure 6.6: BH-01: Coefficient of consolidation

6.2.2. Geo-hydrology

No data regarding the initial pore pressure distribution was available for the Marine Soft Clay and underlying layers. It is therefore assumed that the initial pore pressure distribution is governed by the Mean Sea Level. As the Marine soft Clay lays on top of GTF clay, influence of a higher hydraulic head in a deeper layer, if present, will be limited.

After placement of the fill, the phreatic surface rises to 0.5m MSL, as is displayed in figure 6.7. The new phreatic surface is used for the calculation of the effective fill weight.

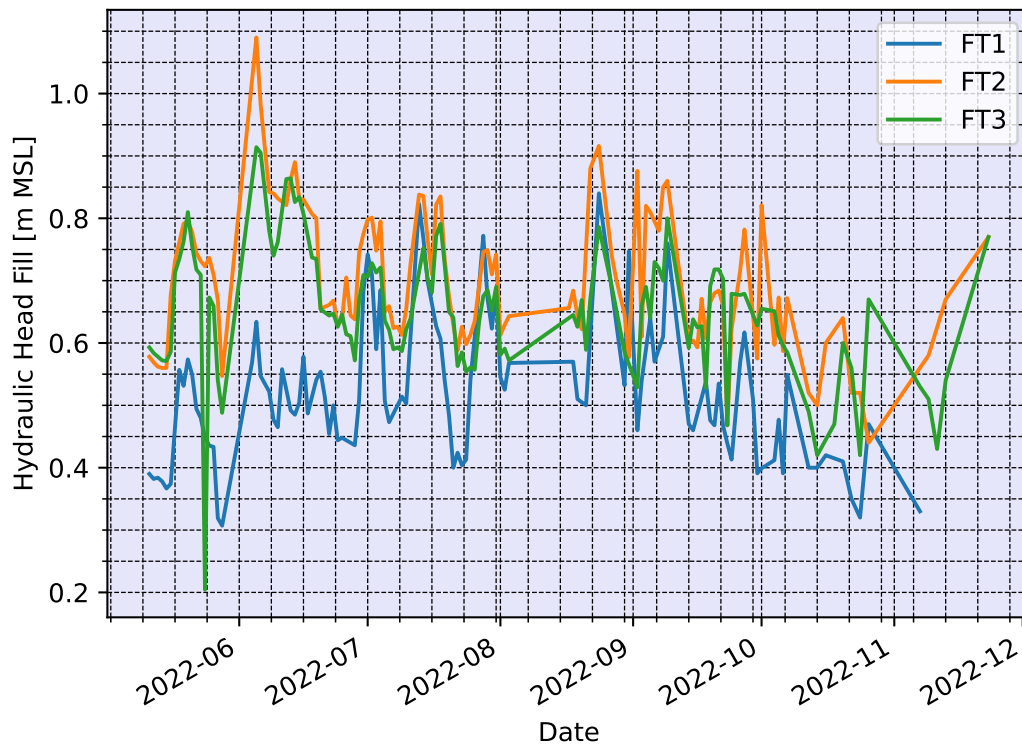


Figure 6.7: Hydraulic head in the sand fill

6.2.3. N_{kt} and SHANSEP S

To establish the N_{kt} factor for the correlation between undrained shear strength (s_u) and corrected cone resistance (q_t), a procedure involves plotting the s_u values obtained from undrained shear stress tests against the corrected cone resistance minus the total vertical stress at the corresponding depth. The laboratory undrained shear strength tests are carried out on samples extracted from boreholes BH-01, BH-02, BH-05, and BH-06. Additionally, field vane tests are conducted in boreholes BH-03 and BH-04.

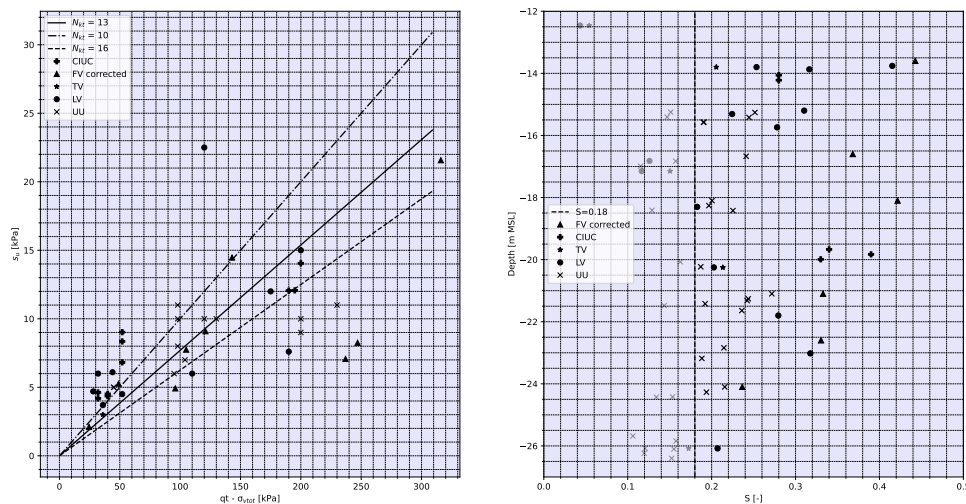


Figure 6.8: N_{kt} and SHANSEP S

On the right-hand side, figure 6.8 showcases the SHANSEP S factor variation with depth. The SHANSEP S factor values are obtained from various tests, including Fieldvane (FV), Torvane (TV), Laboratory vane (LV) tests, and UU triaxial tests. The tests results are adjusted for overconsolidation ratio (OCR) using the SHANSEP framework, with a SHANSEP m equal to 0.91. Tests yielding a SHANSEP S factor lower than 0.18 are depicted with reduced opacity. Investigation of marine clays by the Norwegian Geotechnical Institute (NGI) were summarized by Yang et al. (2019), the SHANSEP S values in triaxial compression are generally between 0.27 and 0.35. An exception was found by DeGroot (2000) who found a SHANSEP S value of 0.18 which will be used as the minimal value. The general picture is that most laboratory shear tests show small values for the SHANSEP S factor. For the tests individually, the following was observed:

- The results from the UU tests exhibit a wide range of values, with a significant portion yielding very low shear strengths and SHANSEP S values as low as 0.12. The majority of UU tests recorded SHANSEP S values below the predetermined threshold of 0.18, necessitating their exclusion from the analysis. These findings align with the conclusions drawn by Ladd and DeGroot (2003) as referenced in the literature study.
- The LV tests demonstrate a substantial range of SHANSEP S factors, with the majority of tests surpassing the threshold of 0.18.
- Only a limited number of TV tests were conducted, and the SHANSEP S factors obtained from these tests exhibit values that are in close proximity to the 0.18 boundary.

The relatively low SHANSEP S values observed in the laboratory tests may be attributed to sample disturbance. This is despite that samples with unusually low water content, which deviated significantly from the expected values based on weight tests, were eliminated from the analysis.

The field vane (FV) tests yield higher SHANSEP S values compared to the laboratory tests. Figure 6.9 (right) provides evidence that the field vane results align well with existing literature. Further elaboration on this observation will be provided later. Considering the laboratory tests presented in figure 6.8, a SHANSEP S value of 0.25-0.32 appears to be a reasonable estimation for MSC1 and MSC2. For MSC3, a lower SHANSEP S of 0.20-0.25 seems suitable, although little tests on this layer were performed.

The left side of figure 6.8 depicts the relationship between undrained shear strength obtained from both laboratory tests and field tests, plotted against the corrected cone resistance minus the total vertical stress at the respective depth. Laboratory tests with SHANSEP S values below 0.18 were excluded from the analysis. The N_{kt} factor is determined by fitting a line through the data points originating from

the origin. Based on the test data, a N_{kt} factor of 13 appears to be a suitable fit.

Figure 6.9 (left) showcases the variation of undrained shear strength over depth using a Cone Penetration Test (CPTu) with an N_{kt} factor of 13, alongside the results obtained from laboratory tests. The CPTu results exhibit a strong correlation with the corrected field vane tests in the first 10 meters of depth. However, the laboratory vane tests yield higher strength values compared to the correlated strength derived from CPTu. On the other hand, the UU triaxial tests provide a lower bound estimate of the measured shear strength obtained from CPTu.

Figure 6.9 (right) exhibits the results of field vane tests without OCR correction, displayed over depth. Additionally, the graph illustrates the relationships between liquid limit, preconsolidation stress, and undrained shear strength derived from field vane tests according to the studies conducted by Hansbo (1957). The relationships between plasticity index, preconsolidation pressure, and undrained shear strength obtained from field vane tests as described by Chandler (1988) and Larsson (1980) are also plotted. The field vane tests demonstrate a notable correspondence with the relationships established in the literature.

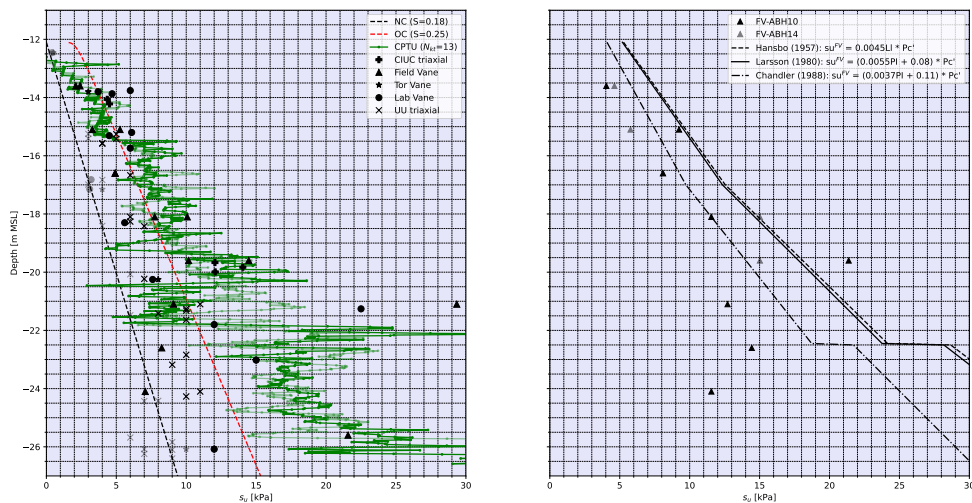


Figure 6.9: Labtests and CPTu

6.2.4. Site investigation summary

The soil parameters obtained from the site investigation campaign are presented in Table 6.1, providing a summary of the geotechnical properties. Appendix B contains further details on the additional site investigation conducted to determine parameters such as preconsolidation stress, compression ratio, recompression ratio, and creep coefficient.

Table 6.1: Summary of geotechnical soil properties

Property	Unit	MSC1	MSC 2	MSC 3
γ	[kN/m ³]	13.0	14.0	14.5
w	[%]	150	130	100
PI	[%]	90	67	74
LL	[%]	130	105	110
PL	[%]	40	38	36
CR	[-]	0.28	0.26	0.25
RR	[-]	0.02	0.02	0.02
C_α	[-]	0.01	0.007	0.006
C_h^1	[m ² /s]	1e-8	1e-7	2.5e-8
SHANSEP S	[-]	0.30	0.30	0.30
SHANSEP S + creep	[-]	0.25	0.25	0.25
SHANSEP m	[-]	0.92	0.92	0.92
m_{isotach}	[-]	26	34	38
p_c'	[kPa]	10	10	10

¹ $C_h = C_v$ derived from 1D consolidation tests

6.3. Consolidation

An excess pore pressure calculation is required to determine the SHANSEP undrained shear strength during consolidation. The excess pore pressure in the field trials is described by the radial consolidation theory of Barron (1948). The extended version by Conte and Troncone (2009) was implemented to simulate the load of the surcharge. The results of the model are displayed in figure 6.10 (FT1), figure 6.11 (FT2) and figure 6.12 (FT3). The graph includes the following elements:

- red dotted line: fill load over time, corrected for submersion using settlement plate data as displayed in figure B.4.
- black triangle: the excess pore pressure based on the minimal coefficient of consolidation obtained from 1D consolidation tests.
- black cross: the excess pore pressure based on the maximum coefficient of consolidation obtained from 1D consolidation tests.
- blue line: excess pore pressure of MSC1 measured by a piezometer, installed at depths of -16.5m MSL and -17.5m MSL for FT1 and FT3 respectively. For FT2, no piezometer was placed in MSC1. To account for settlement, the measured pore pressure is adjusted with the data of extensometers, which are also installed at the center of the field trials. For detailed monitoring data, please refer to Appendix B.
- orange line: the excess pore pressure of MSC2 measured by a piezometer installed at a depth of -22.5m MSL, -24.0m MSL and -22.0m MSL for FT1, FT2 and FT3 respectively. The measured pore pressure is corrected for settlement using extensometers.
- green line: the excess pore pressure measured by a piezometer installed at a depth of -27.5m and -24.0m MSL for FT1 and FT2. The measured pore pressure is corrected for settlement using extensometers.
- blue stars: the excess pore pressure of the piezometer in MSC1 fitted with the radial consolidation model using the horizontal consolidation coefficient as provided in the legend.
- yellow stars: the excess pore pressure of the piezometer in MSC2 fitted with the radial consolidation model using the horizontal consolidation coefficient as provided in the legend.
- green stars: the excess pore pressure of the piezometer in MSC3 fitted with the radial consolidation model using the horizontal consolidation coefficient as provided in the legend.

- vertical coloured lines: the moments at which CPTu's have been taken with the colours corresponding to the CPTu colours in section 6.4.

Although the construction of the fill took 60 to 80 days, the assumptions is made that the consolidation starts after placement of the PVD's. This assumptions simplifies the modelling of the horizontal consolidation since the dissipation during filling can be discarded. This simplified analysis is unlikely to influence the results because:

1. The vertical consolidation coefficient is very low, especially for the top layer.
2. The piezometers fitted with the consolidation model will be installed at least 1.5m under the seabed. The dissipation of excess pore water pressure is very limited below the top 1m of the subsoil, see figure B.3
3. A significant part of the load is applied after placement of the PVDs.

The horizontal coefficient of consolidation based on piezometer data is summarized in table 6.2.

Table 6.2: C_h based on piezometer data

	FT1 C_h [m^2/s]	FT2 C_h [m^2/s]	FT3 C_h [m^2/s]
MSC 1	1.60e-8	-	8.5e-8
MSC 2	6.20e-8	7.50e-8	9.0e-8
MSC 3	9.00e-8	1.10e-7	-

The fitted C_h value for FT1 is in correspondence with the C_h values derived from the 1D consolidation tests while FT2 and FT3 show higher values for C_h . This could be related to spacial variation as the distance from the location of sampling to FT2 and FT3 is around 300m. FT1 is relatively close ($\pm 100m$) to Borehole BH-01 compared to FT2 and FT3.

6.3.1. Consolidation Field Trial 1

The results of the radial consolidation model with a drain spacing of 1.0m in a triangular grid are displayed in figure 6.10. The VWP at -17.5m MSL (MSC 1) fits with a horizontal coefficient of consolidation (C_h) of $1.60e-8m^2/s$. This value is in the same order as the minimum C_h value obtained in the 1D consolidation tests ($1e-8m^2/s$) at corresponding depth. The VWP at -22.5m MSL (MSC 2) is fitted by a C_h of $6.20e-8m^2/s$. This is in the order of the 1D consolidation tests, where a C_v value of $7e-8m^2/s$ was found for the corresponding depth. The VWP at -27.5m MSL is fitted by a C_h value of $9.00e-8m^2/s$. This VWP is installed in or close to the GFT formation.

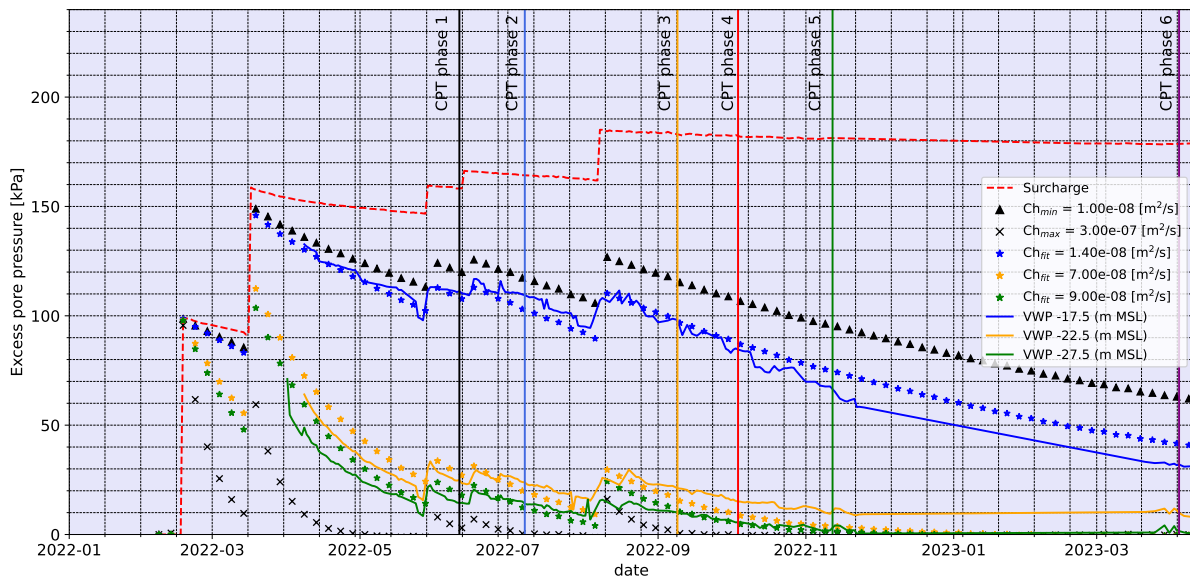


Figure 6.10: FT1: Radial Consolidation

6.3.2. Consolidation Field Trial 2

The results of the radial consolidation model with a drain spacing of 2.5m in a triangular grid are displayed in figure 6.11. The VWP at -17.5m MSL (MSC 2) is fitted with a C_h value of $7.5e-8m^2/s$. This value is close to the minimum C_h derived from 1D consolidation tests ($7e-8m^2/s$) at corresponding depth. The VWP at -22.5m MSL (MSC 3) is fitted with a horizontal consolidation coefficient of $1.00e-7m^2/s$. This is higher than the vertical consolidation coefficient derived from tests in the 1D consolidation apparatus, where a C_v coefficient of $7e-8m^2/s$ was found for the corresponding depth.

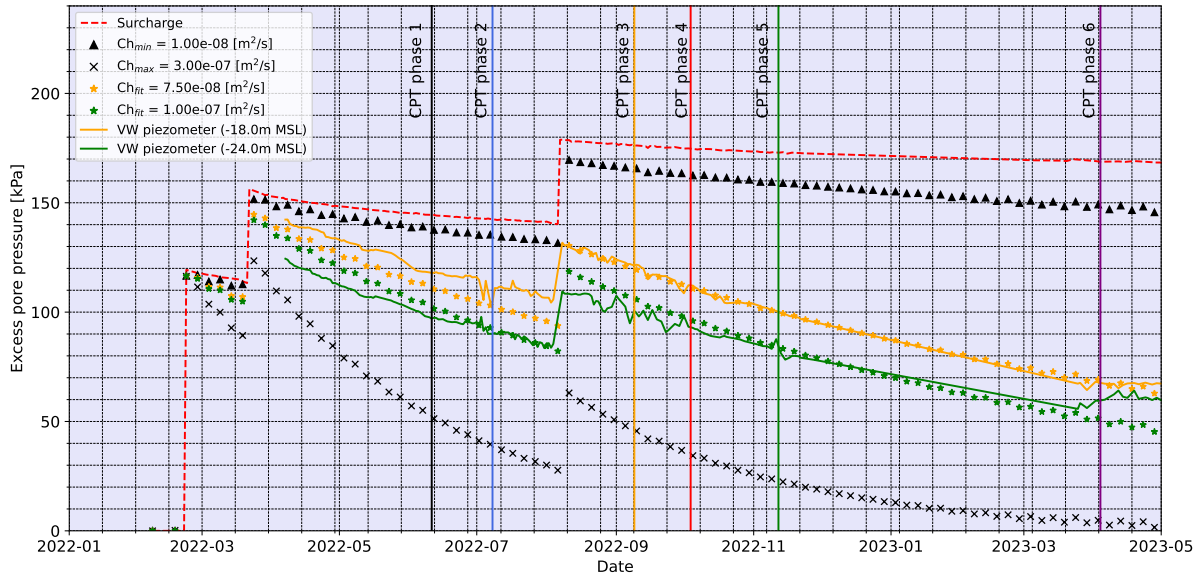


Figure 6.11: FT2: Radial Consolidation

6.3.3. Consolidation Field Trial 3

The results of the radial consolidation model with a drain spacing of 2.5m in a triangular grid and 2.0m of extra surcharge is displayed in figure 6.12. The VWP at -16.5m MSL can be fitted with a C_h of $6e-8m^2/s$. This value is larger than the value of vertical consolidation obtained in the 1D consolidation tests ($1e-8m^2/s$) at corresponding depth. The VWP at -22.0m MSL (MSC2) is fitted with a horizontal consolidation coefficient of $6.80e-8m^2/s$. This is close to the 1D consolidation test derived C_h of $7e-8m^2/s$.

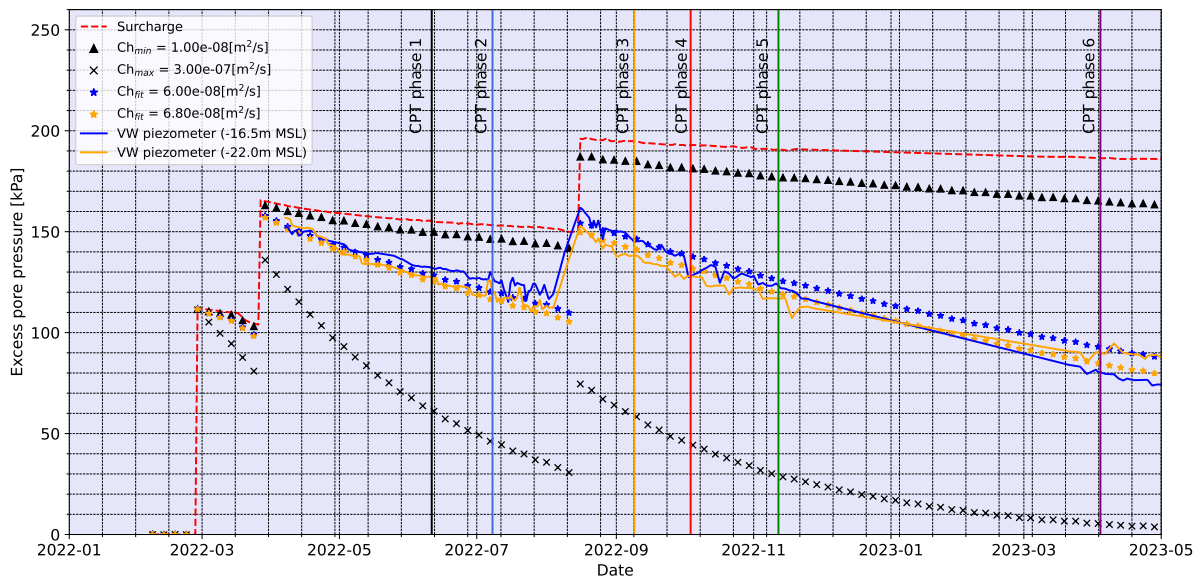


Figure 6.12: FT3: Radial Consolidation

6.4. Comparison SHANSEP and CPTu

Cone Penetration Tests (CPTu) were conducted at six different time points. Tables 6.3, 6.4, and 6.5 provide an overview of the CPTu dates and the corresponding fill elevation during those dates. The transition from fill (sand) to Soft Marine Clay is identified by a significant reduction in cone resistance, determining the bottom of the fill. The starting ground level recorded by the CPT rig establishes the top of the fill. It is important to note that the fill thickness can vary by up to 1m across the field trial.

Table 6.3: CPTu information FT1

	CPTu date	Fill elevation [m MSL]	Fill bottom [m MSL]
phase 1	2022-06-11	3.8	-15
phase 2	2022-07-08	4.8	-15.6
phase 3	2022-09-08	5.8	-15.8
phase 4	2022-10-04	5.9	-15.9
phase 5	2022-11-12	5.7	-16.15
phase 6	2023-04-04	5.5	-16.5

Table 6.4: CPTu information FT2

	CPTu date	Fill elevation [m MSL]	Fill bottom [m MSL]
phase 1	2022-06-10	4.2	-13.5
phase 2	2022-07-09	3.8	-14.2
phase 3	2022-09-10	5.9	-14.3
phase 4	2022-10-01	5.9	-14.4
phase 5	2022-11-09	5.8	-14.7
phase 6	2023-04-04	5.2	-15.1

Table 6.5: CPTu information FT3

	CPTu date	Fill elevation [m MSL]	Fill bottom [m MSL]
phase 1	2022-06-10	5.8	-13.5
phase 2	2022-07-09	5.6	-13.9
phase 3	2022-09-10	8.3	-14.3
phase 4	2022-10-01	8.2	-14.6
phase 5	2022-11-09	7.9	-15.0
phase 6	2023-04-04	7.3	-15.3

Figures 6.13, 6.16 and 6.19 show the undrained shear strength development in the Marine Soft Clay over time for each individual field trial. The figures contains the following elements:

- There are six graphs available, each representing a specific point in time during the consolidation process. The colors used to indicate different phases in the graphs align with the colored vertical lines shown in Figures 6.10, 6.11, and 6.12. The date of the corresponding Cone Penetration Tests (CPTu's) is provided above each graph. The time interval between the first five graphs is either 1 or 2 months. The final set of CPTu's is conducted approximately 5 months after Phase 5.
- For each phase of the field trial, a total of 5 Cone Penetration Tests (CPTu's) were conducted at specific locations: North, East, South, West, and center. The CPTu results from each location within a phase are depicted using the same color, but with varying brightness levels in the plots. This allows for a visual distinction between the individual CPTu measurements within each phase.
- A dotted line is included in the graph, representing the lower and upper bounds of strength determined by SHANSEP. This strength is derived using the theoretical excess pore pressures

calculated using the radial consolidation model. The input parameters for the model include the minimum and maximum values of horizontal coefficient of consolidation (C_h), C_h is assumed to be equal to C_v , C_v is determined in 1D consolidation tests. An OCR value due to creep for the SHANSEP calculation is determined with the isotach framework, see figures B.10, B.11 and B.12.

- A triangular marker is used to represent the undrained shear strength calculated using the piezometers and SHANSEP framework. The strength calculation is based on an effective stress estimated with the pore pressures measured by piezometer data. The contribution of creep to the OCR is accounted for using the Isotach model. The calculation of the OCR due to creep for the field trials can be found in figures B.10, B.11 and B.12.

The zero readings before and after each CPTu were checked to make sure that the tests were properly calibrated. The difference between the zero readings before and after for each CPTu is found in appendix B in figure B.5, figure B.6 and figure B.7. No significant deviation in zero readings were observed.

6.4.1. Field Trial 1

All CPTu's in figure 6.13 start at the interface of the seabed and the sand fill, hence the large strength at the very top of the graphs. The following observations can be made for FT1, with a 1.0m PVD spacing.

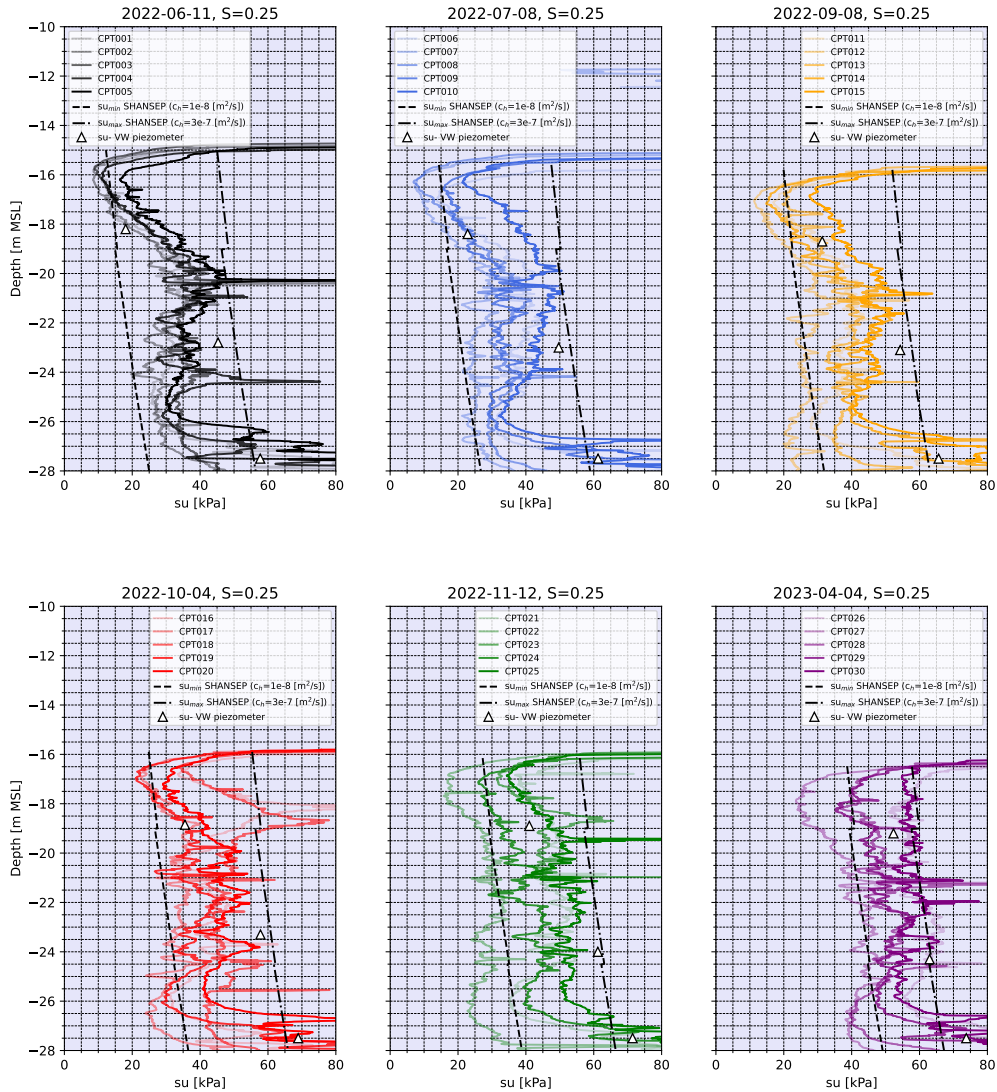


Figure 6.13: FT1: General strength comparison

The upper layer, spanning from -15.0m MSL to -18.5m MSL, exhibits a slow development of undrained shear strength, with a minimum strength of only 9kPa. Surprisingly, this minimum strength is even lower than the minimum predicted value based on SHANSEP with the lowest horizontal coefficient of consolidation based on the 1D consolidation test. In contrast, MSC2 from -18.5m MSL to -24.0m MSL demonstrates a higher strength, in line with a larger horizontal coefficient of consolidation found in the 1D consolidation test. A 2-meter thick layer between -24.0m MSL and -26.0m MSL poses lower strength than MSC2, likely a result of a lower SHANSEP S factor.

MSC2 in phase 6 reached, according to the piezometer at -22.5m MSL, a degree of consolidation of over 95%. The strength can be regarded as end of consolidation strength. The SHANSEP prediction in case of a C_h of $3e-7m^2/s$ can also be regarded as fully consolidated, since all pore pressures are dissipated as figure 6.10 indicates. For an SHANSEP S factor of 0.25, the SHANSEP prediction includ-

ing creep shows a strength prediction which is close to the CPTu correlated strength. The SHANSEP factor should be increased to 0.30 in case creep is not considered, see figure B.8 in appendix B. The SHANSEP S of 0.25 including creep is preferred since it is capable of capturing strength increase due to creep. Future CPTu's will show higher strength values as a result of creep, using a higher SHANSEP S of 0.3 while excluding creep can not account for this strength increase.

The SHANSEP undrained shear strength, calculated using pore pressure data from the piezometer located at -17.5m MSL, exhibits a reasonably good agreement when creep is taken into account, as indicated by the triangular marker. However, the strength estimation based on the VW piezometer appears to be lower than expected during the initial two phases. The introduction of an additional surcharge between phase 2 and phase 3 significantly increases the piezometer-based strength, while the impact on the CPTu correlated strength is comparatively less pronounced. In phase 6, the VW piezometer-based strength aligns well with the CPTu correlated strength.

The back calculation of SHANSEP strength for the piezometer installed at -22.5m MSL is substantially larger than the strength found in the CPTu's. This mismatch reduces over time as the piezometer measures low excess pore pressures from phase 3 (orange), most strength increase due to pore pressure dissipation has already occurred according to the piezometer. The CPTu measurements slowly catch up with the piezometer based strength. This phenomenon can be explained by the following considerations:

- Piezometer location relative to the PVDs: Although efforts were made to position the piezometer in the middle of two drains, the exact placement remains uncertain. Consequently, deviations from the ideal central position can significantly influence pore pressure measurements, particularly within the densely spaced PVD grid of 1m x 1m. It is worth noting that the CPTu's conducted in each phase also deviate from the center, implying that some of the CPTu measurements likely capture strengths close to those indicated by the VW piezometer.
- The CPTu estimated strength increases slower than consolidation would suggest. A similar deviation was noticed during the application of extra surcharge between phase 2 and phase 3: the piezometer based strength increased more than the CPTu based strength.
- It is possible that the piezometer was installed either within or near a thin permeable layer, as indicated by the presence of spikes in the CPTu profile between -23m MSL and -25m MSL. These layers may enhance the dissipation of pore pressure, potentially affecting the readings of the VW piezometer.

The relationship between the CPTu derived strength and the SHANSEP strength becomes closer as the excess pore pressure dissipates during consolidation. In Phase 6, it is observed that more than 95% of the excess pore pressures are dissipated, considering a C_h value of $3e-7m^2/s$. Specifically, CPT026 and CPT030 closely follow the SHANSEP prediction, except for the clay layer between -24m MSL and -26m MSL. This deviation is attributed to a lower SHANSEP S for MSC3, as will be discussed later. A reasonable SHANSEP S factor for MSC3 is 0.22, see figure B.9

After approximately one year of consolidation, the achieved strength exhibits significant variation over the 30m distance between the CPTu's in FT1. The measured strength ranges from 25kPa to 65kPa, corresponding to 38% to 100% of the final expected strength. The large range of strength is likely caused by variation in the distance between the CPTu's and the PVD's. On average, the strength reached after one year of consolidation is approximately 49kPa, which represents around 75% of the final predicted strength.

Figure 6.14 presents the initial undrained shear strength obtained from a marine Cone Penetration Test (CPTu) and the average of five CPTu's conducted during each of the six phases. To facilitate comparison between phases, the CPTu measurements are adjusted for settlement. The CPTu's from phases 1 to 5 are scaled to match the length of phase 6.

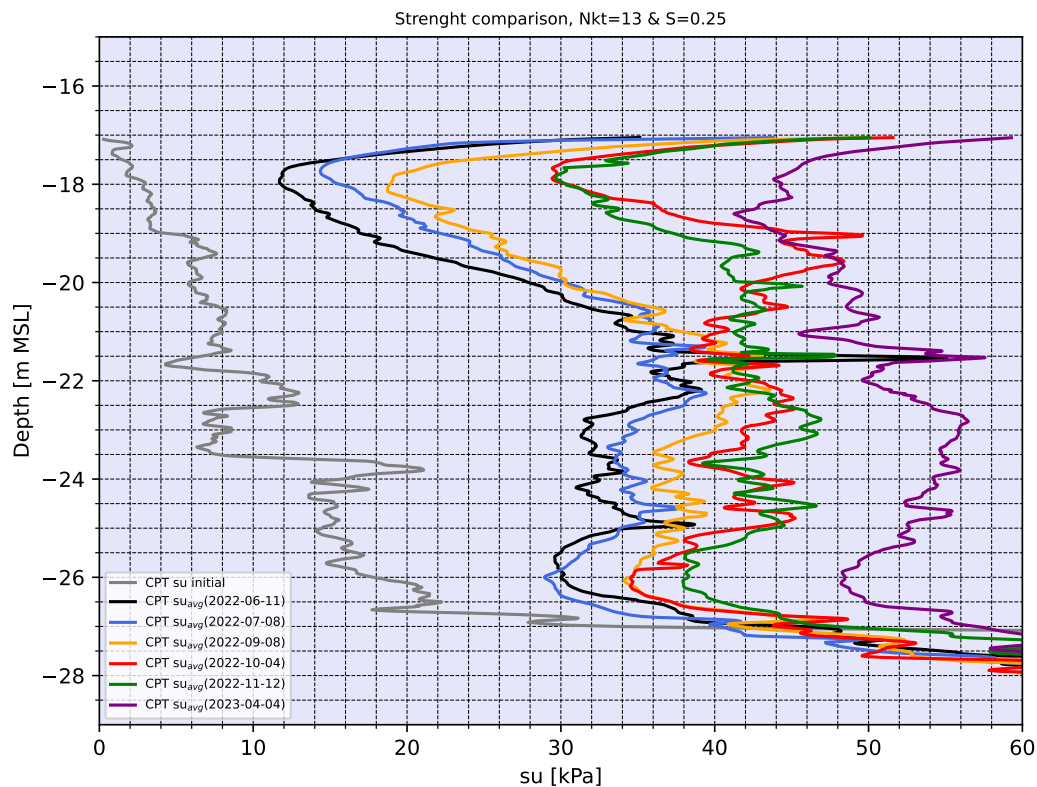


Figure 6.14: FT1: Average strength comparison

It is observed that, at certain depths, the average strength decreases relative to the earlier phases. This decrease can be attributed to averaging effects. Specifically, the average strength in October (red) is higher than the average strength in November (green) due to the influence of local high cone resistance values recorded in CPT016 and CPT018, which heavily impact the average value for October. The overall trend indicates that the average undrained shear strength increases as consolidation progresses, aligning with the expectations set by the effective stress theory. In the first layer, MSC1, a relatively slow consolidation process is observed, as evidenced by a modest 10kPa increase in strength based on the marine CPTu before the placement of the prefabricated vertical drains (PVD's) and phase 1 CPTu's.

On the other hand, MSC2 exhibits a more rapid increase in strength during the same time period, with the strength increasing from 12kPa prior to filling to 35kPa in phase 1. Subsequently, the rate of strength development diminishes after phase 1 due to a higher degree of consolidation that has already been achieved in this layer. As mentioned earlier, CPTu data indicates MSC3 having a lower strength due to a lower SHANSEP S factor. This is supported by the following observations:

- Although not many tests are available, the laboratory and field vane tests in figure 6.8 indicate a lower SHANSEP S between -24m MSL and -26m MSL.
- The lower strength is unlikely a result of slower consolidation: in that case, the average strength difference between MSC2 and MSC3 would decrease over time, as is observed for MSC1.

Figure 6.15 presents the temporal evolution of strength at different locations within the field trial. The left graph includes the piezometer data, as the VWP's are installed at the center of the field trial. The maximum distance between the CPTu's at each location (North, East, South, West, center) is only 2.5 meters. Despite this small distance, distinct local variations in the form of strength peaks are clearly evident. This phenomenon is particularly prominent within the first three meters of the clay layer. Notable examples of this variation can be observed in CPT016, CPT017, and CPT018, where a distinct

strong layer with a thickness of approximately two meters is identified. The presence of these localized variations highlights the spatial variability within the clay layer, particularly within the shallow depths.

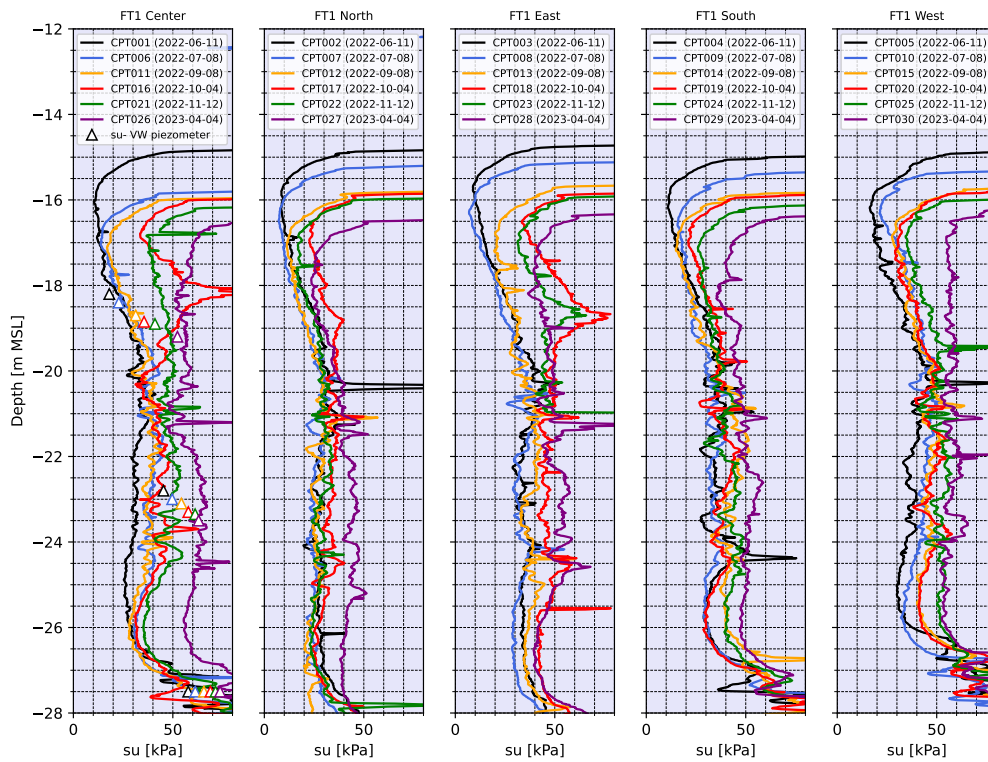


Figure 6.15: FT1: Strength per location

The center and western locations exhibit a tendency to approach the final strength range of 60kPa to 65kPa. It is plausible that the center location undergoes faster consolidation due to the limited influence of the field trial boundary. Outside the field trial, the drain spacing is maintained at 2.5m, which could potentially impact the consolidation process near the boundary and subsequently affect the rate of strength increase over time.

6.4.2. Field Trial 2

All CPTu's in figure 6.17 start at the interface of the seabed and the sand fill, explaining the high strength values at the top of the graphs. The following observations can be made for FT2, which has a 2.5m PVD spacing.

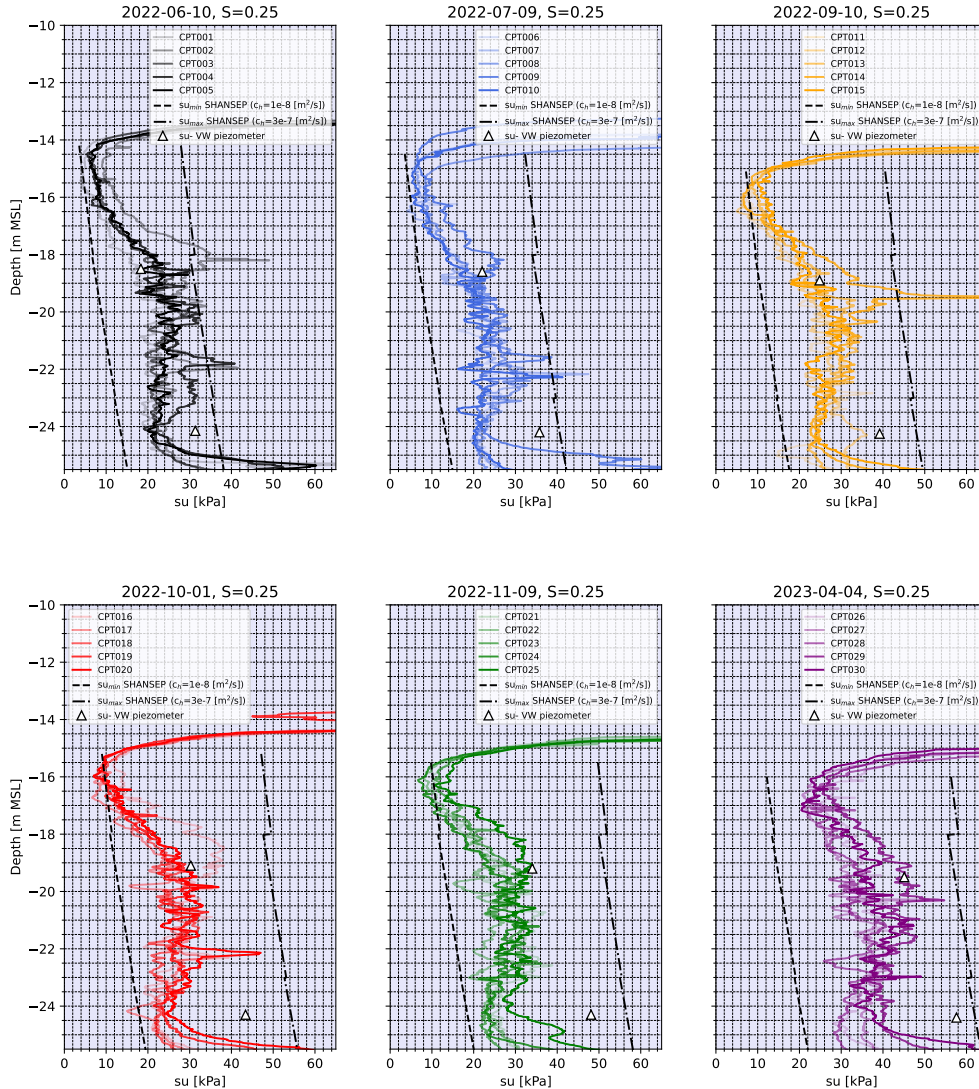


Figure 6.16: FT2: General strength comparison

The top layer from -14.0m MSL to -18.0m MSL shows a slow development of undrained shear strength and a minimum strength of only 5kPa, approaching the minimum predicted value based on SHANSEP combined with the lowest vertical coefficient of consolidation found in the 1D consolidation test. The layer from -18.0m MSL to -22.0m MSL shows a higher strength, a result of a higher horizontal coefficient of consolidation as confirmed by figure 6.6. A 2m thick layer between -22.5m MSL and -24.0m MSL shows similar behaviour as the top layer: the strength is low and develops slowly towards the SHANSEP predicted value. The strength based on the maximum 1D consolidation test coefficient of consolidation is not reached. The actual coefficient of consolidation lies between the minimum and maximum 1D consolidation test value.

The strength based on the pore pressure measurements of the piezometer installed at -18.0m MSL in MSC2 demonstrates reasonable agreement with the strength derived from the CPTu measurements.

However, a significant disparity is observed between the back-calculated SHANSEP strength for the piezometer located at -24.0m MSL in MSC3 and the strength determined from the CPTu's. The difference between the VWP strength and the CPTu strength exhibits an increasing trend from phase 1 to phase 5, followed by a reduction in phase 6. This observation suggests several potential explanations:

- The placement of the VWP may not be precisely at the midpoint between two PVDs. Consequently, most of the CPTu measurements are performed in the middle of two PVD's, with the exception of CPT012 and CPT024, which are in closer proximity to the VWP location.
- The VWP may be situated within a coarser layer, as indicated by the characteristics observed in CPT012 and CPT025, showing local increase in strength.

After one year of consolidation with a PVD spacing of 2.5m x 2.5m, it is observed that the achieved strength levels are still below the SHANSEP predicted final strength. The strength values obtained after approximately one year of consolidation range from 20kPa to 45kPa, which corresponds to 33% to 70% of the anticipated final strength. The average strength measured after one year of consolidation is approximately 38 kPa, representing 58% of the predicted final strength.

The disparity between the minimum and maximum strengths obtained from CPTu data is less pronounced than what was noted in FT1. The increased spacing between drains reduces the impact of the CPTu distance to the PVD's. This is because any deviation from the midpoint between two PVDs results in a smaller disparity in pore pressure compared to the 1m spacing of FT1.

Figure 6.17 displays the initial undrained shear strength based on a marine CPTu and the average of the 5 CPTu's taken during each of the 6 phases. Settlement was corrected to facilitate the comparison of the phases. The CPTu's of phases 1 to 5 are scaled to the length of phase 6.

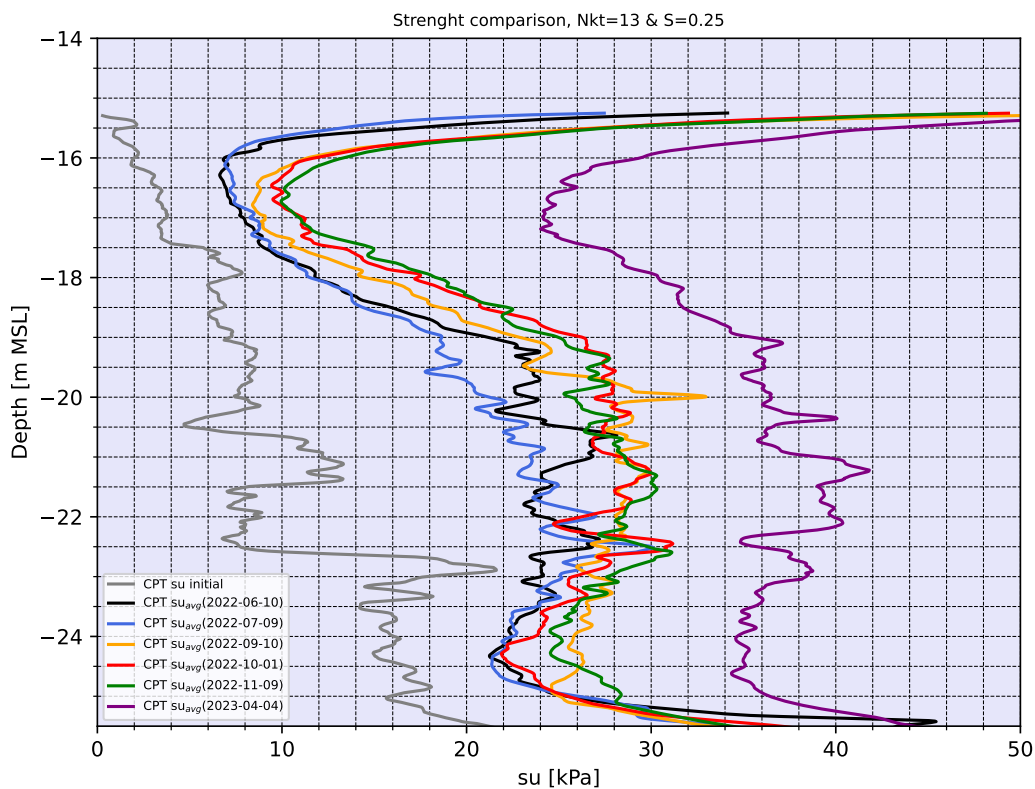


Figure 6.17: FT2: Average strength comparison

The strength development in FT2, particularly in the top layer, exhibits an interesting trend. The undrained shear strength, as correlated with CPTu measurements, increases from 7kPa in phase 1

(2022-06-10) to 10kPa in phase 5 (2022-11-09), indicating a modest increase of only 3kPa over a period of 5 months. Surprisingly, in the subsequent 5 months, the undrained shear strength further rises from 10kPa to 24kPa, representing a substantial increase of 14kPa. This observation appears contrary to the expectations based on consolidation theory, where consolidation typically slows down as excess pore pressure dissipates.

In the first five phases, the minimum undrained shear strength derived from CPTu measurements aligns with the minimum shear strength ($s_{u,min}$) determined by combining the minimal horizontal coefficient of consolidation obtained from 1D consolidation tests with the SHANSEP model. However, in phase 6, the minimum CPTu-correlated shear strength is approximately twice the value of $s_{u,min}$.

One possible explanation for this discrepancy is the influence of averaging. The depth difference between the lowest point in phase 6 CPTu measurements and the lowest point in phase 5 is approximately 1.0m, leading to variations in the average strength. Additionally, the CPTu's conducted in phase 6 exhibit small spikes in strength within the first 2 meters, further contributing to the overall average.

However, it remains unclear why the smallest measured CPTu strength increases from 4kPa to 7kPa in the initial 5 months and then experiences a significant jump from 7kPa to 20kPa in the subsequent 5 months. No additional preload or PVDs were introduced in or near the field trial. Settlement data and piezometer data do not show an acceleration in consolidation.

Figure 6.18 illustrates the evolution of strength over time at different locations within the field trial. The first graph includes the piezometer data, as the VWP's are positioned at the center of the field trial. At the surface, the maximum distance between CPTu's at each location is only 2.5m. Unlike in FT1, there is less presence of localized high strength areas within the first 3 meters of the soil profile. However, some localized strength variations are observed around a depth of approximately -19m MSL, as indicated by CPT02, CPT014, and CPT016. Considering the boundaries of the field trial, no significant influence is expected, as PVD's with the same spacing are installed outside the field trial. The strength development observed at the center location is consistent with the overall trend observed at other locations in the field trial.

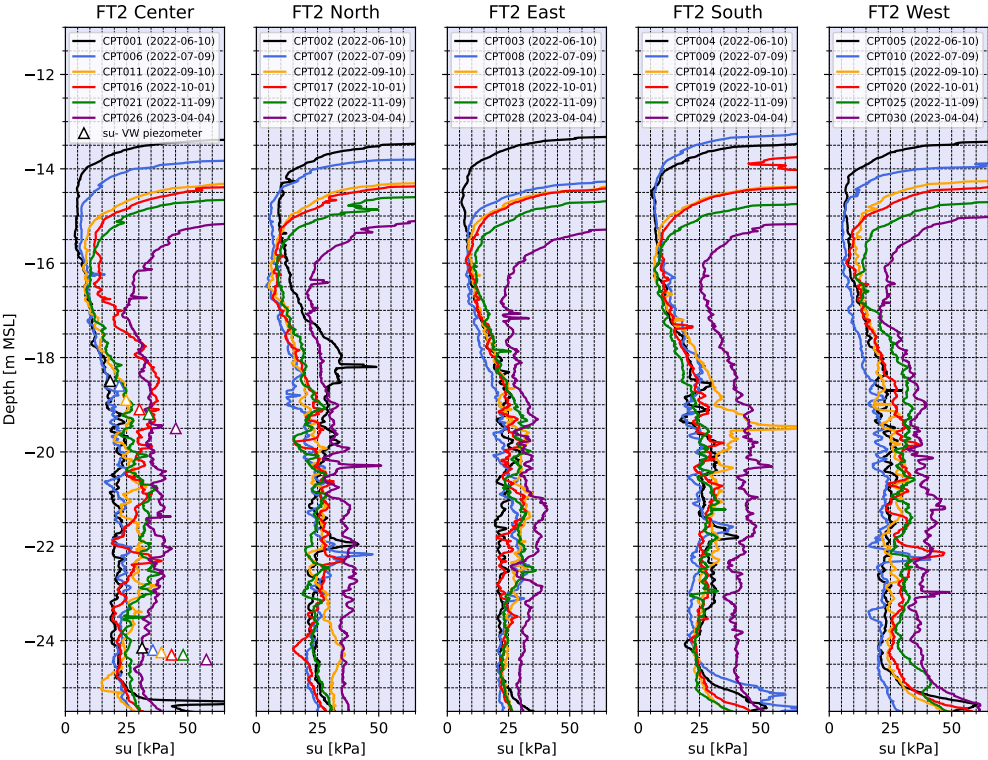


Figure 6.18: FT2: Strength per location

The piezometers installed in MSC2 at -18m MSL correspond well with the correlated CPTu strength. However, the piezometer installed in MSC3 at -24.0m MSL yields a calculated strength that is twice the value of the CPTu-correlated strength.

6.4.3. Field Trial 3

All CPTu's depicted in Figure 6.19 commence at the interface between the seabed and the fill. The following observations can be derived from the FT3 field trial, which features a PVD spacing of 2.5m and an additional 2.0m surcharge.

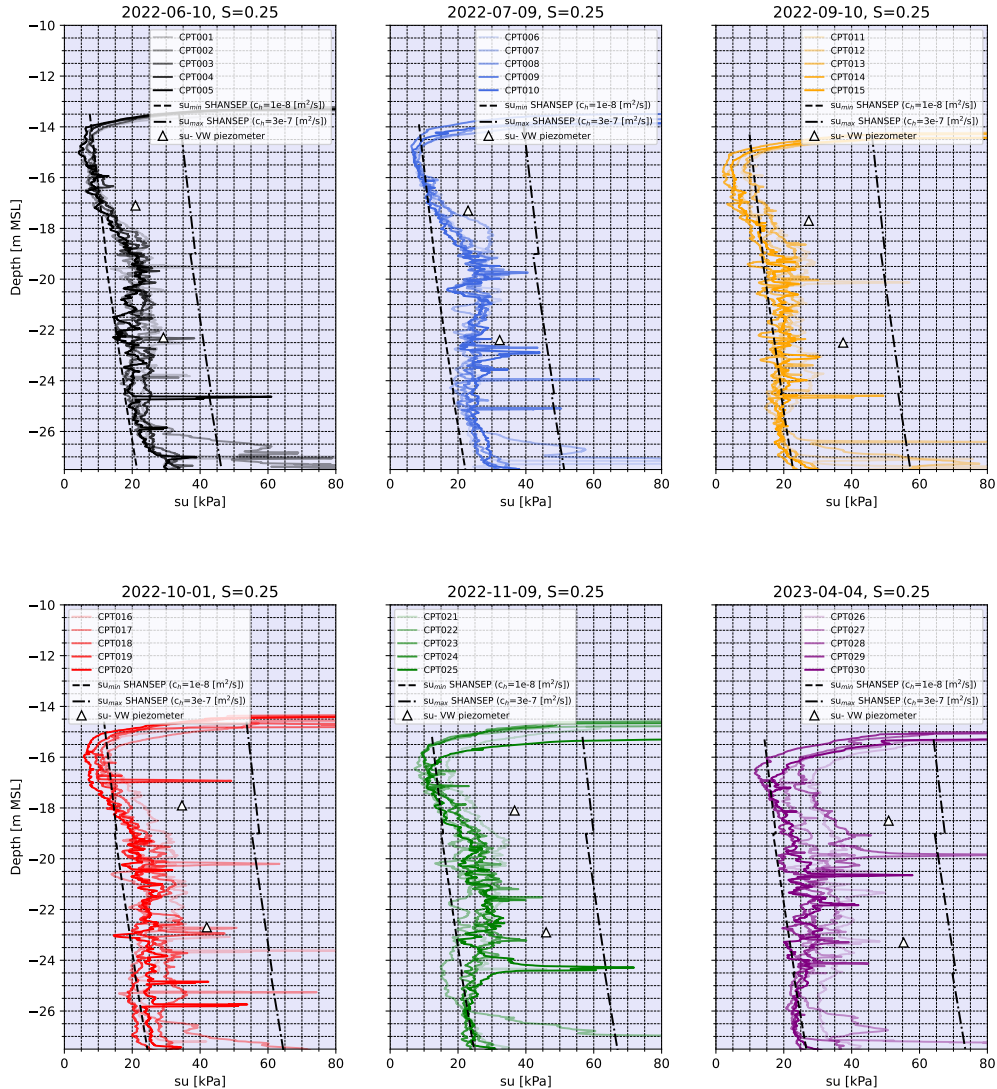


Figure 6.19: FT3: General strength comparison

The MSC1 layer, between -14.0m MSL to -18.0m MSL, exhibits a relatively low strength and gradual strength development. The minimum shear strength obtained from CPTu measurements closely aligns with the predicted minimal undrained shear strength based on SHANSEP analysis. In contrast, the intermediate layer MSC2, ranging from -18.0m MSL to -25.0m MSL, demonstrates higher strength due to more advanced consolidation resulting from a higher consolidation coefficient. The thin layer of MSC3 displays a similar trend as MSC1, characterized by slow strength development attributed to sluggish consolidation processes.

The back calculation of undrained shear strength using the SHANSEP framework, based on pore pressure measurements from the piezometer located in MSC1 at -16.5m MSL, consistently yields higher values compared to the CPTu correlated strength throughout all phases. Similarly, the piezometer installed in MSC2 at -22.0m MSL demonstrates an overestimation of undrained shear strength values when back calculated using SHANSEP, particularly following the introduction of a 2m extra surcharge

between phase 2 and phase 3. Notably, the placement of this 2m extra surcharge has minimal impact on the CPTu correlated strength, similar to the conclusions drawn for FT1.

After one year of consolidation, the piezometer data indicates a degree of consolidation of approximately 65%. In phase 6, the CPTu measurements exhibit a strength ranging from 12kPa to 35kPa, corresponding to a degree of consolidation of 20% to 58%.

Figure 6.20 depicts the temporal evolution of average strength based on the 5 CPTu measurements conducted in each phase, along with the initial strength derived from a marine CPTu. The observed average strength development aligns with the anticipated pattern: the strength of MSC1 gradually converges with the more rapidly consolidating MSC2 layer, while MSC3 lags behind in terms of strength development. It is worth noting that Phase 3 (orange) exhibits unexpectedly low values, even lower than the strength recorded in Phase 1.

There is no significant discernible effect on the strength development in terms of the additional 2.0m surcharge when comparing FT3 to FT2 (see Figure 6.17). In fact, the average strength recorded in phase 6 of FT3 is observed to be even lower than the strength measured in FT2 without the additional surcharge. It is noteworthy that the distance between the two field trials is merely 100m, with identical seabed depths and PVD spacing.

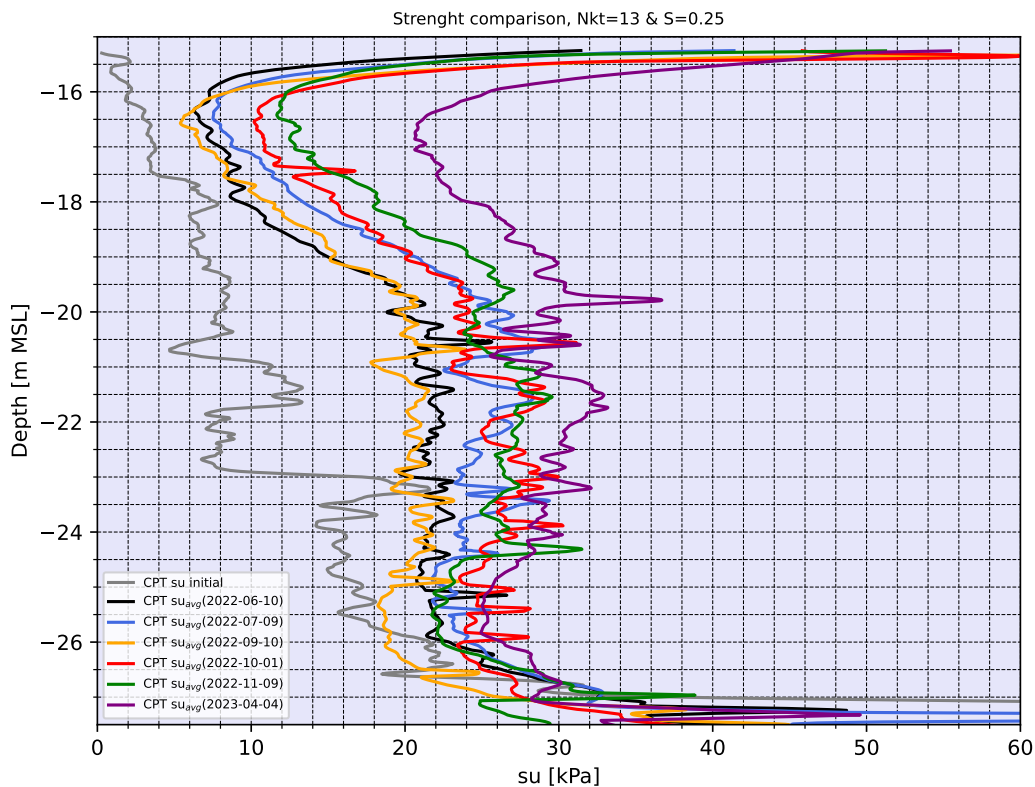


Figure 6.20: FT3: Average strength comparison

However, it should be noted that the impact of the 2.0m extra surcharge becomes evident in terms of settlement, as it leads to an accelerated settlement rate after its placement. Consequently, the total settlement observed in phase 6 of FT3 surpasses that of FT2, this is partly explained by the fact that the soft soil deposit is 2m thicker.

Figure 6.21 illustrates the undrained shear strength per location, as determined through CPTu correlations. The center location incorporates the data obtained from piezometer measurements, given their installation at the center of the field trial. Notably, localized zones with higher strength values are

observed in the northern and eastern locations.

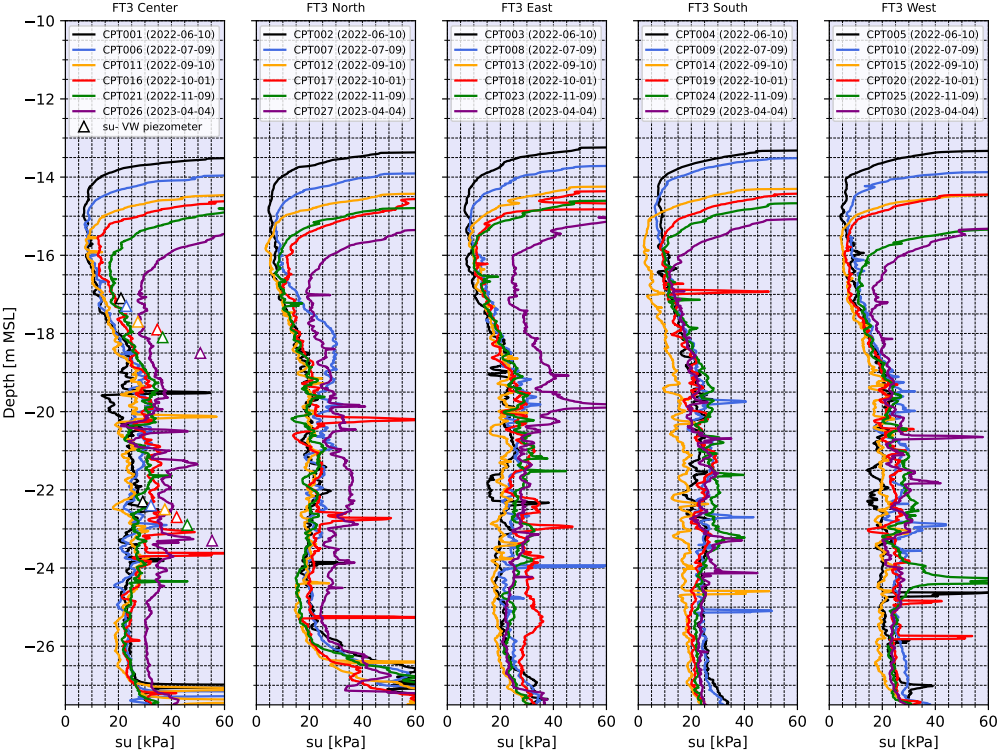


Figure 6.21: FT3: General strength comparison

7

Project comparison

Strength development for a dike reinforcement project at the Markermeerdijken was considered in Chapter 5, while strength development for a reclamation project was investigated in chapter 6. The nature of both project types introduces challenges, some of which are project dependent, others valid for both project types. This chapter will consider differences and similarities between both projects.

7.1. Strength characteristics

The SHANSEP parameters and the N_{kt} factors used for the CPTu correlated strength are summarized in table 7.1. The strength ratio of clay Calais is similar to the strength ratio of Marine Soft Clay 1 and Marine Soft Clay 2. The strength ratio of clay Duinkerke and Peat are larger than those of the Marine Soft Clay.

The SHANSEP m factor of the Marine Soft Clay is larger than for the soils present at the Markermeerdijken, a smaller strength lost due to preload removal is expected for the reclamation.

In terms of N_{kt} factor, the reclamation site requires a lower value compared to the Markermeerdijken. A separate N_{kt} value for peat was computed, which turned out to be not very different from the N_{kt} of the clay layers.

Table 7.1: Strength parameters

	SHANSEP S + creep	SHANSEP S	SHANSEP m	N_{kt}
<i>Reclamation</i>				
Marine Soft Clay 1	0.25	0.29	0.92	13.0
Marine Soft Clay 2	0.25	0.29	0.92	13.0
Marine Soft Clay 3	0.22	0.25	0.92	13.0
<i>Markermeerdijken</i>				
Peat	0.33	0.43	0.88	16.6
Duinkerke Clay	0.27	0.35	0.85	16.0
Calais Clay	0.22	0.30	0.85	16.0

7.2. Similarities

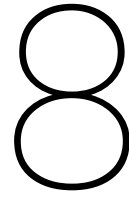
The following similarities between SHANSEP strength prediction for the dike project and the Reclamation project were observed:

- End of consolidation strength prediction: for both projects the end of consolidation strength is predicted with reasonable accuracy, silty layers excepted.
- Settlement of preload: although the fill measured settlements up to 4m, where the dike project settles 1.4m, both cases submersion of the preload should be considered. Due to the larger fill thickness compared to the preload thickness of the Markermeerdijken field trials, the relative reduction of preload effectiveness is similar.

7.3. Differences

Most differences between the reclamation project and the dike project are in the fact that for one project, strength during consolidation is considered which brings many more uncertainties, while the dike project did not consider strength during consolidation. A large uncertainty in pore pressure is caused by local variations in consolidation coefficient and unknown position of measurement equipment relative to the PVD's. More general differences between the two projects are mainly:

- Availability of site investigation data: the collection of data offshore is expensive, this results in a lower availability of good quality data, increasing prediction uncertainty. Ideally, the N_{kt} is determined with laboratory tests as close as possible to the CPTu. In the reclamation project, this distance is often more than hundreds of meters, while in the dike project a higher density of site investigation tests are available.
- Thickness of the preload: the preload at Markermeerdijken has a height of 5m, while the reclamation fill has a thickness of 15m to 22m. In the first place, this leads to a larger settlement and strength increase due to the larger preload magnitude. Second, predrilling can negatively effect CPTu accuracy according to Sandven (2010). Predrilling through 20m of fill, in case of the reclamation project, could have a larger influence on CPTu accuracy then predrilling through a 5m preload, as is the case at the Markermeerdijken.



Discussion

8.1. Research Limitations

The assessment of undrained shear strength was carried out using CPTu tests with a class 1 cone. However, Sandven (2010) pointed out that CPTu tests might not retain their class 1 categorization when penetrating rigid layers, even with prior drilling. In the context of the Philippines field trials, the CPTu tests were executed through a sand fill with a thickness exceeding 20 meters. This situation raises apprehensions regarding the reliability of the CPTu outcomes, particularly due to the notable variations observed. Furthermore, the absence of documentation detailing the operators responsible for each CPTu test introduces an additional source of uncertainty. The operator's influence on the precision of a CPTu is noteworthy, as discussed by Kardan et al. (2016).

Moreover, there has been a scarcity of site investigation carried out in the immediate vicinity of the field trials for the Philippines reclamation project. When combined with the significant variability observed in the boreholes throughout the site, it gives rise to uncertainties regarding the applicability of the soil parameters established from the field trials.

8.2. Suggestions for future research

This research focused on the accuracy of undrained shear strength prediction with the SHANSEP framework. As often is the case, research leads to new questions and research recommendations, those are presented in this subsection.

The first suggestion for future research is to examine the enhancement of strength using a Finite Element Method (FEM). FEM can offer a more advanced way to assess how stress increases due to preloading, which could improve the prediction of undrained shear strength. Another benefit of using FEM is that it can help calculate a more accurate OCR (overconsolidation ratio) considering creep effects. Lastly, FEM can be used to more precisely determine how pore pressure is distributed, especially in cases where the distribution of pore pressure is not linear, as seen in the Markermeerdijken field trials.

The second suggestion is to research how large the influence of creep is on the undrained shear strength. The two case studies in this research focused on end of consolidation strength, performing extra CPTu's some months or years after consolidation could potentially reveal the practical strength gain due to creep.

Lastly, a research suggestion regarding the development of strength during consolidation could be put forward. In the context of the reclamation project, the observation was made that there is uncertainty in verifying strength due to an unknown distance between measurement equipment and PVD's. Additionally, the strength derived from CPTu measurements, piezometer-based assessments, and settlement data did not exhibit consistent patterns of development. It would be valuable to conduct a field trial similar to the Markermeerdijken trials, incorporating CPTu measurements during the consolidation phase. In this study, installing PVD's and piezometers before placing the preload could notably improve the accuracy of their placement. This might also reduce uncertainties related to the separation

distance between CPTu and PVD locations. This proposed approach could offer a more comprehensive understanding of the complex relationship among settlement, dissipation of pore pressure, and strength development.

Conclusion and Recommendations

9.1. Conclusions

The primary objective of this thesis was to acquire a comprehensive understanding of the various aspects that play a role in determining the accuracy of predictions generated by the SHANSEP (Stress History And Normalized soil engineering properties) framework. A key focus of interest was to identify and examine the limitations inherent in the SHANSEP framework, as well as to gain insights into the simplifications employed that may result in a reduction of SHANSEP prediction accuracy. This section summarizes the (sub)questions that were addressed during the research and provides a concise overview of the answers obtained.

The following aspects should be considered for the SHANSEP prediction of undrained shear strength development:

- Uncertainty in Pre Overburden pressure (POP): underestimating the POP results in an overestimation of the strength gain due to preloading.
- Depth influence: the efficacy of preload diminishes when the load area is relatively small in comparison to the depth.
- Submersion of surcharge: in case of high water tables, settlement leads to submersion of surcharge which significantly reduces the preload effectiveness, therefore reducing undrained shear strength increase.
- Creep: the SHANSEP S factor should be reduced if creep is considered. The end of consolidation strength will be the same, but strength increase due to creep after consolidation can be captured using the OCR computed with the isotach framework.
- Quality of laboratory data: prediction quality of the SHANSEP framework is largely determined by the amount of high quality laboratory tests available. The constant height DSS yields consistent values of SHANSEP S . Unconsolidated Undrained (UU) triaxial tests yield large spread and unrealistically low values of SHANSEP S , just as was observed by Ladd and DeGroot (2003). The Field Vane (FV) test results in SHANSEP S values in line with the findings of Chandler (1988). The Labvane (LV) tests yields realistic values of SHANSEP S , but also a fairly large spread.

For the verification of undrained shear strength during consolidation, the following aspects should be considered:

- The presence of courser particles in soft soils, indicated by a low pore pressure parameter B_q and higher corrected cone resistance q_t , induces higher strengths in CPTu tests due to partial drainage. This negatively affects correspondence between SHANSEP predicted strength and CPTu correlated strength.
- CPTu based strength and piezometer based strength show a poor correspondence: specifically, this discrepancy was most pronounced in layers which exhibit a relatively small horizontal coefficient of consolidation ($\approx 1e-8 m^2/s$). In these layers, the piezometer measurements consistently

indicated higher strength values compared to the CPTu results. However, the CPTu results layers with a higher coefficient of consolidation ($\approx 1e-7 m^2/s$) demonstrated a decent match with the piezometer measured based values.

- Prefabricated Vertical Drain (PVD) spacing: piezometers located in areas with larger drain spacing (2.5m) tend to exhibit a higher degree of overestimation in strength compared to the piezometers in the field trial with a 1m x 1m drain spacing. This overestimation of undrained shear strength based on piezometer readings could potentially be attributed to their placement relative to the PVD's, their positioning within or near thin permeable layers or installation effects.
- The short term increase in strength as determined by piezometers was found to be greater than the estimated strength increase based on CPTu measurements following the application of an additional surcharge. In the case of Field Trial 3 in the Philippines, where a 2.0m additional surcharge was applied, it resulted in the dissipation of pore pressure and additional settlement. However, the rate of strength increase in Field Trial 3 was not faster compared to Field Trial 2, which exhibited similar site characteristics.

The results of the Markermeerdijken field trials and the Philippines field trials can be compared. The strength development during consolidation is not compared since no CPTu data was acquired during consolidation at Markermeerdijken. The following was observed:

- The prediction of the end of consolidation strength of soft soils was accurate in the Markermeerdijken field trials. This can be attributed to high-quality laboratory tests, high-quality CPTu measurements, and low spatial variability. In the Philippines reclamation, the end of consolidation strength was predicted with decent accuracy and aligned well with piezometer-based strength. However, due to local variability and uncertainty in the distance between PVD and CPTu, only 2 out of 5 CPTu measurements provided values for the end of consolidation strength.
- The SHANSEP S factors excluding creep for the clay at Markermeerdijken (0.35 for Clay Duinkerke and 0.30 for Clay Calais) are slightly higher than the SHANSEP S at the Philippines (0.29 for MSC1 and MSC2, 0.25 for MSC3).

Site conditions play a major role in the development of undrained shear strength. The question was raised which conditions influence strength development. Based on the field trials, the following can be concluded:

- The consolidation process and the resulting strength development primarily depend on the spacing of drains, as was observed in the reclamation field trials. In the 1m x 1m field trial, it was observed that the undrained shear strength, as determined by CPTu measurements, reached a degree of consolidation ranging from 38% to 100% one year after the installation of PVD's. However, in field trials with a 2.5m drain spacing, the average consolidation based on CPTu measurements was limited to 20% to 70% only.
- The application of a preload does not yield a short-term increase in strength as measured by Cone Penetration Test (CPTu) correlations. However, a notable short-term effect is observed in the piezometer data, potentially due to the proximity of the piezometers to the PVDs. Interestingly, in the comparison between Field Trial 3 (FT3) and Field Trial 2 (FT2), the introduction of an additional 2.0m surcharge does not result in an additional increase in strength. Nonetheless, it does lead to the generation of additional pore pressure and settlement.

The overall conclusion suggests that the SHANSEP framework demonstrates suitability for predicting undrained shear strength in clay and peat. However, accurately predicting undrained shear strength during the consolidation process proves challenging. This challenge primarily arises from the inherent uncertainties associated with the consolidation phenomenon rather than limitations within the SHANSEP framework itself. It is worth emphasizing that the reliability and precision of predictions strongly depend on the availability of high-quality laboratory tests, preferably excluding Undrained Unconsolidated triaxial tests. Furthermore, it is important to note that the SHANSEP predicted strength shows a poor match with CPTu strength for soils responding partially drained in CPTu's, such as silts.

9.2. Recommendations

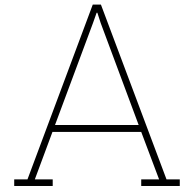
Based on this research, it is suggested to consider the following points when predicting the undrained shear strength using the SHANSEP framework:

- In scenarios characterized by elevated water tables, it is recommended to undertake predictions of final settlement and adjust the effective preload considering the influence of submersion. The presence of submersion exerts a significant effect on the ultimate strength due to preloading. It is imperative to account for this effect when estimating the final strength of the soil.
- It is advised to evaluate the presence of silt in soil by utilizing the parameter Bq , as the SHANSEP framework does not provide accurate results for soils which partially drain during CPTu. The DSS tests on silt yield a high SHANSEP S value which provide a bad fit with the CPTu strength. The question rises whether the undrained strength of soils responding partially drained to CPTu's should be considered. Eventually, drained or undrained response is dependent on the combination of consolidation coefficient and rate of loading. Furthermore, excess pore pressure should be able to drain somewhere, inclusion between two layer with a low consolidation coefficient could prevent this in case no PVD's are installed.
- To enhance the accuracy of soil testing, it is advisable to invest in high-quality Direct Simple Shear tests and field vane tests, while avoiding the utilization of Unconsolidated Undrained (UU) tests. Eventually, calculating slope stability is often done with the DSS strength ratio: this value is often lower than the triaxial compression strength and is reached at larger strains. usually, the largest part of a slope fails under a failure mode as simulated in a DSS tests, see figure 3.9.
- If long term strength prediction is required, the inclusion of creep in the SHANSEP prediction should be considered.
- It is not recommended to rely solely on piezometer data for obtaining in situ strength, as its positioning relative to the PVD's is uncertain.
- In case of a small preload area, account for depth effects.

References

- Barron, R. A. (1948). Consolidation of fine-grained soils by drain wells by drain wells. *Transactions of the American Society of Civil Engineers*, 113(1), 718–742.
- Bjerrum, L. (1967). Engineering geology of norwegian normally-consolidated marine clays as related to settlements of buildings. *Géotechnique*, 17(2), 83–118. <https://doi.org/10.1680/geot.1967.17.2.83>
- Casagrande, A. (1936). The determination of the preconsolidation load and its practical significance. *Proc. 1st Int. Conf. Soil Mech.*, 3–60.
- Chandler, R. J. (1988). *The in-situ measurement of the undrained shear strength of clays using the field vane*. ASTM International West Conshohocken, PA, USA.
- Conte, E., & Troncone, A. (2009). Radial consolidation with vertical drains and general time-dependent loading. *Canadian Geotechnical Journal*, 46(1), 25–36.
- Astm-d6535* (Standard). (2011). ASTM International. 100 Barr Harbor Drive, PO Box C700, West Conshohocken, PA 19428 2959, United States.
- De Koning, M., Simanjuntak, T., Goeman, D., Bakker, H., Haasnoot, J., & Bisschop, C. (2019). Determination of shansep parameters by laboratory tests and cptu for probabilistic model-based safety analyses. *Proceedings of the XVII European Conference on Soil Mechanics and Geotechnical Engineering*.
- DeGroot, D. (2000). Laboratory measurement of undrained shear behaviour of clays. *GEOSHORE-International Conference on Offshore and Nearshore Geotechnical Engineering, December 2-3, 1999., Oxford & IBH, New Delhi(India), 2000*, 133–140.
- Den Haan, E., & Edil, T. (1994). Secondary and tertiary compression of peat. *International Workshop on Advances in Understanding and Modelling the mechanical behaviour of Peat*, 49–60.
- Goodier, J. N., & Timoshenko, S. (1970). *Theory of elasticity*. McGraw-Hill.
- Hansbo, S. (1957). *New approach to the determination of the shear strength of clay by the fall-cone test*. Statens geotekniska institut.
- Jamiolkowski, M. (1985). New developments in field and laboratory testing of soils. *Proc. 11th. Int. Conf. on SMFE., San Francisco, CA, 1985, 1*, 57–153.
- K. Senneset, N. J. (1954). Shear strength parameters obtained from static cone penetration tests. strength testing of marine sediments; laboratory and in situ measurements. *Symposium San Diego, 1984, ASTM special technical publication*.
- Kardan, C., Viking, K., Nik, L., & Larsson, S. (2016). Influence of operator performance on quality of cptu results. *Proceedings of the 17th Nordic Geotechnical Meeting*, 153–158.
- Karlsrud, K., Lunne, T., Kort, D., & Strandvik, S. (2005). Cptu correlations for clays. *Proceedings of the 16th international conference on soil mechanics and geotechnical engineering*, 693–702.
- Ladd, C. (1991). Stability evaluation during staged construction: 22nd terzaghi lecture. *Journal of Geotechnical Engineering, ASCE*, 117, 537–615.
- Ladd, C., & DeGroot, D. (2003). Recommended practice for soft ground site characterization: Arthur casagrande lecture. 12th pcsmgc.

- Ladd, C., & Foott, R. (1974). New design procedure for stability of soft clays. *Journal of the geotechnical engineering division*, 100(7), 763–786.
- Larsson. (1980). Undrained shear strength in stability calculation of embankments and foundations on soft clays. *Canadian Geotechnical Journal*, 17(4), 591–602. <https://doi.org/10.1139/t80-066>
- Larsson, R., & Åhnberg, H. (2005). On the evaluation of undrained shear strength and preconsolidation pressure from common field tests in clay. *Canadian geotechnical journal*, 42(4), 1221–1231.
- Larsson, R., Bergdahl, U., & Eriksson, L. (1984). *Evaluation of shear strength in cohesive soils with special referens to swedish practice and experience*. Statens geotekniska institut.
- Luna, R., II, E. K., Santos, J., & P. (2020). Geohazard and geotechnical assessment for reclamation projects in the philippines. *Symposium San Diego, 1984, ASTM special technical publication*.
- Lunne, T., Eidsmoen, T., Gillespie, D., & Howland, J. D. (1986). Laboratory and field evaluation of cone penetrometers. *Use of In Situ Tests in Geotechnical Engineering*, 714–729.
- Olson, R. E. (1977). Consolidation under time dependent loading. *Journal of the Geotechnical Engineering Division*, 103(1), 55–60.
- Poulos, H. G., & Davis, E. H. (1964). Elastic solutions for soil and rock mechanics. *Geotechnique*, 14(4), 273–293. <https://doi.org/10.1680/geot.1964.14.4.273>
- Rémai, Z. (2013). Correlation of undrained shear strength and cpt resistance. *Periodica Polytechnica Civil Engineering*, 57(1), 39–44.
- Robertson, P. (1986). Use of piezometer cone data. *Proceedings of the ASCE speciality conference in situ '86: Use of in situ tests in geotechnical engineering, Blacksburg, 1263-80, ASCE*.
- Sandven, R. (2010). Influence of test equipment and procedures on obtained accuracy in cptu. *CPT10-2 nd International Symposium on Cone Penetration Testin, USA: Huntington Beach, CA*.
- Sheahan, T. C., Ladd, C. C., & Germaine, J. T. (1996). Rate-dependent undrained shear behavior of saturated clay. *Journal of Geotechnical Engineering*, 122(2), 99–108.
- Skempton, A. (1954). The pore-pressure coefficients a and b. *Geotechnique*, 4(4), 143–147.
- Technische Adviescommissie voor de Waterkeringen. (1989). *Leidraad voor het ontwerpen van rivierdijken deel 2*. Uitgeverij Waltman - Delft.
- Terzaghi, K., & Peck, R. B. (1948). Soil mechanics. *Engineering Practice. John Wiley and Sons, Inc., New York*.
- Verruijt, A. (2017). *An introduction to soil mechanics*. Springer Cham. <https://doi.org/10.1007/978-3-319-61185-3>
- Yang, S., D'Ignazio, M., Lunne, T., Andersen, K., & Yetginer, G. (2019). Undrained shear strength of marine clays based on cptu data and shansep parameters. <https://doi.org/10.32075/17ECSMGE-2019-0048>



Data Markermeerdijken

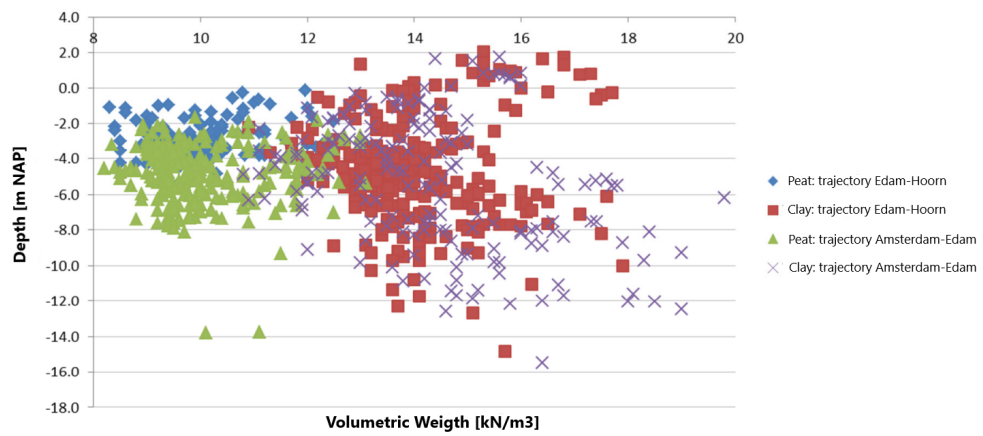


Figure A.1: Volumetric weight measurements Markermeerdijken

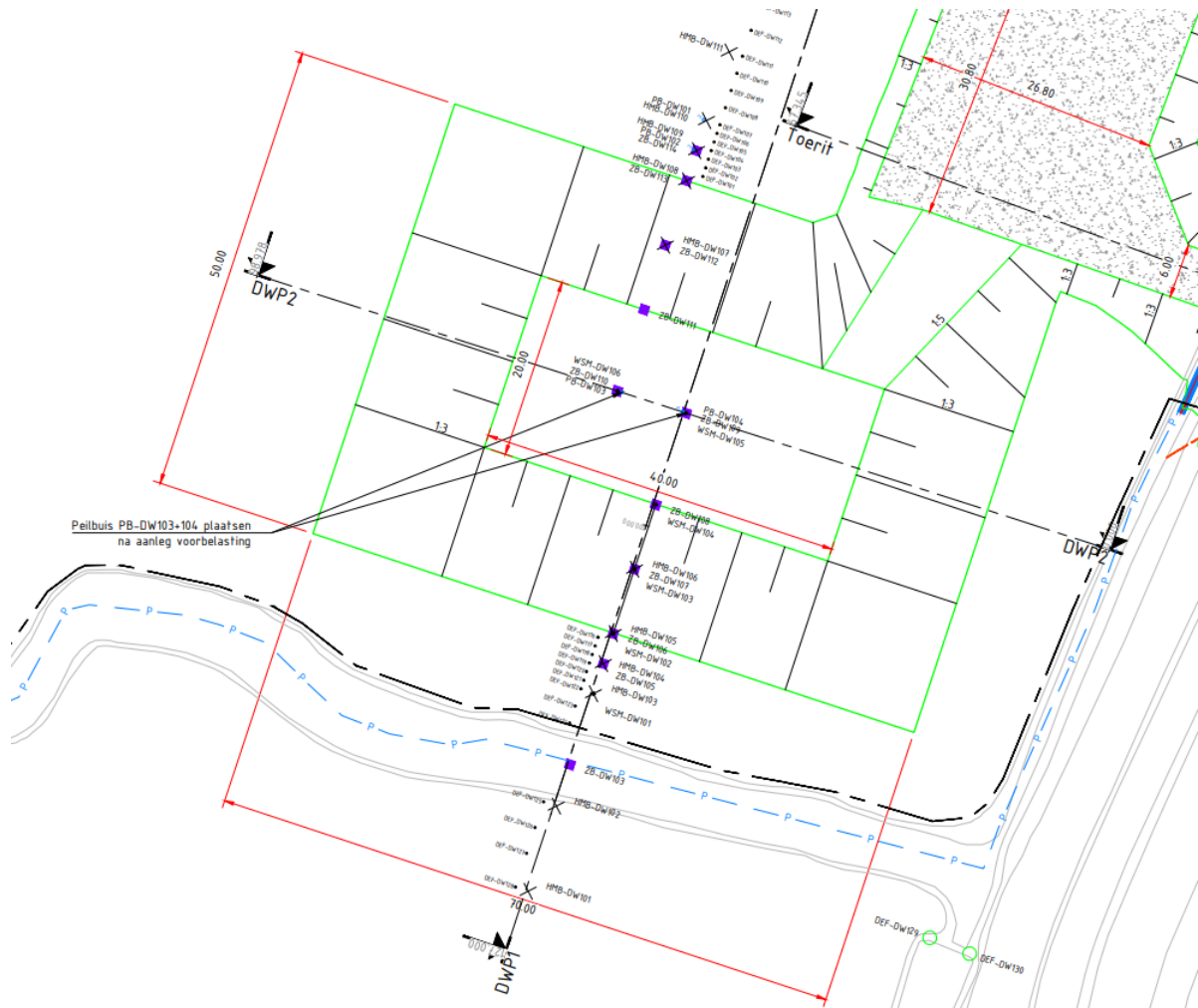


Figure A.2: Top view de Weel

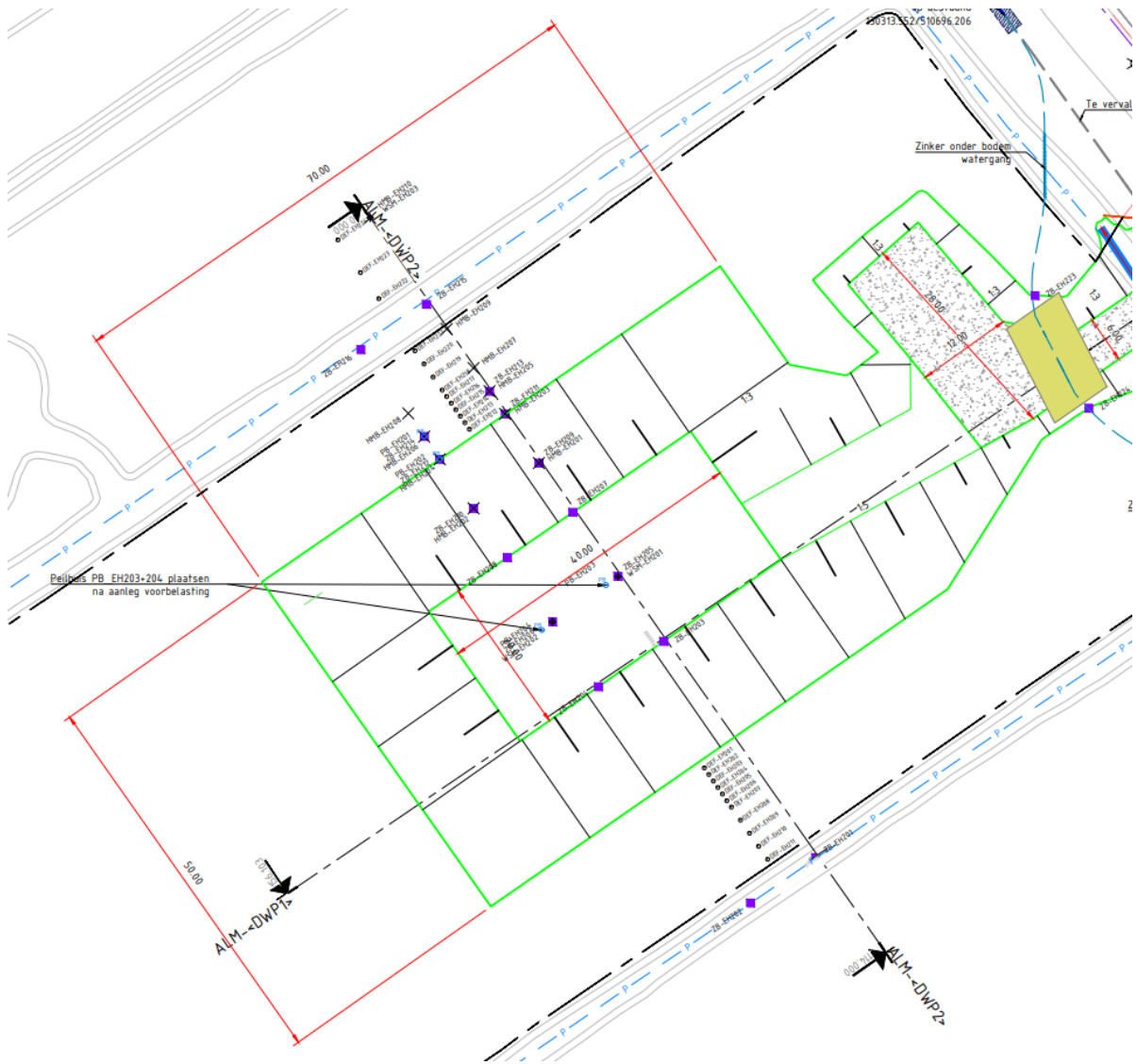


Figure A.3: Top view Ethersheim

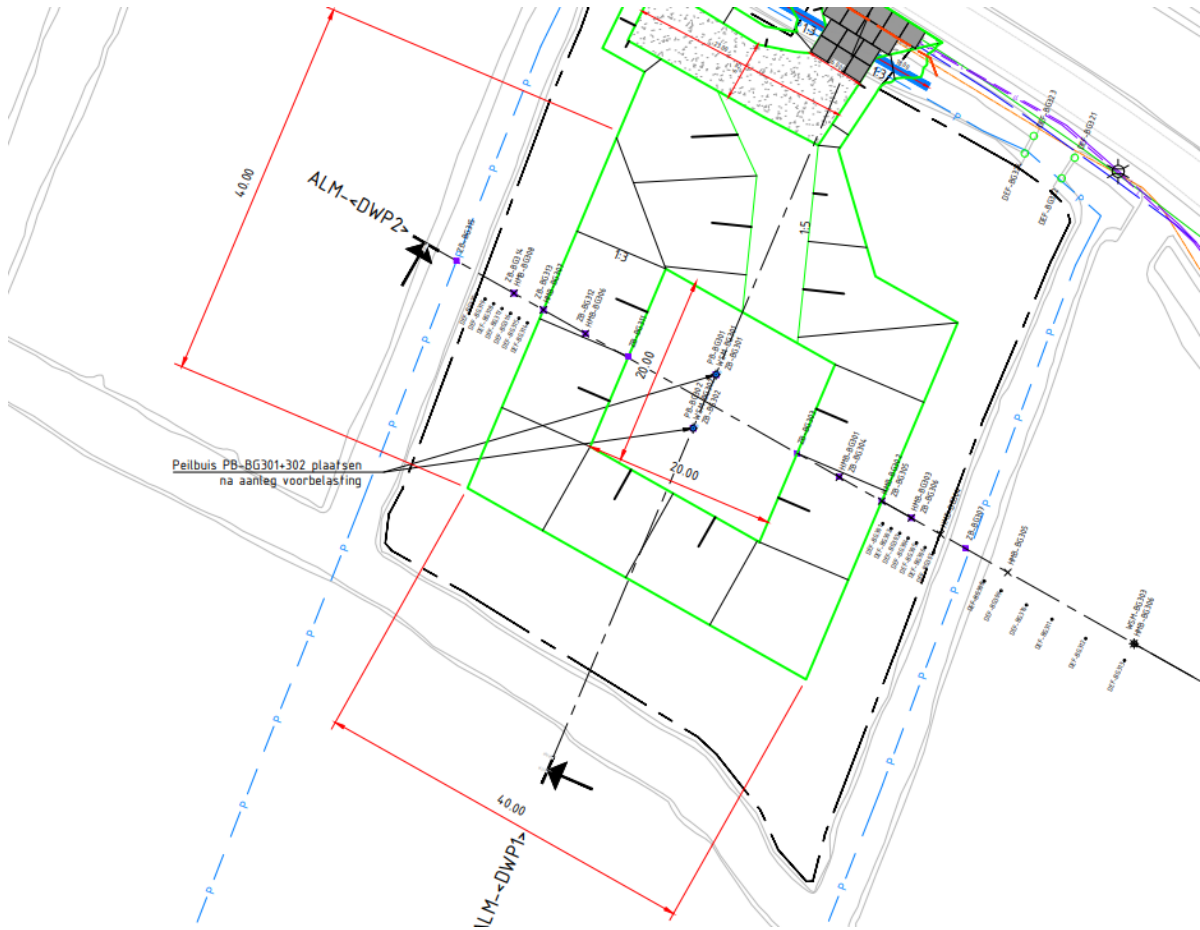


Figure A.4: Top view Broeckgouw

Peat									
initial	start time [days]	preload height [m]	initial stress [kPa]	equivalent age [days]					
	0	0	5	237356					
	tstart [days]	dH [m]	stress [kPa]	equivalent age [days]	duration [days]	t_end [days]	OCR [-]	CPTu phase	
	2,37E+05	0,80	16,71	0,01	30,00	30,01			
	30,01	0,70	26,96	0,03	27,00	27,03			
	27,03	0,50	34,29	0,91	12,00	12,91			
	12,91	0,58	42,71	0,58	108,00	108,58			
	108,58	0,58	51,13	28,13	31,00	59,13			
	59,13	0,35	56,25	15,32	1,00	16,32			
	16,32	1,00	70,89	0,62	156,00	156,62			
	156,62	0,50	78,22	39,03	78,00	117,03	1,40	phase 1	
	117,03	-4,16	17,30	2,15E+11	20,00	2,15E+11	6,33	phase 2	

POP [kPa]	7
CR	0,489
RR	0,079
ca	0,029
isotach m	14,1379

Duinkerke									
initial	start time [days]	preload height [m]	initial stress [kPa]	equivalent age [days]					
	0	0	5	12528458567					
	tstart [days]	dH [m]	stress [kPa]	equivalent age [days]	duration [days]	t_end [days]	OCR [-]	CPTu phase	
	1,25E+10	0,80	16,71	9,32	30,00	39,32			
	39,32	0,70	26,96	0,01	27,00	27,01			
	27,01	0,50	34,29	0,41	12,00	12,41			
	12,41	0,58	42,71	0,27	108,00	108,27			
	108,27	0,58	51,13	20,51	31,00	51,51			
	51,51	0,35	56,25	9,76	1,00	10,76			
	10,76	1,00	70,89	0,19	156,00	156,19			
	156,19	0,50	78,22	28,20	78,00	106,20	1,31	phase 1	
	106,20	-4,16	17,30	2,7E+13		2,7E+13	5,91	phase 2	

POP [kPa]	12
CR	0,247
RR	0,038
ca	0,012
isotach m	17,42

Calais									
initial	start time [days]	preload height [m]	initial stress [kPa]	equivalent age [days]					
	0	0	28	218,29					
	tstart [days]	dH [m]	stress [kPa]	equivalent age [days]	duration [days]	t_end [days]	OCR [-]	CPTu phase	
	218,29	0,80	39,71	0,46	30,00	30,46			
	30,46	0,70	49,96	0,53	27,00	27,53			
	27,53	0,50	57,29	2,47	12,00	14,47			
	14,47	0,58	65,71	1,29	108,00	109,29			
	109,29	0,58	74,13	33,61	31,00	64,61			
	64,61	0,35	79,25	19,87	1,00	20,87			
	20,87	1,00	93,89	1,05	156,00	157,05			
	157,05	0,50	101,22	41,78	78,00	119,78	1,31	phase 1	
	119,78	-4,16	40,30	1,35E+09		1,35E+09	3,29	phase 2	

POP	10
CR	0,229
RR	0,035
ca	0,011
m	17,64

Figure A.5: Markermeerdijken: Isotach model calculation

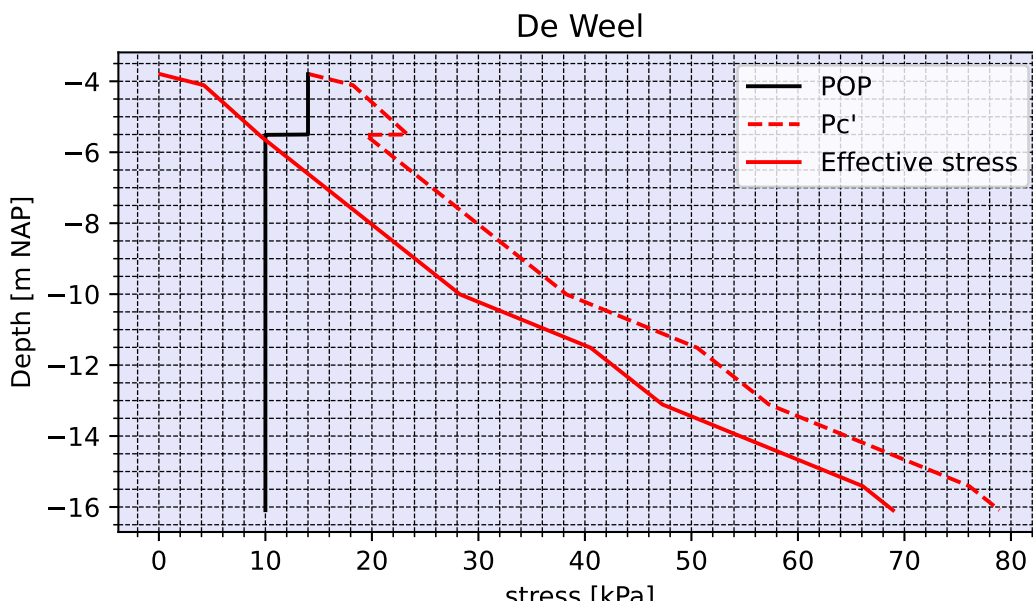


Figure A.6: de Weel stress state

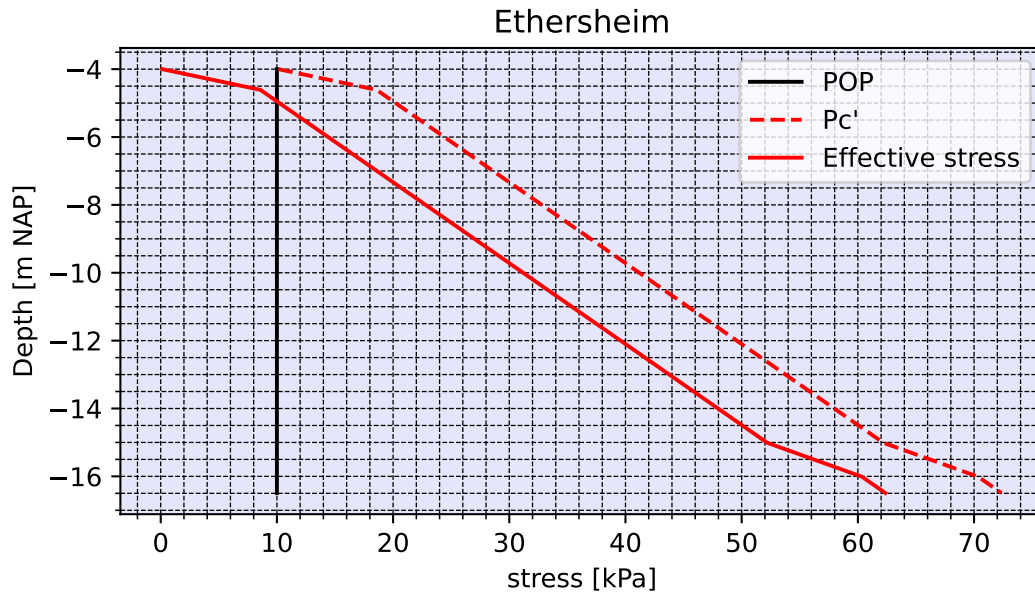


Figure A.7: Ethersheim stress state

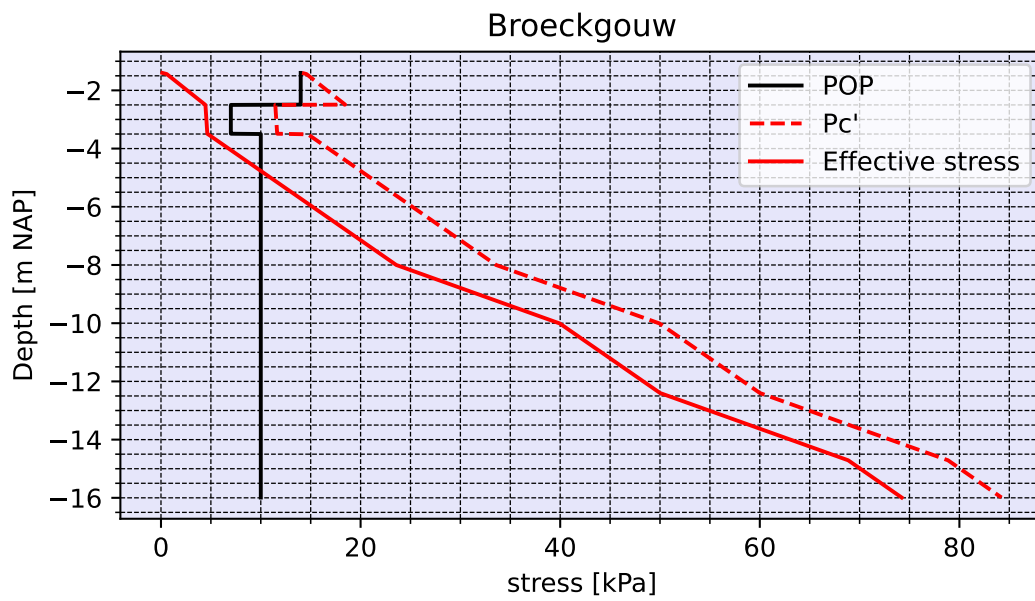


Figure A.8: Broeckgouw stress state

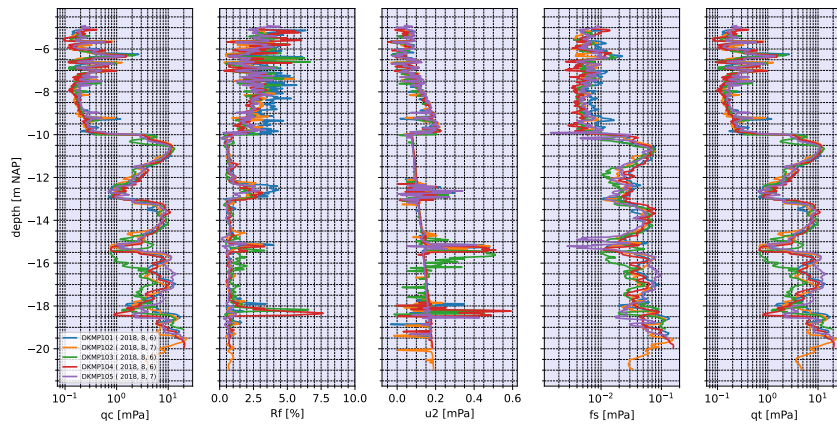


Figure A.9: de Weel phase 0

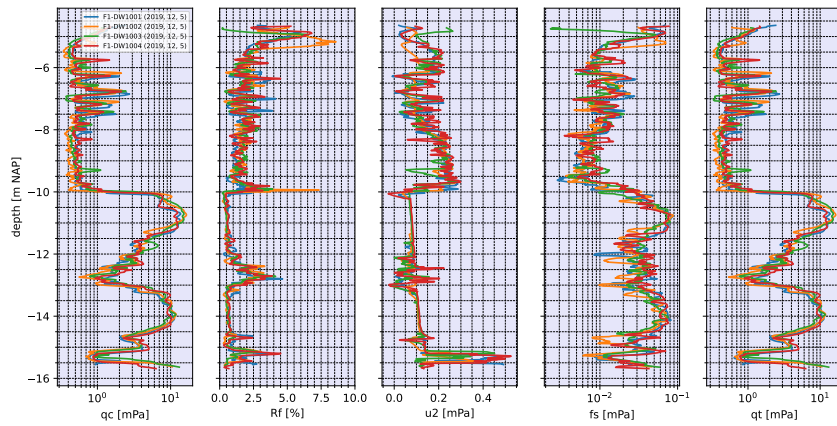


Figure A.10: de Weel phase 1

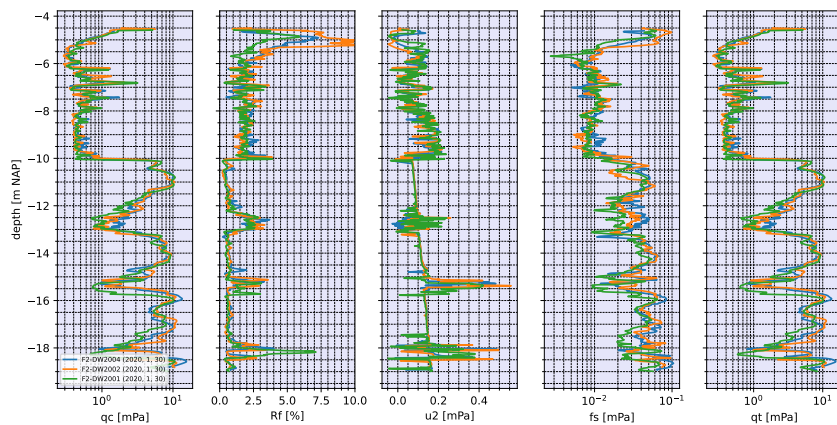


Figure A.11: de Weel phase 2

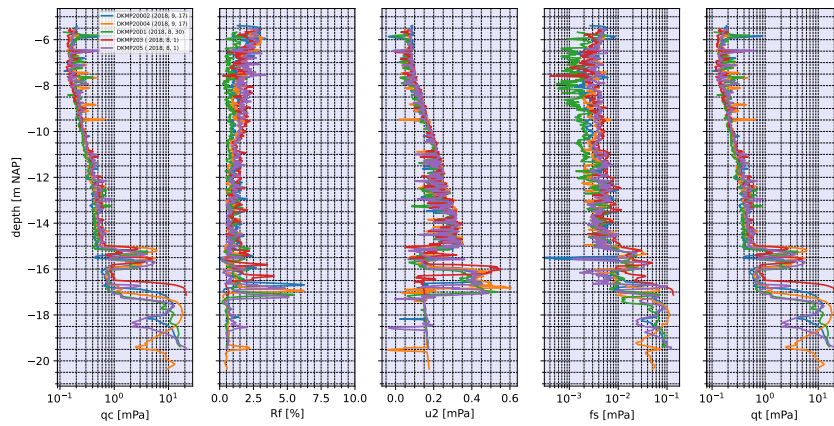


Figure A.12: Ethersheim phase 0

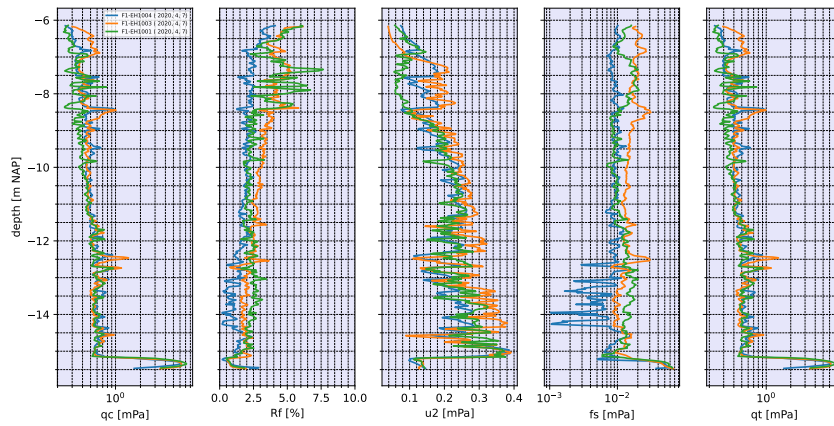


Figure A.13: Ethersheim phase 1

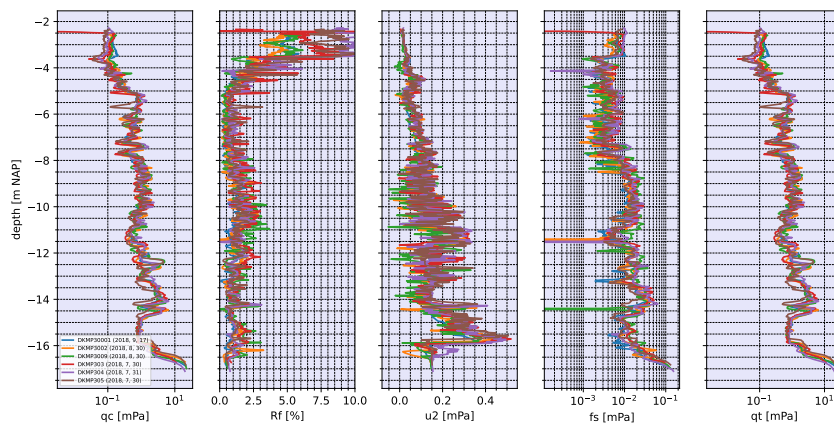


Figure A.14: Broeckgouw phase 0

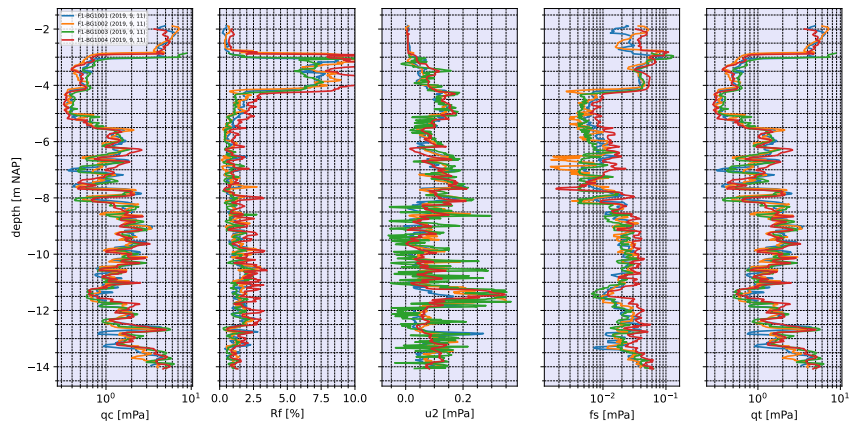


Figure A.15: Broeckgouw phase 1

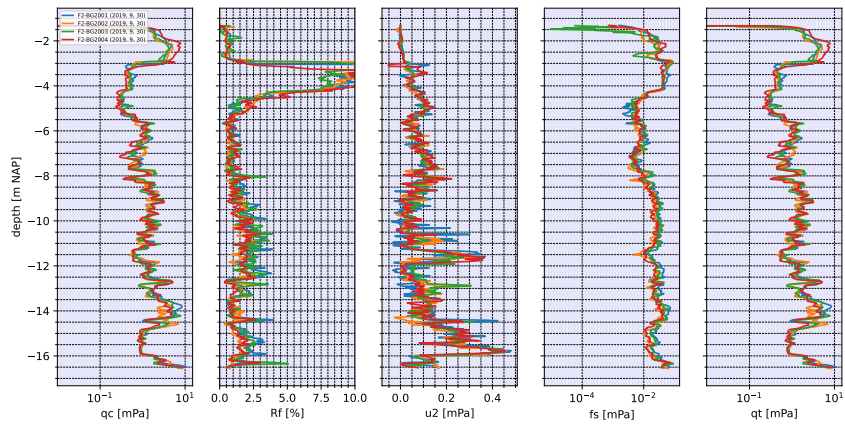


Figure A.16: Broeckgouw phase 2

B

Data Philippines reclamation

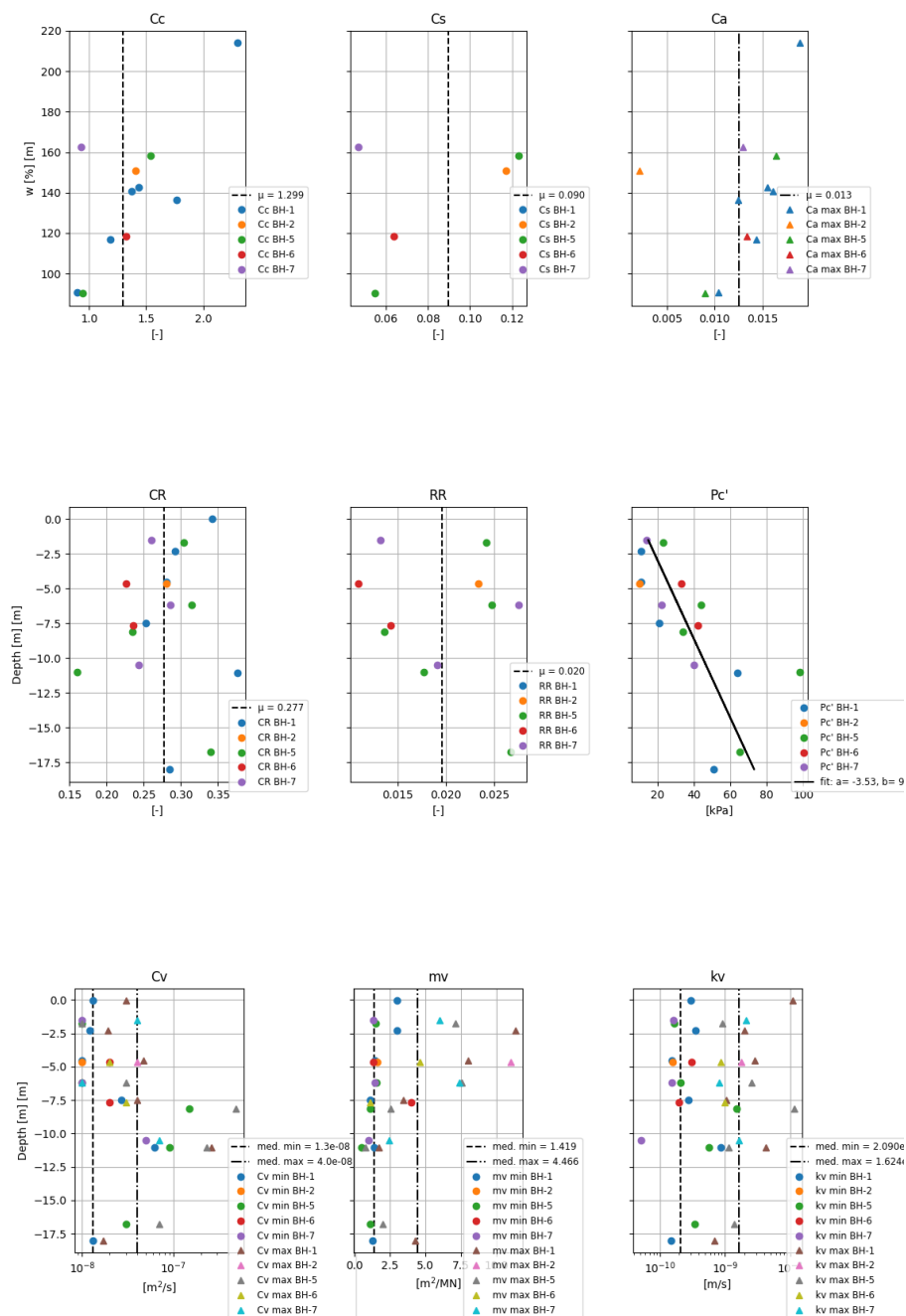


Figure B.1: Site investigation boreholes: BH-01, BH-02, BH-05, BH-06, BH-07

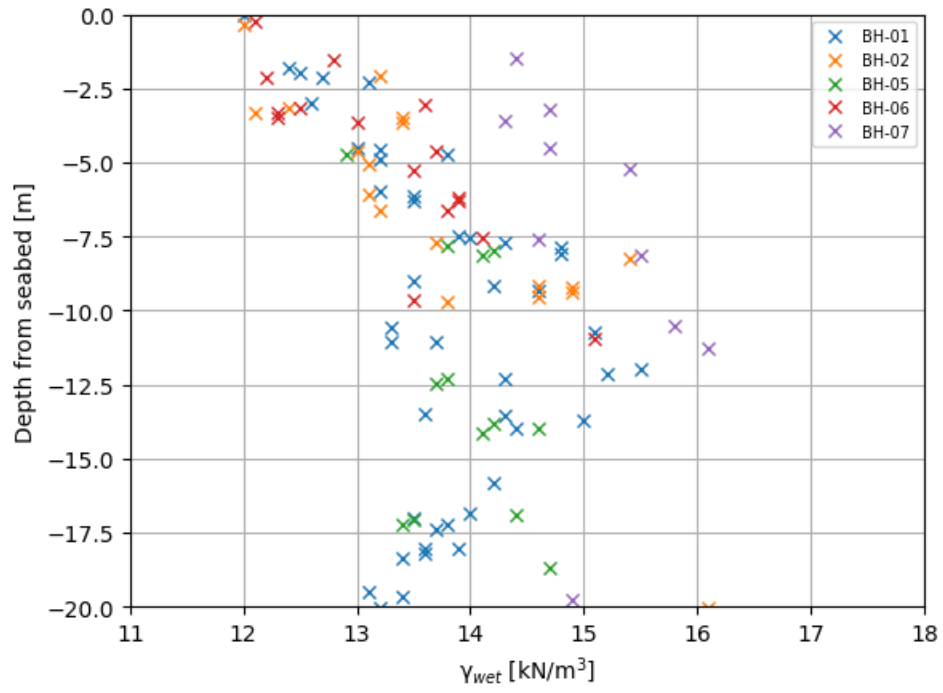


Figure B.2: Bulk unit weight

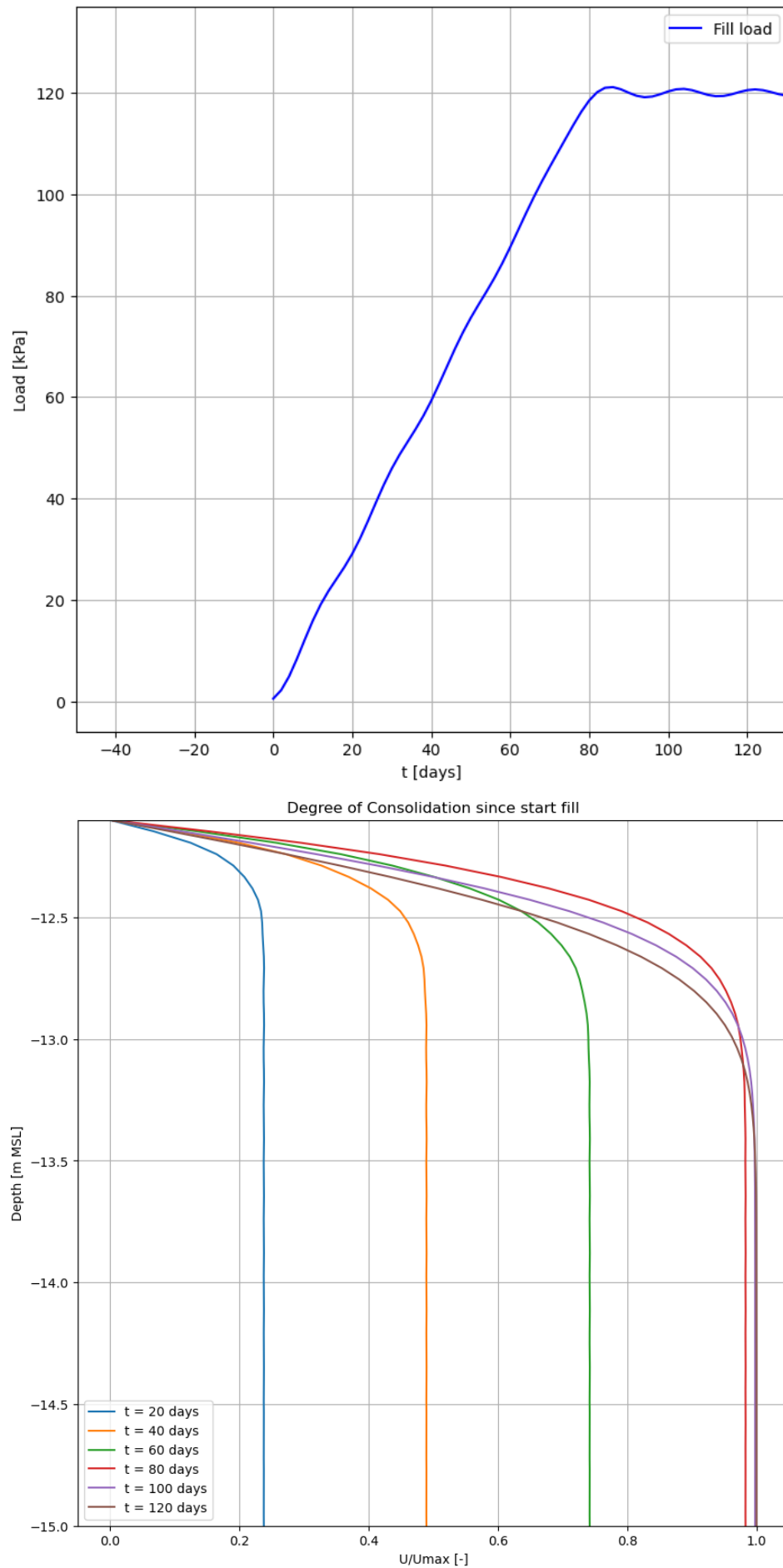


Figure B.3: Consolidation during fill, before PVD installation. Fill was completed in approximately 90 days

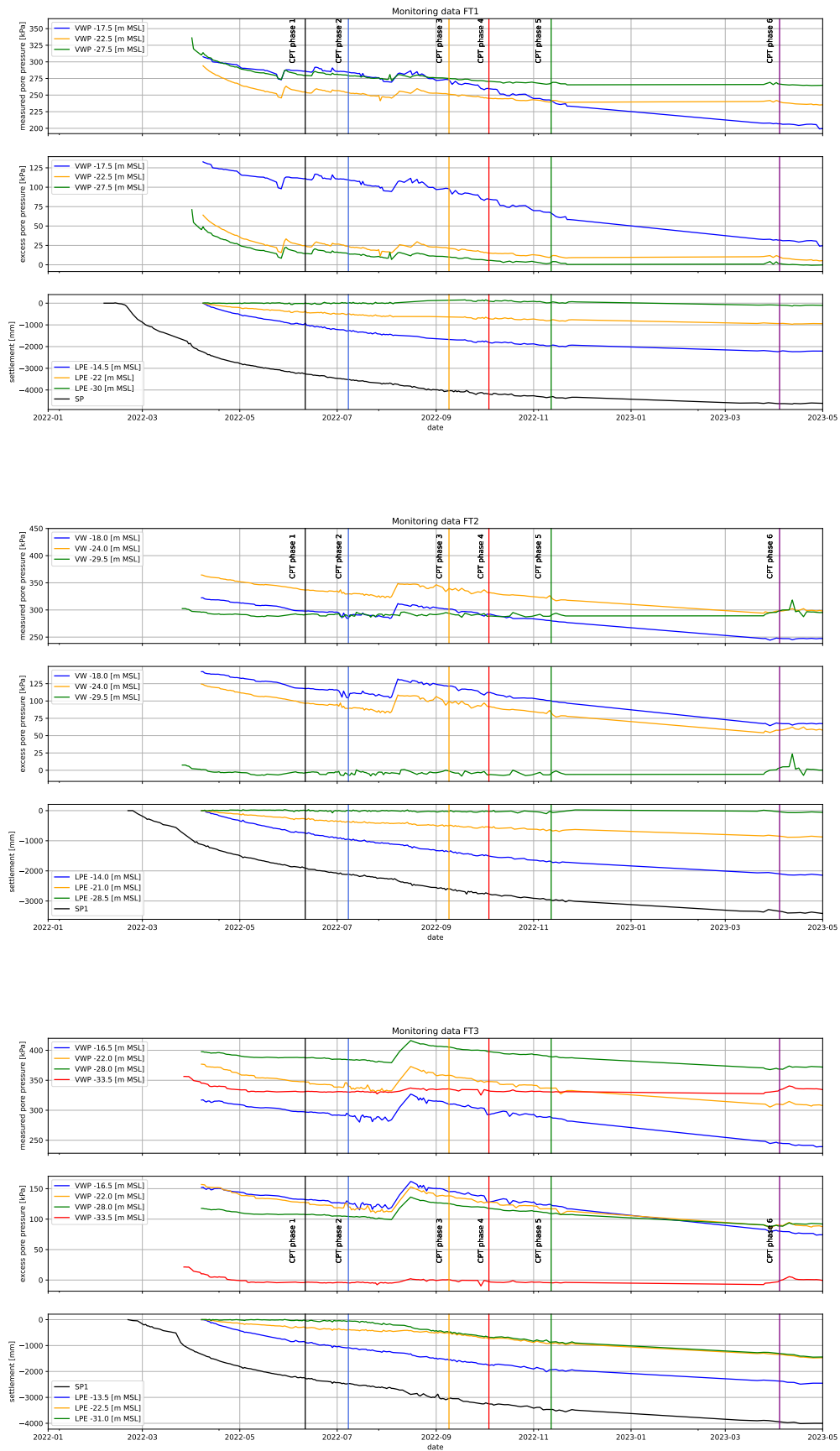


Figure B.4: Monitoring data

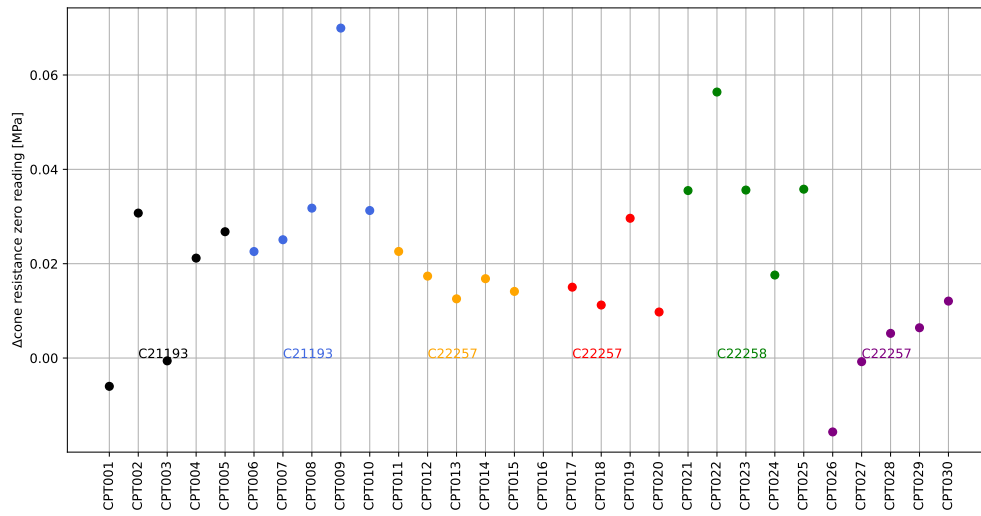


Figure B.5: FT1: Difference between zero measurement cone resistance prior to CPTu and after CPTu

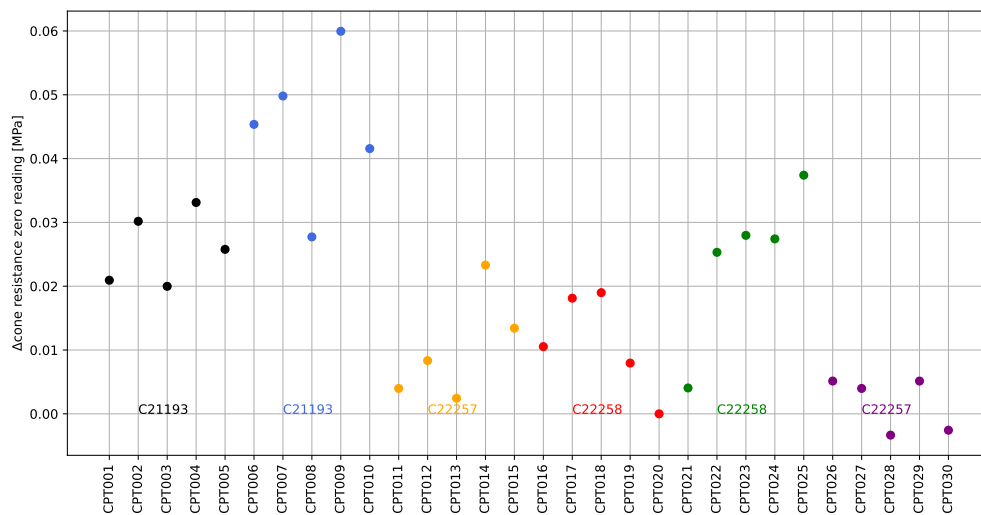


Figure B.6: FT2: Difference between zero measurement cone resistance prior to CPTu and after CPTu

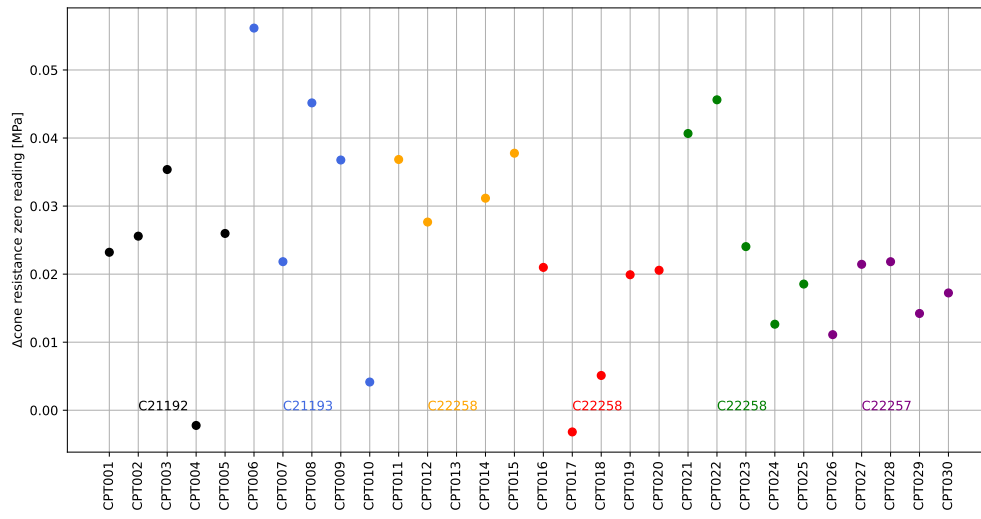


Figure B.7: FT3: Difference between zero measurement cone resistance prior to CPTu and after CPTu

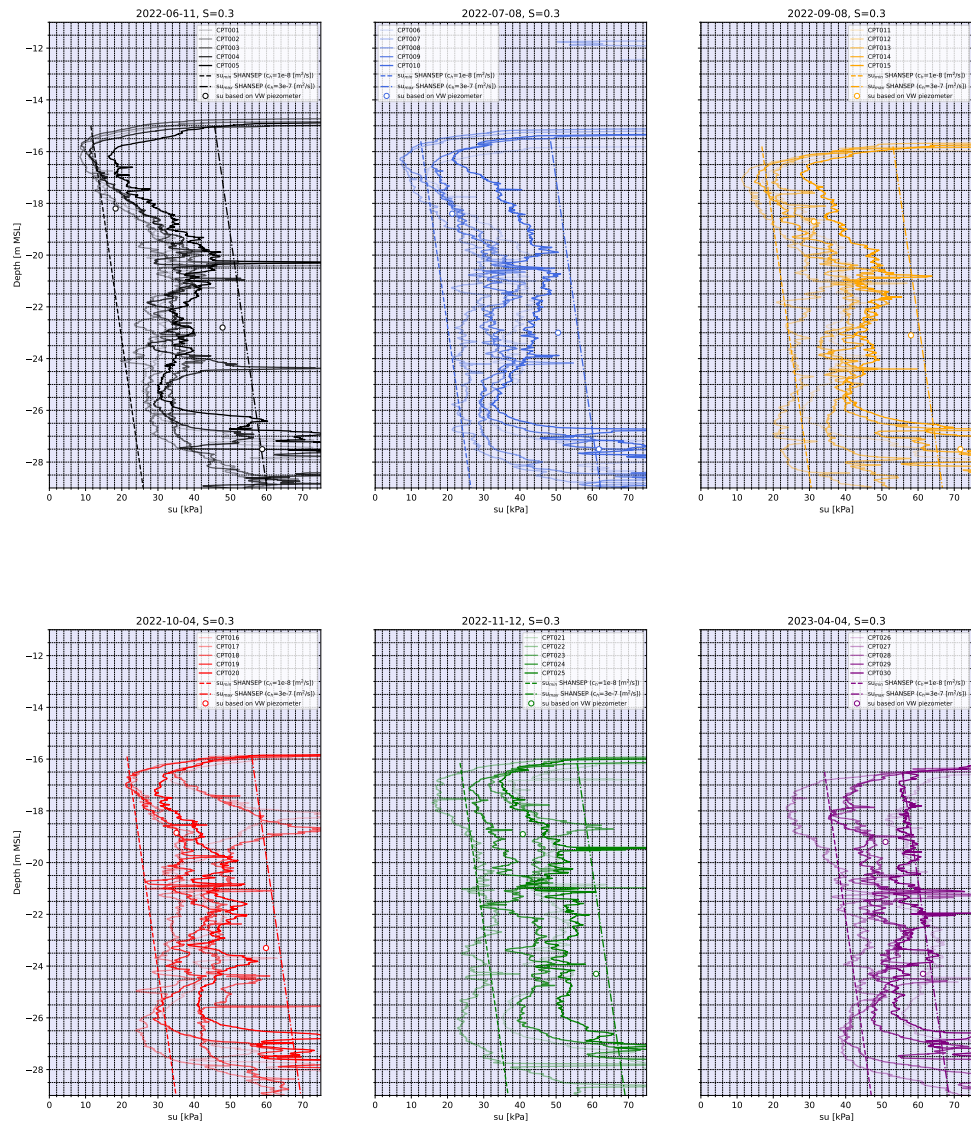


Figure B.8: FT2: General strength comparison excluding creep

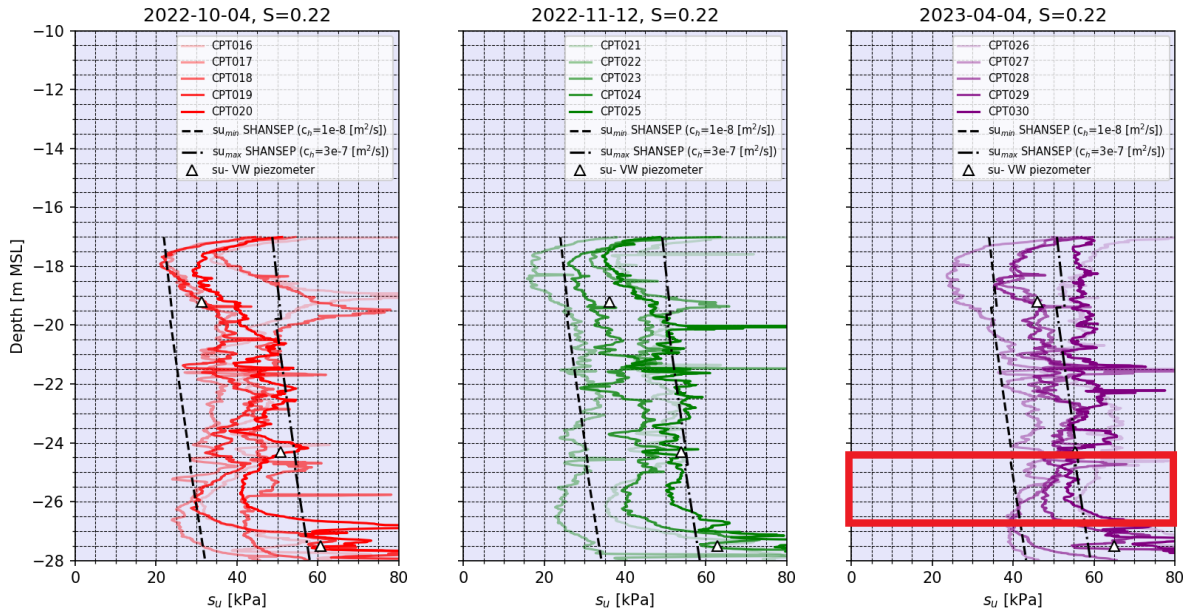


Figure B.9: MSC3: better fit with SHANSEP S of 0.22

FT1-MSC1									
initial	start time [days]	initial stress [kPa]	equivalent age [days]						
	1		10	67108864					
days after PVD placement	preload + initial stress [kPa]	tstart [days]	Δt [days]	t_end [days]	OCR [-]	CPTu phase	POP [kPa]	10	
100	158	9,31E-25	105	105	1,20				
115	171	13,44	30	43,44	1,16	phase 1			
135	180	11,45	20	31,45	1,14	phase 2			
172	180	31,45	37	68,45	1,18				
195	202	3,41	23	26,41	1,13	phase 3			
235	202	1,57	40	41,57	1,15	phase 4			
260	202	41,57	25	66,57	1,18	phase 5			
410	202	66,57	150	216,57	1,23	phase 6			
							m [-]	26	

FT1-MSC2									
initial	start time [days]	initial stress [kPa]	equivalent age [days]						
	1	18	18	3342781					
days after PVD placement	preload + initial stress [kPa]	tstart [days]	Δt [days]	t_end [days]	OCR [-]	CPTu phase	POP [kPa]	10	
100	166	1,58E-28	105	105,00	1,15				
115	179	8,09	30	38,09	1,11	phase 1			
135	188	7,19	20	27,19	1,10	phase 2			
172	188	27,19	37	64,19	1,13				
195	210	1,49	23	24,49	1,10	phase 3			
235	210	0,63	40	40,63	1,12	phase 4			
260	210	40,63	25	65,63	1,13	phase 5			
410	210	65,63	150	215,63	1,17	phase 6			
							m	34	

FT1-MSC3									
initial	start time [days]	initial stress [kPa]	equivalent age [days]						
	1	24	24	559979					
days after PVD placement	preload + initial stress [kPa]	tstart [days]	Δt [days]	t_end [days]	OCR [-]	CPTu phase	POP [kPa]	10	
100	172	1,23E-29	105	105,00	1,13				
115	185	6,59	30	36,59	1,10	phase 1			
135	194	6,02	20	26,02	1,09	phase 2			
172	194	26,02	37	63,02	1,12				
195	216	1,06	23	24,06	1,09	phase 3			
235	216	0,44	40	40,44	1,10	phase 4			
260	216	40,44	25	65,44	1,12	phase 5			
410	216	65,44	150	215,44	1,15	phase 6			
							m	38	

Figure B.10: OCR due to creep in FT1: layers MSC1, MSC2 and MSC3

FT2-MSC1							
initial	start time [days]	initial stress [kPa]	equivalent age [days]				
	1	10	67108864				
days after PVD placement	preload + initial stress [kPa]	tstart [days]	Δt [days]	t_end [days]	OCR [-]	CPTu phase	POP [kPa]
110	160	6,8E-25	110	110	1,20	phase 1	10
140	160	110,00	30,00	140,00	1,21	phase 2	
170	160	140,00	30,00	170,00	1,22		
200	190	1,95	30,00	31,95	1,14	phase 3	m
240	190	31,95	40,00	71,95	1,18	phase 4	
265	190	71,95	25,00	96,95	1,19	phase 5	
415	190	96,95	150,00	246,95	1,24	phase 6	26

FT2-MSC2							
initial	start time [days]	initial stress [kPa]	equivalent age [days]				
	1	18	3342781				
days after PVD placement	preload + initial stress [kPa]	tstart [days]	Δt [days]	t_end [days]	OCR [-]	CPTu phase	POP [kPa]
110	168	1,09631E-28	110	110	1,15	phase 1	10
140	168	110,00	30,00	140,00	1,16	phase 2	
170	168	140,00	30,00	170,00	1,16		
200	198	0,64	30,00	30,64	1,11	phase 3	m
240	198	30,64	40,00	70,64	1,13	phase 4	
265	198	70,64	25,00	95,64	1,14	phase 5	
415	198	95,64	150,00	245,64	1,18	phase 6	34

FT2-MSC3							
initial	start time [days]	initial stress [kPa]	equivalent age [days]				
	1	24	559979				
days after PVD placement	preload + initial stress [kPa]	tstart [days]	Δt [days]	t_end [days]	OCR [-]	CPTu phase	POP [kPa]
110	174	8,4E-30	110	110	1,13	phase 1	10
140	174	110,00	30,00	140,00	1,14	phase 2	
170	174	140,00	30,00	170,00	1,14		
200	204	0,40	30,00	30,40	1,09	phase 3	m
240	204	30,40	40,00	70,40	1,12	phase 4	
265	204	70,40	25,00	95,40	1,13	phase 5	
415	204	95,40	150,00	245,40	1,16	phase 6	38

Figure B.11: OCR due to creep in FT2: layers MSC1, MSC2 and MSC3

FT3-MSC1									
initial	start time [days]	initial stress [kPa]	equivalent age [days]						
	1	10	67108864						
days after PVD placement	preload + initial stress [kPa]	tstart [days]	Δt [days]	t_end [days]	OCR [-]	CPTu phase	POP [kPa]		
110	185	1,9E-26	110	110	110	1,20	phase 1		
140	185	110,00	30,00	140,00	140,00	1,21	phase 2		
170	185	140,00	30,00	170,00	170,00	1,22			
200	232	0,47	30,00	30,47	30,47	1,14	phase 3	m	26
240	232	30,47	40,00	70,47	70,47	1,18	phase 4		
265	232	70,47	25,00	95,47	95,47	1,19	phase 5		
415	232	95,47	150,00	245,47	245,47	1,24	phase 6		

FT3-MSC2									
initial	start time [days]	initial stress [kPa]	equivalent age [days]						
	1	18	3342781						
days after PVD placement	preload + initial stress [kPa]	tstart [days]	Δt [days]	t_end [days]	OCR [-]	CPTu phase	POP [kPa]		
110	193	1,5E-30	110	110	110	1,15	phase 1		
140	193	110,00	30,00	140,00	140,00	1,16	phase 2		
170	193	140,00	30,00	170,00	170,00	1,16			
200	240	0,10	30,00	30,10	30,10	1,11	phase 3	m	34
240	240	30,10	40,00	70,10	70,10	1,13	phase 4		
265	240	70,10	25,00	95,10	95,10	1,14	phase 5		
415	240	95,10	150,00	245,10	245,10	1,18	phase 6		

FT3-MSC3									
initial	start time [days]	initial stress [kPa]	equivalent age [days]						
	1	24	559979						
days after PVD placement	preload + initial stress [kPa]	tstart [days]	Δt [days]	t_end [days]	OCR [-]	CPTu phase	POP [kPa]		
110	199	0,00	110,00	110,00	110,00	1,13	phase 1		
140	199	110,00	30,00	140,00	140,00	1,14	phase 2		
170	199	140,00	30,00	170,00	170,00	1,14			
200	246	0,05	30,00	30,05	30,05	1,09	phase 3	m	38
240	246	30,05	40,00	70,05	70,05	1,12	phase 4		
265	246	70,05	25,00	95,05	95,05	1,13	phase 5		
415	246	95,05	150,00	245,05	245,05	1,16	phase 6		

Figure B.12: OCR due to creep in FT3: layers MSC1, MSC2 and MSC3